NEW LIQUID HOLDUP, LOAD POINT AND FLOODING VELOCITY MODELS IN DIFFERENT REGIONS OF OPERATIONS FOR A STRUCTURED PACKED COLUMN

By

ANIL KRISHNA JAMMULA

Bachelor of Technology in Chemical Engineering
Acharya Nagarjuna University
Guntur, Andhra Pradesh, India
2007

Master of Engineering in Chemical Engineering
Lamar University
Beaumont, Texas, USA
2008

Submitted to the Faculty of the
Graduate College of the
Oklahoma State University
in partial fulfillment of
the requirements for
the Degree of
DOCTOR OF PHILOSOPHY
December, 2014

NEW LIQUID HOLDUP, LOAD POINT AND FLOODING VELOCITY MODELS IN DIFFERENT REGIONS OF OPERATIONS FOR A STRUCTURED PACKED COLUMN

Dissertation Approved:

Dr. James R. Whiteley

Dissertation Adviser

Dr. Arland H. Johannes

Dr. Tony Cai

Dr. Danielle D. Bellmer

ACKNOWLEDGEMENTS

I would like to thank my advisor, Dr. Rob Whiteley, for his encouragement, supervision, guidance, and support throughout my Ph.D. program. I would also like to thank my committee members, Dr. Arland H. Johannes, Dr. Tony Cai, and Dr. Danielle D. Bellmer for their guidance and valuable suggestions.

I specially need to thank my wife Sravanthi Vupputuri for her help in my work and writing, financially, emotionally, and also for her constant encouragement. Furthermore, I would like to thank my family members and friends for all their support.

Finally, I'd like to thank Fractionation Research Inc. (FRI), Flowserve, Optimized Gas Treating, and Bayer for their partial financial support either through projects or employment.

"Acknowledgements reflect the views of the author and are not endorsed by committee members or Oklahoma State University."

TABLE OF CONTENTS

LIST OF TABLES

Table Page

LIST OF FIGURES

Figure Page

Nomenclature

a	packing surface area, m^2/m^3
g	gravitational constant, m/s^2
d_e	equivalent diameter, $4\varepsilon/a$, m
D	packing dimension, m
F	Force, N
u	superficial velocity, m/s
s	packing crimp side length, m
b	packing crimp base length, m
h	packing crimp height, m
U	actual velocity after accounting for liquid holdup effect, m/s
Re	Reynolds number, $\frac{u_L \rho_L}{a\ \mu_L}$
h_L	Liquid holdup, m^3/m^3
j*	Dimensionless fluxes, $\frac{\rho_G^{\frac{1}{2}}\ U}{[g\ D\ (\rho_L - \rho_G)]^{\frac{1}{2}}}$
m, c, C_1, C_2, C_3	constants

Greek Letters

ρ	Density, kg/m^3
μ	Viscosity, Pas
θ	Corrugation angle, Deg
δ	Liquid film thickness, m
ε	void fraction of packing
σ	surface tension, N/m

Subscripts

L	Liquid phase

V	Vapor phase
Pre	Preloading region
Load	Loading region
c	Critical
A	preloading
fl	Flooding region

CHAPTER I

1. INTRODUCTION

Separation of mixtures into the desired products is necessary in chemical or petrochemical industries. Among different separation methods, distillation is most popular because of its simple operating principle which is to separate different components based on differences in their boiling points [1, 2]. In addition to its simple operating principle, distillation, when compared to other separation technologies, has a few distinctive advantages which are summarized below [3]:

- Distillation has an economic advantage compared to other technologies at large throughputs
- Distillation does not require any mass separating agent other than energy
- Distillation has been used over the past 100 years, and we know a great deal about it, such as its limitations and scaling up from laboratory to industrial scale
- A huge database of vapor/liquid equilibria is available

These distinctive advantages made distillation king of separations with an overall throughput of 5.23 billion tons per year [4]. In financial terms, this throughput is valued at approximately $2.5 trillion/year, using an average barrel price of $85 [4]. It was estimated that simply improving the design of a distillation column would save approximately 20% of the capital

expenditure and 5% of energy usage. Since distillation accounts for almost 3% of all the energy consumption in the U.S, even the energy savings are huge [5]. In addition, strict EPA regulations are making it difficult to construct new distillation columns, and in turn are encouraging the process industries to operate the distillation columns at higher capacities by revamping the existing columns [6]. Because of this, there is a constant need for improving the efficiency and capacity of column internals. Furthermore, there is a need for accurate models to help design columns that will realize the improvement in efficiency and capacity of new columns without compromising on the column safety.

However, the design equations of a distillation column vary depending on the type of internal used. The two most popular internals of a distillation column are,

- Trays
- Packings

1.1. Trays

Trays are the oldest and most widely used internals in a distillation column [1]. The main objectives of any distillation internal is to provide a large surface area which increases the vapor and liquid contact which in turn will improve the mass transfer between the two phases. In trays, contact between vapor and liquid phase occurs due to bubbling of vapor phase through the continuous liquid phase present on top of the tray.

Over the years many different types of trays have come into existence. The most popular among them are bubble cap trays (1808), sieve trays (1832), and valve trays (1960) [2]. For these trays, a number of researchers developed the overall efficiency models and point efficiency models in different regions of operation [7-9]. Even in the flooding region, the amount of work available

for trays is more than any other distillation internals [10]. A more detailed discussion of this work on trays can be found elsewhere [1, 2].

1.2. Packing

In addition to trays, packings are also another popular internal choice. Packings can be further divided into two sub categories:

- Random packing
- Structured packing

1.2.1. Random Packing

Similar to trays, random packings are also used to provide area for vapor and liquid contact. However, in packed columns the vapor phase is the continuous phase and the liquid phase is the dispersed phase. In a random packed column, packings are dumped into the column and form a random structure for the liquid and vapor phases to pass through [2].

The main advantage of random packings is their availability in different shapes and sizes. In addition, packings can also be manufactured using nonmetals such as ceramics and plastics. There has been a lot of advancement in random packings over the years (1830-present) [2], and for this reason different random packings were classified into four generations of packings. The current and most popular generation is the high capacity random packings which are most popular as revamp tools because of their higher capacities [6, 11]. A more detailed discussion on different versions of random packings can be found in Kister (1991) [2].

After trays, the amount of modeling work is significant for random packings [12-15]. Among different random packing models, the Billet [16] model is popular because it includes

liquid holdup term as the main parameter in its pressure drop and mass transfer model, and it also accounts for the vapor and liquid flow behavior changes in different regions of operation. However, random packings have complex structures, and for this reason, the Billet model relies on packing specific constants for model predictions. This often limits the usability of the Billet model for new packings.

1.2.2. Structured packings

The necessity for lower pressure drop and higher efficiency led to the development of structured packings. In addition, structured packed columns also have higher capacity than trayed columns. In structured packed columns, the packing element is arranged in a systematic arrangement which causes lower pressure drop. However, without a proper liquid and vapor distributor, it is not possible to achieve the desired efficiency and pressure drop of the structured packing. A more detailed discussion on liquid maldistribution and its effects can be found in Stichlmair (1987) [17]
.

Similar to random packings, structured packing evolution can be classified into four generations. This evolution was summarized in Fig. 1.1. Among different generations of structured packings, first and second generations were not popular because of their higher manufacturing costs. Still, their efficiency was significantly higher and pressure drop was significantly lower compared to trays, so they were mostly used in vacuum or very low pressure operations which typically involved thermo sensitive materials. Structured packings, however, became very popular from the third generation onward due to the introduction of sheet metal structured packings. The use of sheet metal reduced the overall manufacturing costs of structured packings, which caused

them to be competitive with other conventional internals such as trays and random packings. From the third generation, the use of structured packing rose to the point where it became the most popular internal choice. Due to the continuous requirement for higher capacity, new fourth generation packings were introduced into the market. These packings have lower resistance to vapor flow which caused these packings to have higher capacity with the same efficiency as the third generation packings.

In the present work, the focus will be on the third generation structured packed columns. These structured packed columns can be modeled either with the equilibrium stage model or with the non-equilibrium stage model [2]. Among these models, the equilibrium stage model is most popular and most widely used because of its simplicity. In the equilibrium stage approach, a column is divided into a number of equilibrium stages and it is assumed that vapor and liquid leaving each stage are in thermodynamic equilibrium. However, this approach is far from reality since theoretical stages are converted into actual packing height using the concept of HETP. These equilibrium concepts are adequate for a binary system, but do not do a good job for multicomponent systems.

In order to properly model multicomponent and non-ideal systems, a non-equilibrium model or rate-based approach was developed [18-20]. In this approach, thermodynamic equilibrium is only assumed at the interface between the vapor and liquid phases. Rate equations can be used to calculate the rate of mass and energy transfer from interface to the bulk phases of a non-equilibrium stage.

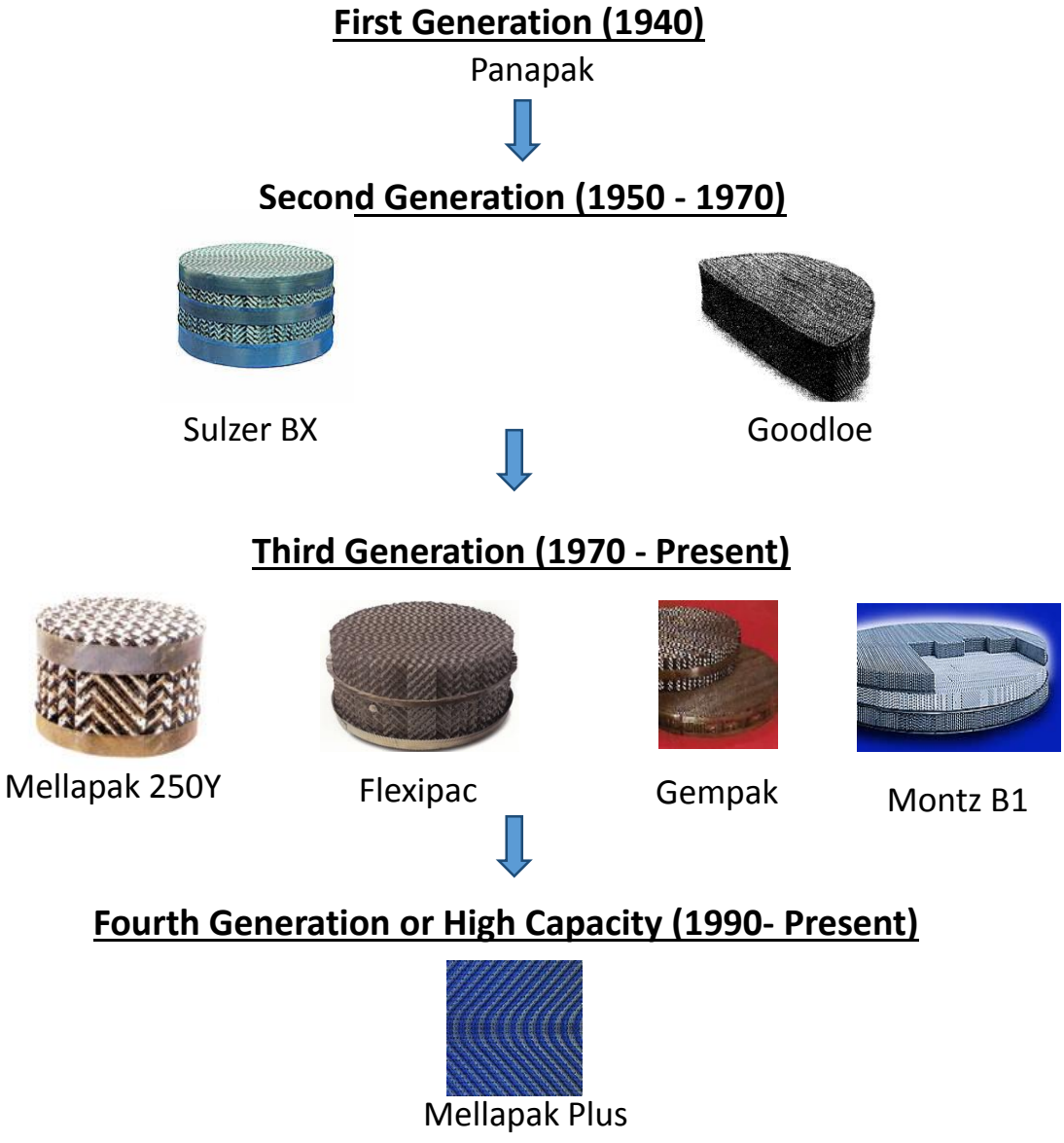

Figure 1.1. Different generations of structured packings

But for both equilibrium and non-equilibrium modeling approaches, hydraulic and mass transfer equations are necessary. The design equations necessary for a structured packed column are

- Hydraulic equations
    - Liquid Holdup
    - Pressure drop
    - Flooding velocity
- Mass transfer equations
    - HETP (k_G, k_L, a_e)

Various researchers [16, 21-25] developed different models for both hydraulic and mass transfer taking place inside a structured packed column. However, a majority of these models were either adopted from random packed column models or restricted to the preloading region. In addition, a majority of these researchers did not develop a proper liquid holdup model for different regions of operation. Without a proper liquid holdup model, it will not be possible to develop a good pressure drop and mass transfer model, since both pressure drop and mass transfer behavior is effected by liquid holdup. In addition to a good liquid holdup model, good models are also necessary to properly identify different regions of operation in a structured packed column. The limited modeling work in the loading and flooding region was especially limiting the overall understanding of the structured packing.

The best example of a model which uses liquid holdup as a principle component in pressure drop and mass transfer model development is the Billet random packed model. However, a major limitation of this model is its dependency on packing specific constants for model predictions. So

models similar to the Billet model are necessary for structured packing without any of the Billet model's limitations.

From the previous discussion, it can be observed that structured packing is a relatively new technology compared to trays and random packings. Therefore, the amount of experimental and modeling work is limited compared to other internals. So there is a clear need for liquid holdup model in different regions of operation, a loading point model and a flooding point model for a structured packed column before developing any other models. In addition to the above discussed gaps, the American Institute of Chemical Engineers in conjunction with the US Department of Energy recently published Vision 2020: 2000 Separations Roadmap [26]. In this document, a discussion on the technical barriers and research needs for various separation technologies were addressed. Prominent barriers and research needs addressed are as follows:

1. The need for a better understanding of mass transfer and multiphase flow in both trayed and packed columns
2. The need of database for mass transfer and hydrodynamic data
3. The need of better understanding of basic distillation phenomena
4. The need for developing a fundamentals-based model for predicting mass transfer and hydrodynamics in complex systems

1.3. Objectives of the present work

- Develop liquid holdup models for different regions of operation which can be used to improve pressure drop and mass transfer models in different regions
- Develop databases for liquid holdup, pressure drop, and HETP test data from the open literature
- Develop a load point model and a flooding velocity model to clearly identify different regions of operations which will help in understanding the complex flow behavior taking place in a distillation column

1.4. Chapter Organization

Structured packing column operation can be divided into three regions of operation. They are

- Preloading region
- Loading region
- Flooding region

The current thesis is also divided into three chapters

Chapter 1: Summarizes the liquid holdup behavior in the preloading region and the preloading liquid holdup model development

Chapter 2: Summarizes the liquid holdup behavior in the loading region and model development for both liquid holdup and load point in the loading region

Chapter 3: Summarizes the liquid holdup behavior in the flooding region and model development for both liquid holdup and flooding velocity in the flooding region

CHAPTER II

2. DEVELOPMENT AND EVALUATION OF LIQUID HOLDUP MODELS IN PRELOADING REGION FOR A SHEET METAL STRUCTURED PACKING. PART I

Abstract:

Liquid holdup model is one of the important hydraulic design equations for a sheet metal structured packed column. In addition, liquid holdup is also an important model parameter for developing pressure drop, mass transfer, and flooding velocity models for structured packing. Therefore, numerous researchers have developed various theoretical models for liquid holdup. However, majority of these models rely on packing specific constants and packing dimensions for model predictions. But this information was not readily available for many structured packings. So in the current work, new preloading liquid holdup model was developed using packing surface area and void fraction as main model parameters. The performance of the newly developed model and other literature models were evaluated and summarized using experimental liquid holdup database obtained from the open literature. The newly developed model did a better job in reducing the offset between experimental data and in capturing the overall effect of flow rate, liquid properties, and packing geometry on liquid holdup. The gaps in the existing experimental data were discussed.

2.1. Introduction

Structured packings have been gaining popularity among internals for distillation and other separation equipment in industry [2, 27-29]. Despite having high mass transfer efficiency and low pressure drop, structured packings are associated with high cost per unit volume compared to other internals such as random packings [30]. Therefore the improvisation of structured packed column design is of great importance to reduce the capital and operating costs. This is necessary for the evaluation of hydraulic models such as liquid holdup, pressure drop, and flooding capacity, as well as for mass transfer models such as HETP that affect the design of a structured packed column. Although, both hydraulic and mass transfer models are equally important in the design of a structured packed column, evaluating all these models at one time is highly improbable, so, a step-wise evaluation was adopted. In the present study, liquid holdup models were evaluated.

Liquid holdup is a hydrodynamic property and can be classified as static and dynamic. The static liquid holdup accounts for the liquid accumulated in the dead zones and will not be influenced by vapor and liquid flow rates. The static liquid holdup does not change significantly over the course of operation and does not participate in the mass transfer operation, whereas the dynamic liquid holdup actively participates in the mass transfer operation and will be influenced by both the liquid and vapor loads. The total liquid holdup in the column is the sum of these two liquid holdups which can be expressed using equation 2.1.

$$h_{L,tot} = h_{L,stat} + h_{L,dyn} \tag{2.1}$$

The liquid holdup model estimates total liquid holdup during the operation of the column, and this will help in estimating the support required for the column at the desired operating conditions [31].

Apart from using the liquid holdup model as a design equation, a number of researchers also used it as a key parameter in pressure drop and mass transfer models [21, 25, 32]. So a good liquid holdup model not only improves the design of the column, but also improves the performance of other models. A brief discussion of the literature liquid holdup models were presented below.

In order to design the structured packed columns, researchers such as Billet (1999) and Mackowiak (1991), adopted liquid hold model which was developed for random packings. The geometry of structured packings, however, differs greatly from random packings, thereby causing the existing models to give inaccurate results. To account for these variations, researchers incorporated packing specific constants into the model. However, the packing specific constants are available only for a few types of packings which limit applicability of the model to new packings. In an effort to develop a separate liquid holdup model for sheet metal structured packing, SRP (Rocha (1993)) used the concept of effective gravity that accounts for the forces affecting the flow of liquid film on the structured packing. Their liquid holdup model for structured packing is an implicit equation which requires iterations to obtain both liquid holdup and pressure drop simultaneously. Followed by SRP, Olujic (1997) [25, 33-35] came up with the Delft model. This model assumes the packed column to be completely wetted so that the total liquid holdup is a product of specific surface area and the average liquid film thickness. The Delft model accounts for the variations in different packings by incorporating dimensions of the packing into the model. Similar to Delft model, Valenz (2010), Pondebat (1992), and Macias (1999) models were few other literature models which were relying on packing dimensions to account for variations in different packing. But often these dimensions are not reported by the packing manufacturers to protect their intellectual property. Apart from these popular models, Alix (2008), and Spiegel (1992) were

researchers who came up with an empirical model using experimental liquid holdup data. A full summary of these models is available in appendix A.

The performance of the literature liquid holdup models were evaluated using the literature experimental database assembled from the open literature (please refer Table 2.2 and Appendix A). The literature model performance was clearly limited by relying on packing specific constants and packing dimensions. In addition, literature models were not accounting for the liquid load effect at really high liquid load rates. These shortcomings of the literature models show a clear need of liquid holdup model in the preloading region developed using the packing geometric surface area and void fraction as the main model parameters.

2.2. Model Development

A counter current structured packed column operation can be classified into three regions of operation using two transition points (AA' and BB') (Fig. 2.1). These three different regions explain the change in hydrodynamic behavior of the column with increase in vapor and liquid flow rates. A more detailed discussion on the hydrodynamic behavior of the column at preloading was summarized below:

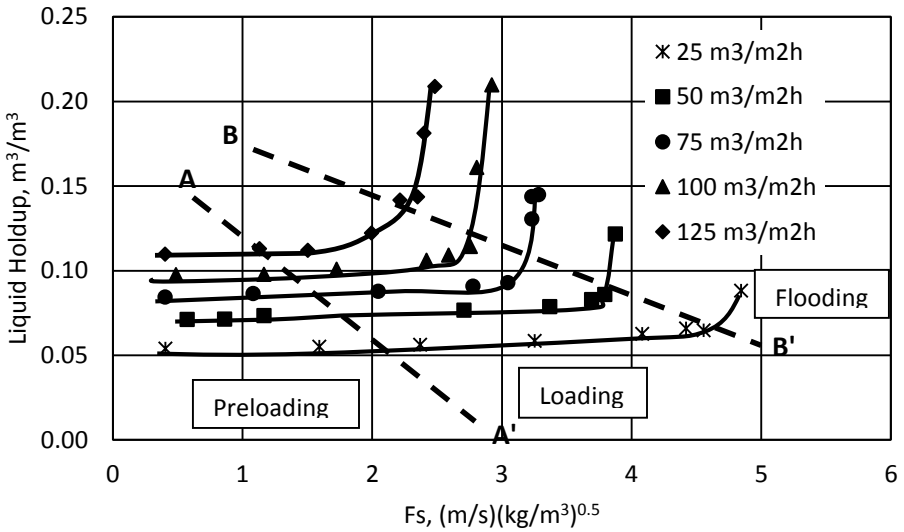

Figure 2.1. Experimental liquid holdup data in different regions of operation (Sulzer Mellpak 250X data at different liquid flow rates, air/water, 1 bar [31])

Preloading Region

In the preloading region, liquid flows freely onto the structured packing without any influence from the counter current vapor flow. Therefore, the liquid holdup is only a function of liquid film formed on the structured packing surface, which again is a function of liquid properties and the liquid flow behavior. Therefore, we hypothesized that identifying a good film thickness model which accounts for the variation in liquid properties and liquid flow behavior on a flat plate is necessary to develop a structured packing liquid holdup model in the preloading region. Also, flat plate can be correlated with structured packing, since the latter one is a collection of plates packed together to promote film flow.

Nusselt [36] film theory is the most popular model among the existing film thickness models. This model was developed based on the assumptions of laminar flow

and no wave formation on the film surface. The final form of the model is shown in equation 2.2

$$\delta = \left(\frac{3\mu_L^2 \, Re}{4 \, \rho^2 \, g \sin\theta} \right)^{\frac{1}{3}} \tag{2.2}$$

Zhou [37] and Lel [38] experimentally measured the thickness of the liquid film on a flat plate over a wide range of flow rates and showed that the experimental data agreed well with the performance of the Nusselt model at low liquid flow rates (i.e. in laminar region). However, the model underpredicts the film thickness at higher liquid flow rates (i.e. in turbulent region). Therefore, a modified form of Nusselt model was proposed by Zhou [37] and Lel [38], which has been estimating the film thickness over a wide range of flow rates without any underpredictions. The final form of the model proposed by Zhou and Lel is shown in equation 2.3.

$$\delta = C_1 \, Re^{C_2} \left(\frac{\mu_L^2}{\rho^2 \, g \sin\theta} \right)^{\frac{1}{3}} \tag{2.3}$$

Where $C_2 = 0.45$, calculated from experimental film thickness data, which shows the strong dependence of film thickness on the liquid flow rate.

$$Re = \frac{D \, \rho_L u_L}{\mu_L} \tag{2.4}$$

In the Reynolds number, term D corresponds to side dimension of the packing, which is not often disclosed by the packing manufacturers to protect their intellectual property. Compared to the packing dimensions (D), packing surface area (a), which can be calculated using equation 2.5, is readily available from the manufacturers. So in the present

study, packing dimension has been replaced with packing surface area (a) in the modified Reynolds number equation (Equation 2.6), which in turn modifies liquid film thickness model (Equation 2.7).

$$a = \frac{4\,s}{bh} \tag{2.5}$$

$$Re_{modified} = \frac{\rho_L u_L}{a\,\mu_L} \tag{2.6}$$

$$\delta = C_1\, Re_{modified}^{C_2} \left(\frac{\mu_L^2}{\rho^2\, g \sin\theta}\right)^{\frac{1}{3}} \tag{2.7}$$

To develop a new liquid holdup equation for the preloading region, the modified liquid film thickness model over a flat plate (Equation 2.7) was adopted to the structured packing by multiplying with packing surface area (a) and dividing with metal surface area ($1 - \varepsilon$') available for wetting to account for the entire structured packing area and void fraction, respectively. After including these terms, regressing the equation using experimental preloading liquid holdup data obtained from literature database gives the final liquid holdup model for the preloading region (Equation 2.8)

$$h_{L,preload} = 0.114\, \frac{a^{1.23}\, Re^{0.41}}{(1-\varepsilon)^{0.28}} \left(\frac{\mu_L^2}{\rho^2\, g \sin\theta}\right)^{\frac{1}{3}} \tag{2.8}$$

The different exponent of 0.41 for Reynolds number compared to the Zhou model can be attributed to the different form of Reynolds number used in the newly developed liquid holdup model.

From now onwards, the newly developed preloading liquid holdup model (equation 2.8) will be referred to as the "OkState preload model".

2.3. Literature Database

To validate the performance of the newly developed liquid holdup models along with other liquid holdup models available in the literature, a huge database of liquid holdup data was assembled from the open literature in all three regions of operation. Data collected from the literature was at atmospheric conditions with air/water as the test system, except in the case of Zakeri's [39] experimental data. In addition to the air/water system, Zakeri added 30 wt. % MEA and sucrose as additives to the air/water system to study the effect of viscosity on liquid holdup. The assembled database also consisted of a wide range of operating conditions with liquid velocities varying between 0.8 mm/s to 48.6 mm/s, vapor velocities varying between 0 m/s to 4.65 m/s, and viscosities varying between 1 cp to 12 cp.

The assembled database was divided into three sub databases depending on the source. Each sub database was briefly summarized below:

- Sulzer database was created using the experimental tests conducted on Mellapak packings at atmospheric pressure using the air/water test system in a 1 m diameter simulation column [31]. The obtained experimental data was used in developing the Suess and Spiegel empirical model [31].
- Delft database was obtained on Montz B1-250 packing tested using a 0.45 m diameter column [40]. This data was used in improving the performance of Delft and SRP models [40].

- Zakeri database was developed using Flexipac 2Y and Montz B1-250M packings using Air/Water, Air/Water/Sucrose, and Air/Water/MEA systems measured in a 0.5 m diameter column [39] to evaluate the effect of viscosity on liquid holdup.

The above three sub databases were further divided into three different regions of operation according to the flow behavior.

Region 1 (Preloading): Liquid holdup data does not change with increasing vapor flow rate

Region 2 (Loading) and region 3 (Flooding) data were omitted intentionally from the present article and will be presented in subsequent articles. Summary of the literature data at preloading region was presented in Table 2.1. Apart from the data summarized in Table 2.1, some more data [21] was collected from the literature and summarized in Appendix B. This data was omitted from the main work due to the lack of packing surface area information.

Table 2.1. Summary of the assembled literature database

Database	Packing	Packing area, m2/m3	Void fraction, ε	h, mm	b, mm	s, mm	Preloading Data Points	Diameter, m	System
TU Delft [40]	Montz B1-250.45	244	98.0	12.00	22.50	16.45	16	0.45	Air/Water
	Montz B1-250.60	245	97.8	12.00	22.30	16.45	17		
Sulzer [31]	Mellapak 250X	250	98.0	12.00	24.10	17.00	16	1.00	Air/Water
	Mellapak 250Y	250	97.5	11.94	24.13	17.00	18		
	Mellapak 500Y	500	97.5	6.53	9.60	8.10	17		
Zakeri [39]	Flexipac 2Y	223	98.9	NA	NA	NA	51	0.5	Air/Water
	Montz B1-250M	250	98.0	11.60	20.00	14.50	52		Air/Water/Sucrose
Total Points							187		Air/Water/MEA

Table 2.2. Performance summary of literature liquid holdup model predictions using literature experimental liquid holdup data in the preloading region

Database	Packing	Mean Absolute Relative Error, %								
		OkState Model (Eqn. 2.8)	Alix [41]	Billet [16]	Delft [33]	Mackowiak [42]	Spiegel [31]	SRP [21]	Stichlmair [43]	Valenz [44]
TU Delft [40]	Montz B1-250.45	**3.6**	11.0	NA	6.9	16.9	9.5	43.1	25.9	12.3
	Montz B1-250.60	**5.0**	16.8	NA	6.0	12.5	4.9	46.9	22.9	19.5
	Average Deviation	**4.3**	14.0	NA	6.4	14.6	7.1	45.1	24.4	16.0
Sulzer [31]	Mellapak 250X	**4.0**	28.4	NA	15.9	10.6	8.7	20.2	42.3	16.6
	Mellapak 250Y	**5.3**	14.1	15.8	15.2	7.1	6.1	27.5	23.3	40.5
	Mellapak 500Y	**6.2**	53.1	NA	17.0	26.2	8.8	40.4	27.8	46.5
	Average Deviation	**5.2**	31.6	NA	16.0	14.6	7.8	29.5	30.8	35.0
Zakeri [39]	Flexipac 2Y	**6.2**	30.6	NA	NA	29.1	17.9	NA	37.1	NA
	Montz B1-250M	7.3	32.8	NA	9.1	18.1	**7.0**	26.5	27.9	35.8
	Average Deviation	**6.8**	31.7	NA	NA	23.5	12.4	NA	32.5	NA

- Lowest error for each packing were bolded
- Billet model error was reported only for the packing with packing specific constants and the ones without them were written as NA
- For models requiring packing dimension information, error was displayed as NA when the packing dimension information was not available

$$MARE,\ \% = \frac{(Measured\ Holdup\ -\ Predicted\ Holdup)}{(Measured\ Holdup)}\ X\ 100$$

2.4. Results and Discussion

As discussed in section 2.1, preloading liquid holdup is a function of the liquid flow rate and liquid properties. So in the present paper, the performance of the new OkState preload model was evaluated for flow, property and geometry effects (Fig. 2.2, 4-6). Fig. 2.2 shows the parity plot of the OkState preload model in the preloading region. Out of the assembled 187 experimental data points, 90% of the points were between ±15% deviation lines. The mean absolute relative error (MARE) of the OkState preload model was 6% with a standard deviation of 6%. These results suggest that the newly developed model was accounting for the liquid flow rate effect on liquid holdup for a wide range of flow rates (Figs. 2.2). These results also proved that the liquid holdup is a function of liquid film formed on the structured packing. Therefore, employing a good liquid film thickness model improved the performance of liquid holdup model. These results proved the need for measuring the film thickness on a flat plate for systems other than air/water.

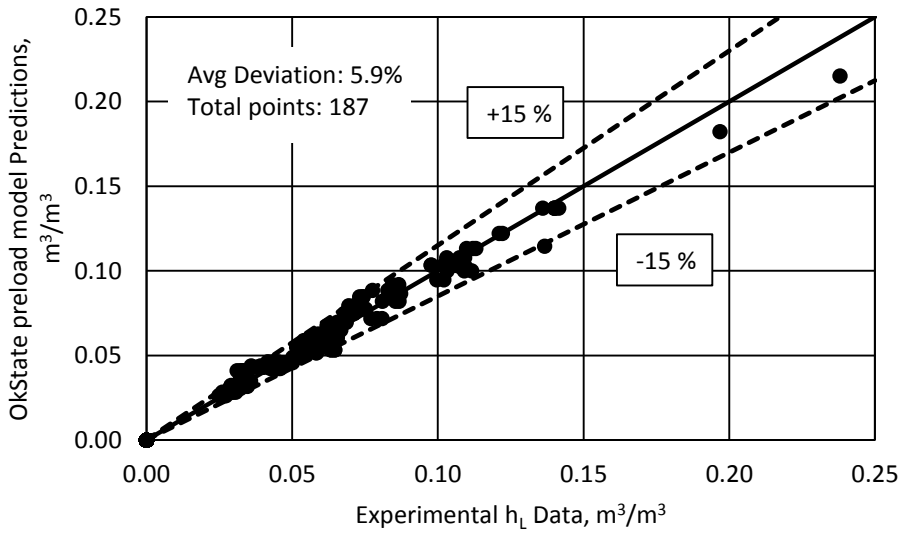

Figure 2.2. OkState preload model predictions vs experimental liquid holdup preloading data

As shown in Fig. 2.3, the Delft liquid holdup model developed based on Nusselt film theory was underpredicting the liquid holdup at high liquid flow rates (Note: typically low liquid holdup

values correspond to lower flow rates and high liquid holdup values correspond to higher liquid flow rates in the preloading region). These results were consitent with the results observed by Zhou [37] and Lel [38] for liquid film thickness model. Their results showed that Nusselt film theory model underpredicts the film thickness at high liquid flow rates.

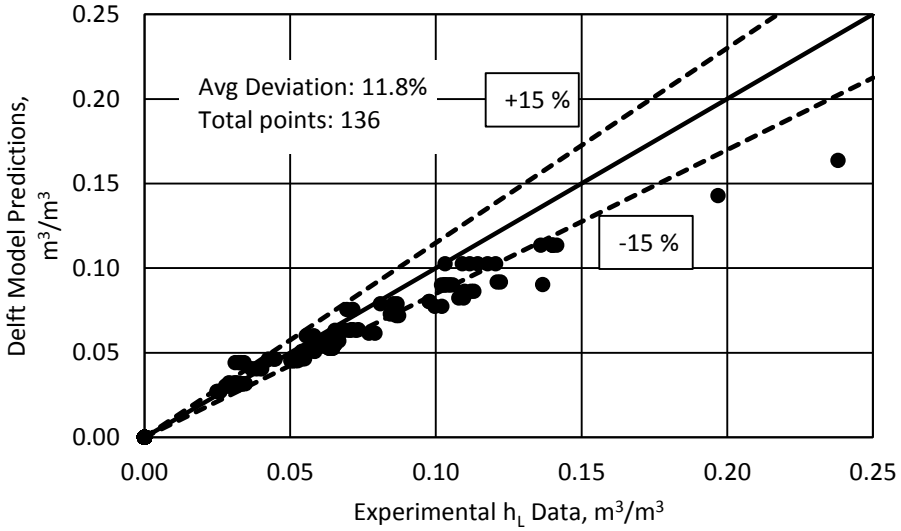

Figure 2.3. Delft preloading model predictions vs experimental liquid holdup preloading data

Average prediction error (MARE) of the newly developed OkState preload model and other literature models for different packings was summarized in Table 2.2. MARE of top performing model for each packing was bolded. Few literature models were omitted from Table 2.2 because of their overall MARE of greater than 30%, however, their parity plots were presented in Appendix A. Also, prediction errors for a few models were not reported either due to lack of packing specific constants (Billet) or packing dimensions (Delft, SRP, and Valenz). Apart from the packings listed in Table 2.1, prediction errors for packings lacking sufficient packing surface area information were attached in Appendix B. Parity plots for the models in Table 2.2 along with some other literature models were presented in Appendix A.

Fig. 2.4 shows the measured liquid holdup values of Mellapak 250X for the air/water system at various liquid flow rates. Liquid flow rates were varied from 25 to 125 m3/m2h. The results showed that with increasing liquid flow rate liquid film thickness increase, thereby increasing the liquid holdup. Moreover, the newly developed OkState preload model also behaved similar to the experimental results obtained at different flow rates.

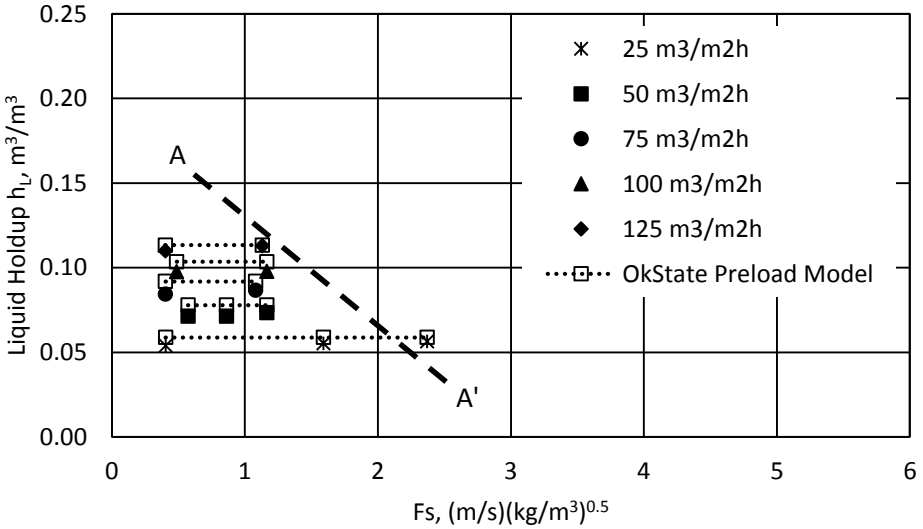

Figure 2.4. OkState preload model predictions over a wide liquid flow rates (Sulzer Mellpak 250X data at different liquid loads, air/water, 1 bar [31])

In addition to the liquid flow rate, viscosity also has a big impact on the liquid film thickness and liquid holdup [20]. Experimental liquid holdup results in the preloading region at different viscosities was plotted for the Montz B1-250M packing. Sucrose was used as an additive to vary the viscosity of the air/water test system. As shown in Fig. 2.5, the liquid holdup in the preloading region increases with increasing viscosity for the experimental results and for the newly developed OkState model. Therefore, the OkState preload model was properly accounting for the effect of viscosity on the liquid holdup in a sheet metal structured packing.

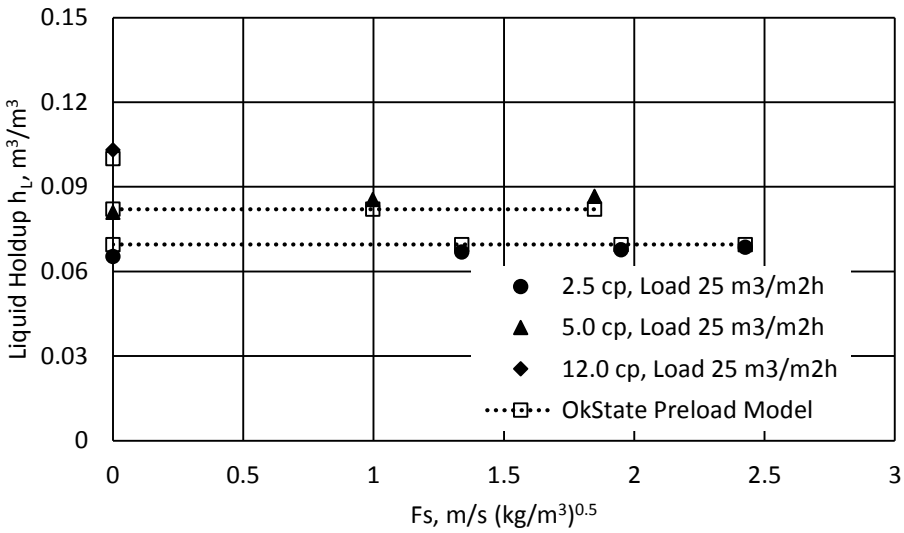

Fig. 2.5. OkState preload model predictions vs experimental liquid holdup preloading data obtained for different viscosities (Montz B1-250M, air/water, 1 bar [39])

In order to study the effect of packing geometry and the corrugation angle on the liquid holdup, experimental liquid holdup results obtained by utilizing different packings 250Y, 250X and 500Y using the air/water test system for different liquid flow rates were plotted. The packings 250Y and 500Y have different packing surface areas, and the effect of each surface area on the liquid holdup can be observed from the plot (Fig. 2.6). At the same liquid flow rate, the liquid holdup is directly proportional to the packing surface area. The newly developed OkState preload model showed the same performance as experimental results.

In addition to the area effect, the effect of corrugation angle on the liquid holdup was studied using Figs. 2.4 and 2.6. From the literature experimental data which was obtained from a few types of packing, the effect of corrugation angle on the liquid holdup was not significant. So there is no need of additional corrugation angle term in the newly developed OkState preload model and the new model is following the trend of both 250Y and 250X packings.

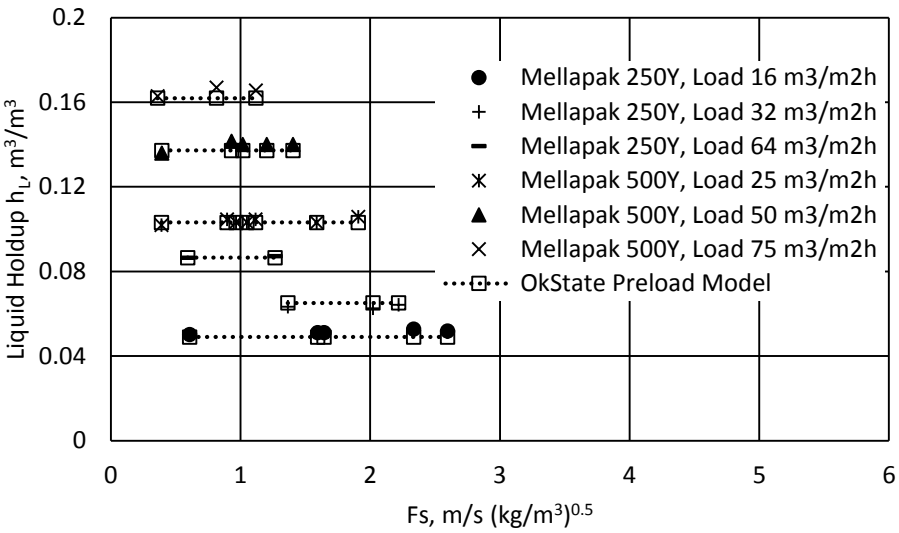

Fig. 2.6. OkState preload model predictions vs experimental liquid holdup data obtained using different packing areas at various load rates (Mellapak 250Y and 500Y, air/water, 1 bar [31])

Overall, the newly developed OkState preload model is accounting for the effect of liquid flow rate, liquid properties and packing geometry on the liquid holdup and capturing the experimental data behavior.

2.5. Conclusion

New OkState preloading and loading models were developed using packing surface area and void fraction as the main parameters, instead of relying on any packing dimensions or packing specific constants. Performance of the newly developed OkState models and other literature models were quantified using experimental liquid holdup data assembled from the literature. Newly developed liquid holdup models are capturing the effects of liquid flow rate, liquid properties, and packing geometry variations on liquid holdup.

All the available literature experimental data is for the air/water system which limits our understanding of liquid holdup behavior for other systems.

Acknowledgement:

We would like to thank Sravanthi Vupputuri, for her help in completing the present work and in preparing the manuscript.

We would also like to thank Dr. Tony Cai and Mike Resetarits from FRI, for their financial support and supervision for part of this work.

Example Problem:

1. An air/water column is being operated at atmospheric conditions using Mellapak 250Y. Please calculate the preloading liquid holdup when the column has a constant liquid flow rate of 32 m^3/m^2h and vapor flow rates of 1.95 m/s. Please use properties below for the calculations:

Water Density	=	1000 kg/m^3
Water Viscosity	=	1 cp
Air Density	=	1.3 kg/m^3
Packing Area (a)	=	250 m^2/m^3
Void fraction (ε)	=	97.5 m^3/m^3
Corrugation angle	=	45

Ans: Given, Liquid velocity U_L = 0.0089 m /s

- At U_G = 1.95 m/s

  From eqn. 2.6,

$$Re = \frac{1000\frac{kg}{m^3} \times 0.0089\frac{m}{s}}{250\frac{m^2}{m^3} \times \left(\frac{1}{1000}\right) Pa\ s} = 35.6$$

$$h_{L,preload} = 0.114\ \frac{250^{1.23}\ 35.6^{0.41}}{(1\text{- }(97.5/100))^{0.28}} \left(\frac{\left(\frac{1}{1000}\right)^2}{1000^2 \times 9.81 \times \sin 45} \right)^{1/3}$$

$= 0.0647\ m^3/m^3$

Actual experimental liquid holdup = $0.0642\ m^3/m^3$

Error, % = $abs\left(\frac{0.0647-0.0642}{0.0642}\right) \times 100 = 0.7\%$

Note: In OkState preload model, if the exponent of the viscosity term $\left[\left(\frac{\mu_L^2}{\rho^2\, g \sin\theta}\right)^{\frac{1}{3}}\right]$ is approximated as 0.33 instead of (1/3), it reduces the overall performance.

CHAPTER III

3. DEVELOPMENT AND EVALUATION OF LIQUID HOLDUP AND LOAD POINT MODELS IN LOADING REGION FOR A SHEET METAL STRUCTURED PACKING. PART II

Abstract:

Model development for a loading region is a difficult process because of complex vapor and liquid flow behaviors compared to preloading and flooding regions. Therefore, only a few loading region models were available in literature to estimate liquid holdup and load point. Also, the available models were developed with few experimental data points at limited operating conditions, thereby affecting their performance. So in the present study, the performance of the literature models was validated using 181 experimental liquid holdup and load point data points obtained from the open literature over a wide range of operating conditions. The results showed that the literature models were not properly accounting for the effect of different thermodynamic and geometrical properties on liquid holdup and load point. Therefore, new models were developed to estimate the liquid holdup and load point in the loading region of a sheet metal structured packed column. The newly developed models were verified using a wide range of experimental database gathered for different systems. The mean relative error of model predictions with experimental data for liquid holdup and load point was less than 10% and 20%, respectively. In addition, the new models require readily available packing geometrical area and void fraction for model predictions instead of

confidential packing specific constants or packing crimp dimensions. This criterion of newly developed models makes them easy to use with new packings.

3.1. Introduction

Structured packing is one of the popular internal among different distillation internals because of its higher mass transfer efficiency and low pressure drop [2, 23, 27-29]. However, there is less amount of experimental data and model development work available in the literature for structured packings compared to trays [2]. Especially there are no models available to account for the liquid holdup in the loading region of a structured packed column. This may be either due to the operation of all columns typically in the preloading region or complexity to operate in the loading region. Unlike the preloading region, in the loading region liquid holdup is affected by both liquid and vapor properties as well as their respective flow rates. Very few researchers have accounted for the effect of counter current gas on liquid flow while developing the liquid holdup model for structured packing [23] or liquid film thickness model for flat plate [45, 46] in the loading region. However, developing a good liquid holdup model in the loading region will aid in improving the performance of pressure drop and other model predictions. Apart from model development, a thorough understanding of high mass transfer efficiency in the loading region will aid in developing new packings and improving the design of the column.

When the operating column transitions from preloading to the loading region, vapor flow rate starts to influence the liquid film formed over the packing. The point where this transition occurs is the loading point and this point will be denoted by $u_{G,Load\ point}$ (AA' in Fig. 3.1). The $u_{G,Load\ point}$ can be defined as the critical point at which the vapor kinetic energy is sufficient to destabilize the liquid film and influence the liquid flow.

The characteristics listed below can be used to identify the load point:

- sudden increase in mass transfer efficiency due to liquid back mixing
- higher liquid holdup which in turn causes higher pressure drop

Load point from experimental liquid holdup and pressure drop data can be observed in Figs. 3.1 and 3.2. These plots show the experimental liquid holdup and pressure drop data of Mellapak 250X and Montz B1-400 packings respectively. From Figs. 3.1 and 3.2, a clear counter current vapor flow effect on both liquid holdup and pressure drop can be observed. However, it is difficult to identify the exact location of load point from the limited literature experimental data, so a shaded region (AA'BB') was shown in the figures to show the approximate region with the loading point.

Verschoof (1999) [40] was the only researcher who developed a model to identify the load point. However the major drawbacks of his model was its small experimental database used for model development and the model requirement of packing crimp dimensions for model predictions. Therefore, when the performance of this model was evaluated using the assembled experimental database, the model performance was not satisfactory (Appendix E). Other researchers, like Mackowiak [23], used a constant fraction of flood point to define the load point. However, this is not a proper way to identify and calculate the load point. Similar to flood point, a good model to identify load point is necessary to account for the effect of liquid properties and liquid load.

In addition to the load point model, liquid holdup models were also limited in the loading region. Billet (1999) [16], Mackowiak (1991) [42], and SRP (1993) [21] were some researchers who tried to predict the liquid holdup in the load region. However, when the performance of these models were evaluated using the assembled experimental database, none of the literature models were capturing the increasing liquid holdup trend observed in the loading region (Fig. 3.1)

(Appendix D). A new liquid holdup model capturing this increasing trend will help in improving the predictions of pressure drop in the loading region because liquid holdup effects the pressure drop of the column.

From the above results and observations, there is a clear need of modeling efforts for sheet metal structured packing in the loading region. In the present work, a new liquid holdup and load point models in the loading region were developed.

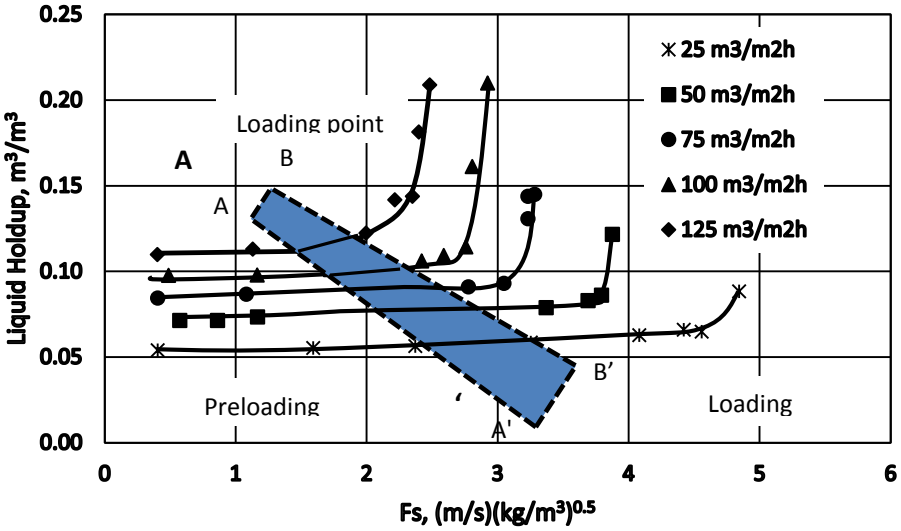

Fig. 3.1. Experimental liquid holdup as a function of gas rate and different liquid flow rates showing different regions of operation and an approximated load point region (Sulzer Mellpak 250X data at different liquid flow rates [31], air/water, 1 bar)

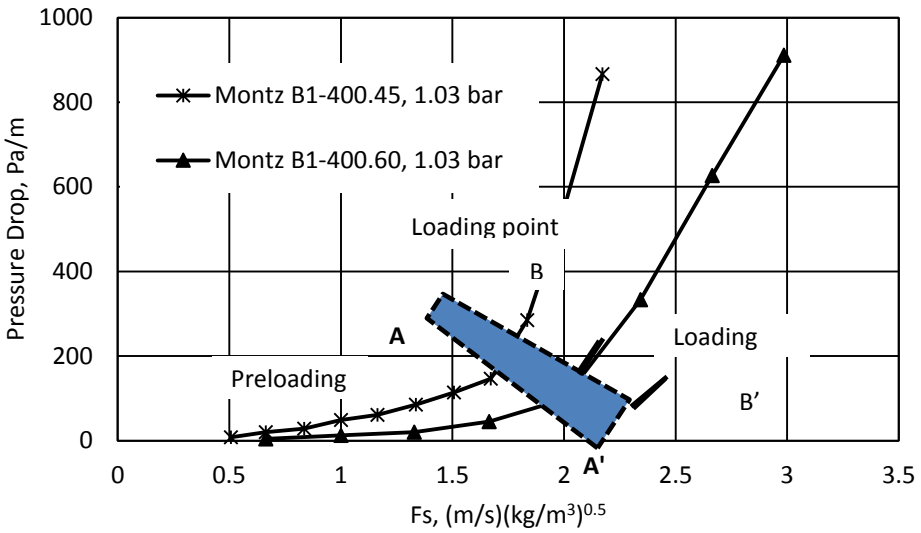

Fig. 3.2. Experimental pressure drop data as a function of gas rate and corrugation angle showing different regions of operation and an approximated load point region (Montz B1-400.45 and B1-400.60, C6/C7 [47], 1.03 bar, total reflux run)

3.2. Model Development

As explained earlier, a counter current structured packed column operation can be classified into preloading and loading regions of operation using the loading point (AA'BB'). In the present article the emphasis was given to develop load point and liquid holdup models in the loading region:

3.2.1. Loading Region

Based on the definition of load point, the kinetic energy at load point will be calculated as [21],

$$Vapor\ kinetic\ energy_{Load\ point} = \left(\frac{u_{G,Load\ point}}{\varepsilon \left(1 - h_{L,pre}\right) \sin\theta} \sqrt{\rho_G} \right)^2 \tag{3.1}$$

After the load point, the additional kinetic energy, $Vapor\ kinetic\ energy_{Operating\ point} - Vapor\ kinetic\ energy_{Load\ point}$, generated due to the increased vapor flow supports the destabilized liquid film and starts to load the column. Since the additional kinetic energy starts loading the column with liquid, this region is called the "loading region" [2]. So for the newly developed liquid holdup model in the loading region, the additional kinetic energy that is supporting the weight of the liquid can be calculated using the equation below.

$$Additional\ Kinetic\ Energy = \left[\left(\frac{u_G}{\varepsilon\,(1-h_{L,load})\sin\theta}\ \sqrt{\rho_G} \right)^{1+\frac{h_{L,load}}{h_{L,pre}}} - \left(\frac{u_{G,Load\ point}}{\varepsilon\,(1-h_{L,pre})\sin\theta}\ \sqrt{\rho_G} \right)^{2} \right] \tag{3.2}$$

In equation 3.2, the first term calculates the kinetic energy at the operating point**,** accounting for the liquid holdup effect on vapor flow [21]. The second term (equation 3.1) calculates the kinetic energy continuously utilized to break the newly formed film due to the continuous liquid flowing down the column.

As discussed earlier, vapor kinetic energy affects the flow of liquid and liquid accumulation on the packing. So in the loading region, in addition to the preloading liquid hold-up due to the flow of liquid, additional liquid is pushed back and being supported by the kinetic energy of the vapor flow. In order to calculate the total liquid holdup in the loading region, the additional kinetic energy (Equation 3.2) will be multiplied by kinetic energy of the liquid spread on the packing surface area (a) and then added to the preloading

liquid holdup. Leading constant and exponents of packing surface area and kinetic energy of the liquid were regressed to obtain the final liquid holdup loading model (Equation 3.3).

$$h_{L,load} = h_{L,pre} + (1.68\ 10^{-6})\left(u_L\sqrt{\rho_L}\right)^{0.671}(a)^{1.15}\left[\left(\frac{u_G}{\varepsilon\left(1-h_{L,load}\right)\sin\theta}\sqrt{\rho_G}\right)^{1+\frac{h_{L,load}}{h_{L,pre}}} - \left(\frac{u_{G,Load\ point}}{\varepsilon\left(1-h_{L,pre}\right)\sin\theta}\sqrt{\rho_G}\right)^{2}\right] \quad (3.3)$$

Terms in the above equation were summarized below,

$h_{L,pre}$ = Preloading liquid holdup calculated using OkState preload liquid holdup model or from experimental data

$\left(u_L\sqrt{\rho_L}\right)^c$ = Liquid kinetic energy distributed over the packing surface area 'a', opposite to vapor flow and also contributing to the additional film formation on the packing

$(a)^c$ = Packing surface area affecting both vapor and liquid flows

Equation 3.3, is an implicit equation of liquid holdup because both vapor flow and kinetic energy terms are a function of liquid holdup at operating conditions. The only information lacking for solving equation 3.3 is the $u_{G,Load\ point}$, which can be obtained either using experimental data (present case) or a model [40]. Therefore, a new model to estimate $u_{G,Load\ point}$ point was presented below, which will be very useful for the liquid holdup loading model calculations and in identifying the loading point for any column operation.

The newly developed liquid holdup loading model (equation 3.3) will be referred to as the "OkState liquid holdup load model" in this article.

3.2.1.1. Algorithm to solve the OkState liquid holdup load model in the loading region

- Rearrange equation 3.3 into the form below

$$\left\{h_{L,pre} + (1.68\ 10^{-6})\left(u_1\sqrt{\rho_L}\right)^{0.671}(a)^{1.15}\left[\left(\frac{u_G}{\varepsilon\left(1-h_{L,load}\right)\sin\theta}\sqrt{\rho_G}\right)^{1+\frac{h_{L,load}}{h_{L,pre}}} - \left(\frac{u_{G,Load\ point}}{\varepsilon\left(1-h_{L,pre}\right)\sin\theta}\sqrt{\rho_G}\right)^2\right]\right\} - h_{L,load} = 0 \quad (3.4)$$

- Take $h_{L,pre}$ as initial guess for $h_{L,load}$
- Solve equation 3.4 with any line search optimization algorithm such as Golden Section with a constraint of $h_{L,load} > h_{L,pre}$

3.2.2. Load Point model

Identification of load point is important to understand the region of operation in distillation column. Further, OkState liquid holdup load model predictions were depended on the load point (Equation 3.3). Load point is defined as a point at which vapor kinetic energy is equal to the liquid film destabilization force. However, there were no models available in the literature to estimate the liquid film destabilization force as it was impossible to measure such force. In order to overcome this obstacle, important parameters which might have an

effect on the liquid film destabilization force were grouped together to obtain a destabilization force model. The final form of the liquid film destabilization force model is presented below,

$$F_{destabilization} = C_1 \frac{\sigma^{C_2}\, h_{L,pre}^{C_5}\, \mu_L^{C_6}}{\varepsilon^{C_5}\, a^{C_4} \left(u_L \sqrt{\rho_L}\right)^{C_4}} \tag{3.5}$$

According to load point definition, the destabilization force (equation 3.5) is equal to the vapor kinetic energy. Therefore

$$U_G^2\, \rho_G = C_1 \frac{\sigma^{C_2}\, h_{L,pre}^{C_5}\, \mu_L^{C_6}}{\varepsilon^{C_5}\, a^{C_4} \left(u_L \sqrt{\rho_L}\right)^{C_4}} \tag{3.6}$$

However, the vapor velocity is a function of the liquid holdup present in the column. The vapor velocity (U_G), can be calculated using equation 3.7.

$$U_G = \frac{u_g}{\varepsilon\left(1 - h_{L.pre}\right) \sin\theta} \tag{3.7}$$

Substituting equation 3.7 into equation 3.6 and rearranging, the final expression for the load point is

$$u_{g,load\ point} = \left[C_1 \frac{\sigma^{C_2}\, \mu_L^{C_6} d_e^{C_5}}{\left(u_L \sqrt{\rho_L}\right)^{C_4}}\, h_{L,pre}^{C_5} \frac{\left(1 - h_{L,pre}\right)^6 \sin^{C_7}\theta}{\rho_G} \right]^{\frac{1}{2}} \tag{3.8}$$

The constants C_1-C_7 were obtained by regressing the model equation with the literature experimental data. The final model equation with the obtained constants is presented below,

$$u_{g,load\ point} = \left[64.6 \frac{\sigma^{0.5}\, d_e}{\mu_L^{0.5} \left(u_L \sqrt{\rho_L}\right)^{0.5}}\, h_{L,pre}^{0.3} \frac{\left(1 - h_{L,pre}\right)^6 \sin^{0.6}\theta}{\rho_G} \right]^{\frac{1}{2}} \quad (3.9)$$

Henceforth, the new load point model will be referred as "OkState Load point model".

3.3. Literature Database

3.3.1. Liquid holdup database

To validate the performance of OkState liquid holdup load model and to compare with available literature liquid holdup models a huge database of liquid holdup experimental data was assembled from the open literature in all three regions of operation. However, the data gathered from loading region was only presented in the present article. A more detail discussion on the preloading and flooding region experimental data can be obtained from our earlier articles [48, 49].

In the current work, the database was divided into three sub categories based on the source of availability. All the literature experimental data gathered in this study was obtained using an air/water test system. However, the data gathered from Zakeri [39] used sucrose and MEA to modify the viscosity of the air/water test system between 1cp to 12 cp. In addition to data obtained at different viscosities, the literature database also consists of experimental liquid holdup data obtained at different vapor and liquid flow rates. A summary of the experimental database was presented in Table 3.2.

3.3.2. Load point database

A wide database of load point experimental data was obtained from the experimental liquid holdup and pressure drop test data from the open literature. A more detailed discussion about these liquid holdup and pressure drop databases can be found in our earlier articles [50, 51]. In addition to air/water test system, load point database also consisted of cyclohexane/n-heptane, cholorbenzene/ethylbenzene, and iso-octane/toluene test systems. A brief summary of the load point database was presented in Table 3.1.

Table 3.1. Variable ranges summarizing the load point database

Variable	**Range**
Operating pressure (bar)	0.033 − 4.14
Liquid density (kg/m^3)	561 − 1850
Vapor density(kg/m^3)	0.14 − 13.14
Liquid velocity (m/s)	0.0008 − 0.049
Vapor velocity (m/s)	0.39 − 9.6
Liquid viscosity (Pa.s)	0.0001 − 0.0012
Vapor viscosity (Pa.s)	0.000006 − 0.000181
Surface tension (N/m)	0.08 − 0.725

Apart from the data summarized in tables 3.1, 3.2 and 3.3, some experimental data lacking sufficient packing geometric information was obtained from the literature. However, these data were not utilized for model development and was summarized in Appendix F.

Table 3.2. Summary of the assembled literature database

Database	Packing	Packing area, m^2/m^3	Void fraction, ε	h, mm	b, mm	s, mm	Loading	Diameter, m	System
TU Delft [40]	Montz B1-250.45	244	98.0	12.00	22.50	16.45	11	0.45	Air/Water
	Montz B1-250.60	245	97.8	12.00	22.30	16.45	10		
Sulzer [31]	Mellapak 250X	250	98.0	12.00	24.10	17.00	22	1.00	Air/Water
	Mellapak 250Y	250	97.5	11.94	24.13	17.00	28		
	Mellapak 500Y	500	97.5	6.53	9.60	8.10	9		
Zakeri [39]	Flexipac 2Y	223	98.9	NA	NA	NA	49	0.5	Air/Water Air/Water/Sucrose Air/Water/MEA
	Montz B1-250M	250	98.0	11.60	20.00	14.50	52		
Total Points							181		

Table 3.3. Summary of OkState liquid holdup load model and other literature liquid holdup model predictions using literature experimental liquid holdup data in loading region

Database	Packing	Mean Absolute Relative Error, %				
		OkState Liquid Holdup Load Model (Eqn. 3.3)		SRP [21]	Mackowiak [42]	Gualito [52]
		Using Preloading Model Predictions	Using Experimental Preloading Data			
TU Delft [40]	Montz B1-250.45	17.8	**12.1**	48.0	45.4	44.6
	Montz B1-250.60	14.7	**13.7**	49.0	41.3	50.2
	Average Deviation	16.3	**12.8**	48.5	43.5	47.3
Sulzer [31]	Mellapak 250X	8.3	**7.1**	21.6	44.3	25.9
	Mellapak 250Y	11.3	**5.1**	27.9	48.4	31.5
	Mellapak 500Y	6.3	**2.8**	38.7	47.4	45.4
	Average Deviation	9.4	**5.5**	27.2	46.7	31.5
Zakeri [39]	Flexipac 2Y	6.1	**1.9**	NA	45.8	NA
	Montz B1-250M	7.0	**2.6**	27.4	37.9	25.7
	Average Deviation	6.6	**2.2**	NA	41.7	NA

- Lowest error for each packing were bolded
- For models requiring packing dimension information, error was displayed as NA where the packing dimension information is not available

$$MARE,\ \% = \frac{(Measured\ Holdup\ -\ Predicted\ Holdup)}{(Measured\ Holdup)}\ X\ 100$$

3.4. Results and Discussion

3.4.1. Loading Model

The performance of the OkState liquid holdup load model along with other literature liquid holdup load models using experimental liquid holdup loading data were summarized in Table 3.3. In addition, the best performed model was bolded for each packing. In the table, a few model mean absolute relative errors (MARE) were reported as 'NA' due to lack of necessary packing dimension information for model predictions.

Figs. 3.3 and 3.4 show the parity plots of the OkState liquid holdup load model in the loading region. To calculate the liquid holdup in the loading region, liquid holdup in the preloading region (hl preload term in equation 3.3) has to be calculated first. Preloading liquid holdup can be obtained in two ways, either by using the newly developed OkState liquid holdup preload model or by using experimental liquid holdup preloading data. In Figure 3.3, the liquid holdup in the loading region was calculated using the newly developed OkState liquid holdup preload model. The OkState liquid holdup load model predictions have an overall MARE of 8.7% with a standard deviation of 7.4% (Fig. 3.3). More than 85% of the 181 experimental data points fell between the ± 15 % deviation lines. In figure 3.4, the loading region liquid holdup was calculated using experimental liquid holdup preloading data. Incorporating preloading experimental data instead of the OkState liquid holdup preload model, further reduced the error by 4.2% (i.e. from 8.7 % to 4.5%). Also, 95% of 181 experimental data points fell in between the ± 15% deviation lines compared to 85% data points in the case of the OkState liquid holdup load model predictions obtained using the OkState liquid holdup preload model. These results clearly demonstrated the advantage of using experimental liquid holdup preloading data compared to the OkState liquid

holdup preload model. Therefore it is advised to use experimental preloading data, where available, in the OkState liquid holdup load model to significantly improve the overall performance.

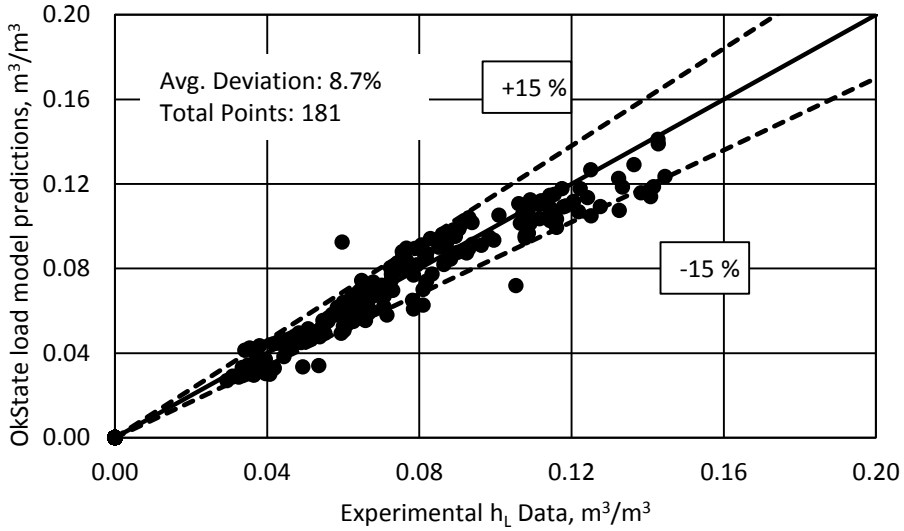

Fig. 3.3. OkState liquid holdup load model (eqn. 3.3) predictions obtained using OkState liquid holdup preload model vs experimental liquid holdup loading data

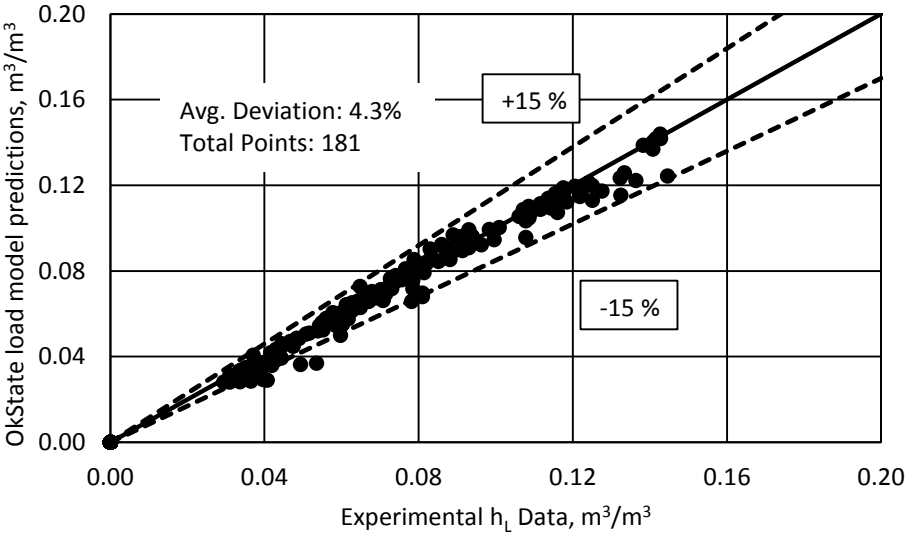

Fig 3.4. OkState liquid holdup load model (eqn. 3.3) predictions obtained using experimental liquid holdup preloading data vs experimental liquid holdup loading data

In Fig. 3.3 and 3.4, loading model predictions were shown deviating at higher liquid holdup values. This is because at this point the column is moving into the flooding region, and it is difficult to clearly differentiate the points in the loading region or flooding region. At higher liquid holdup values, where the operation of the column was moving from the loading region to the flooding region, loading model predictions were under predicting (Figs. 3.3 and 3.4).

Loading and preloading region liquid holdup experimental results were plotted for Montz B1-250M packing using the air/water/MEA system at 25 m^3/m^2hr liquid rate and 2.5 cp viscosity in Fig. 3.5. The plot shows the increase in liquid holdup with increase in vapor flow rate after the load point for both experimental data and the newly developed OkState liquid holdup load model predictions. The observed offset (consistent deviation) of the OkState liquid holdup load model predictions from experimental data in the loading region was due to the usage of the newly developed OkState liquid holdup preload model while calculating the liquid holdup in the loading region, thereby transferring the error of the OkState liquid holdup preload model into the OkState liquid holdup load model. Fig. 3.5 was reproduced using experimental preloading data while calculating the liquid holdup in the loading region (Fig. 3.6). Utilization of experimental data nullified the offset between experimental data and OkState liquid holdup load model predictions in the loading region.

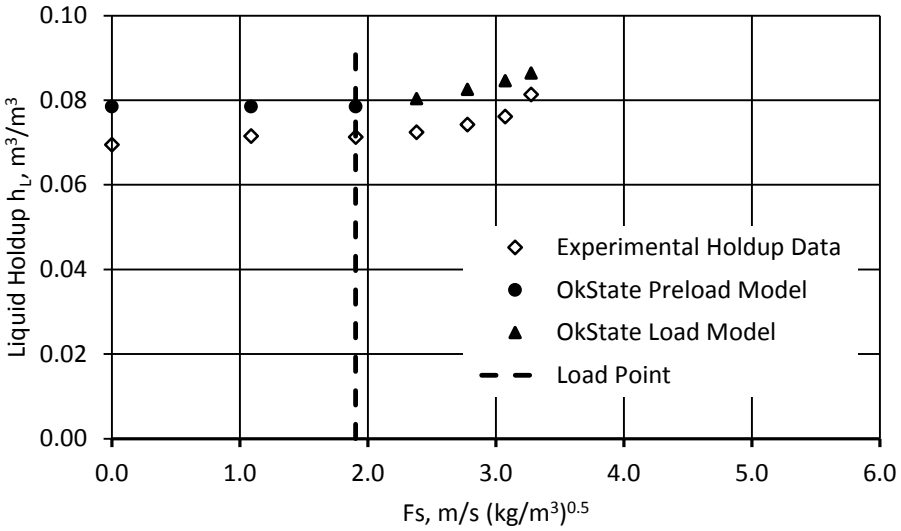

Fig. 3.5. OkState liquid holdup load model (eqn. 3.11) predictions obtained using OkState liquid holdup preload model for Montz B1-250M packing using air/water/MEA at 1 bar, 2.5 cp, and 25 m^3/m^2h [39]

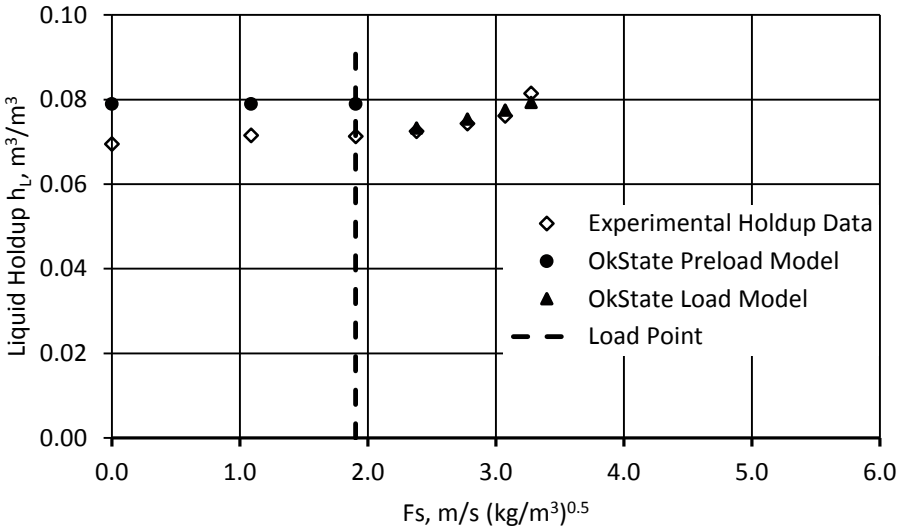

Fig. 3.6. OkState liquid holdup load model (eqn. 3.11) predictions obtained using experimental liquid holdup preloading data for Montz B1-250M packing using air/water/MEA at 1 bar, 2.5 cp, and 25 m^3/m2h [39]

Similar to the preloading model, the performance of the loading model was also evaluated for viscosity and liquid load effect. Loading region experimental holdup data was plotted for

Montz B1-250M packing using the air/water system at viscosities 2.5 cp, 5.0 cp, and 12.0 cp (Fig. 3.7). Similar to the results observed in the preloading region, liquid holdup increases with increasing the viscosity in the loading region (Fig. 3.7). Moreover, the loading region liquid holdup model predictions calculated using experimental preloading data does a better job in reducing the offset compared to the OkState liquid holdup load model predictions calculated using the preloading model.

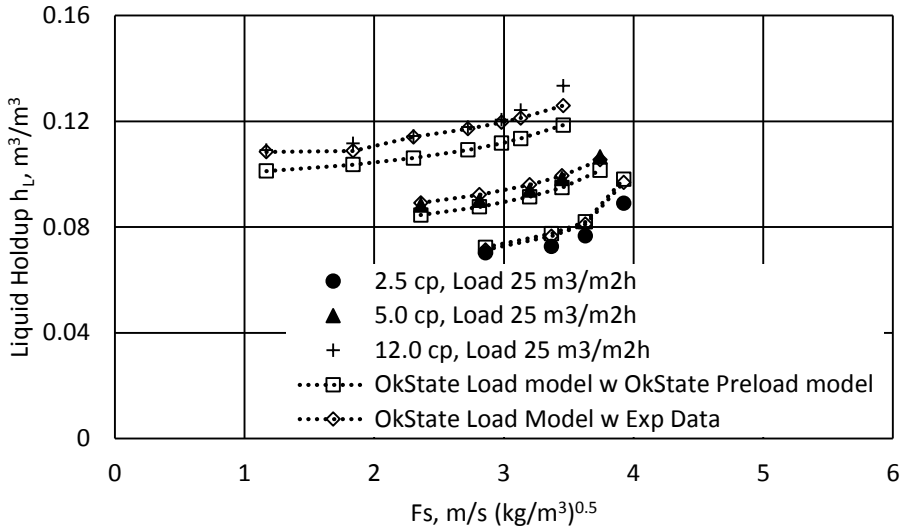

Fig. 3.7. OkState liquid holdup load model predictions vs experimental liquid holdup data obtained for different viscosities in loading region (Montz B1-250M data, 1 bar pressure, air/water [39])

In Fig. 3.8, effect of liquid flow rate on liquid holdup in the loading region was evaluated using Mellapak 250X packing experimental liquid holdup data for the air/water test system. Similar to earlier observations, the OkState liquid holdup load model predictions calculated using experimental liquid holdup preloading data were closer to experimental holdup data in the loading region. Experimental data for additional packings is necessary to study the corrugation angle and packing area effect in the loading region.

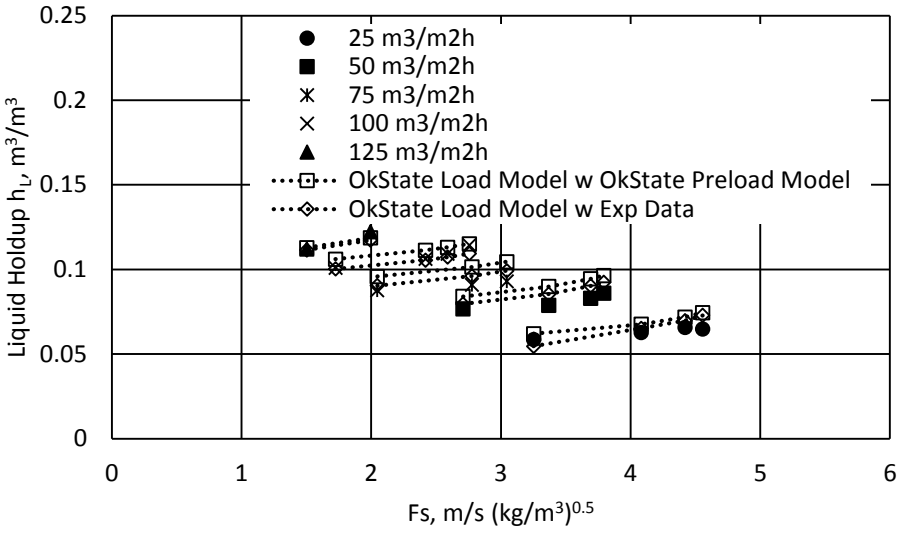

Fig 3.8. OkState liquid holdup load model predictions over a wide liquid flow rates (Sulzer Mellpak 250X data at different liquid loads [31], air/water, 1 bar pressure)

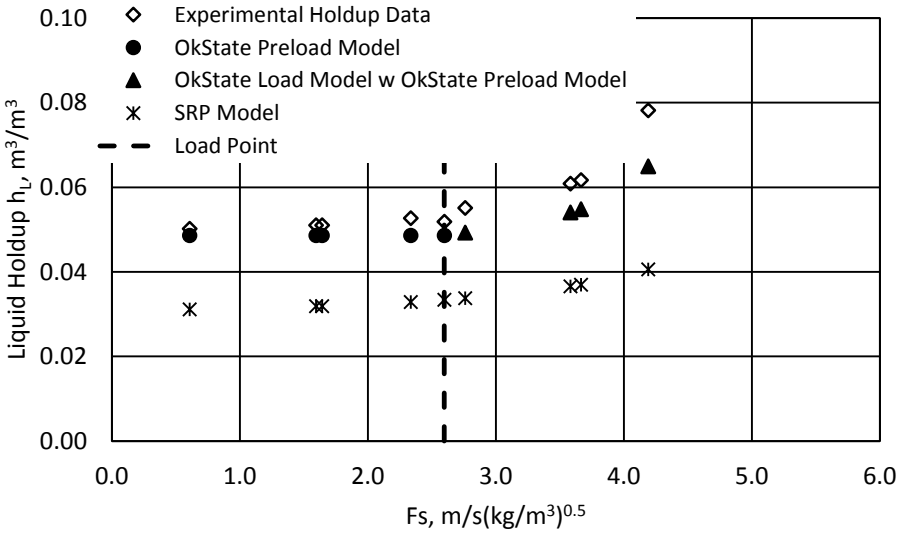

Fig 3.9. Experimental liquid holdup data for Mellapak 250Y and SRP [21] and Okstate model predictions (Mellapak 250Y, liquid load rate 16 m^3/m^2h, air/water, 1 bar pressure)

Fig 3.9 shows the experimental liquid holdup data for Mellapak 250Y packing tested at atmospheric conditions using an air/water test system. The data was collected at a liquid

load rate of 16 m^3/m^3h. As can be observed from the figure, the predictions of the new OkState liquid holdup load model using the OkState liquid holdup preload model were doing a much better job in capturing the increasing experimental liquid holdup trend compared to the SRP model. In addition, the SRP model predictions were showing a constant offset with the experimental data.

Overall, the new OkState liquid holdup load model captures the effect of vapor flow rate on liquid holdup for many different packings under different operating conditions better than any other literature model (Appendix C & D). However, since all the available literature data was for an air/water system, this was limiting further improvement of the model. Therefore, obtaining some additional experimental data for other systems will help in understanding the vapor viscosity effect on the loading region, as well as improving the currently developed model further. Apart from vapor viscosity, liquid surface tension of a system might also have an effect on liquid holdup. However, current literature data is not sufficient to identify this effect.

3.4.2. Loading point model

The performance of the OkState load point model can be observed from the parity plot (Fig. 3.10) (Appendix G). The graph showed that the model has a MARE of 18% with a standard deviation of 17.2%. The MARE was calculated using equation 3.10. However, the calculated error was not true value due to the lack of exact experimental load point.

$$MARE,\ \% = \frac{(Measured\ load\ point\ - Predicted\ load\ point)}{(Measured\ load\ point)}\ X\ 100 \qquad (3.10)$$

The identification of exact experimental load point was difficult due to the discrete experimental data. In addition to that, the conservative model predictions were showing higher MARE than expected in the parity plot. Therefore, to properly evaluate the performance of the OkState load point model, individual plots were created for different types of structured packings. These plots will help to identify the load point over the operating region, making it easy to evaluate the performance of the OkState load point model in capturing the effect of packing and property variations.

Experimental liquid holdup data collected by Sulzer at atmospheric conditions for Mellapak 250X packing was plotted in Fig. 3.11. The data was obtained for air/water test system at different liquid load rates. The load points obtained by OkState load point model predictions at different liquid load rates were also plotted in Fig. 3.11. The results showed an increase in load point with decreasing flow rate, which was expected for liquid load point. In addition, the model predictions were conservative, as explained earlier.

Fig. 3.12 shows the experimental pressure drop data for Montz B1-400.45 and B1-400.60 packings tested at 1.03 bar pressure using the C6/C7 test system under total reflux conditions. Similar to Fig. 3.11, the OkState load point model predictions were conservative compared to the experimental data. In addition, the new model was successfully capturing the effect of corrugation angle on the load point. Fig. 3.12 shows that the OkState model predicted the load point at slightly higher vapor velocity for 60° packing compared to 45° packing. This behavior was consistent with the behavior observed from experimental data.

In addition to the effect of corrugation angle and packing geometric area, the effect of viscosity on load point was also evaluated (Fig. 3.13). Experimental load point data obtained from Montz B1-250M packing at different viscosities using an air/water test system under atmospheric

conditions was plotted in Fig. 3.13. The load point was at lower vapor velocities for higher viscosity systems compared to the lower viscosity systems. The new OkState load point model can be seen following the same trend as experimental data.

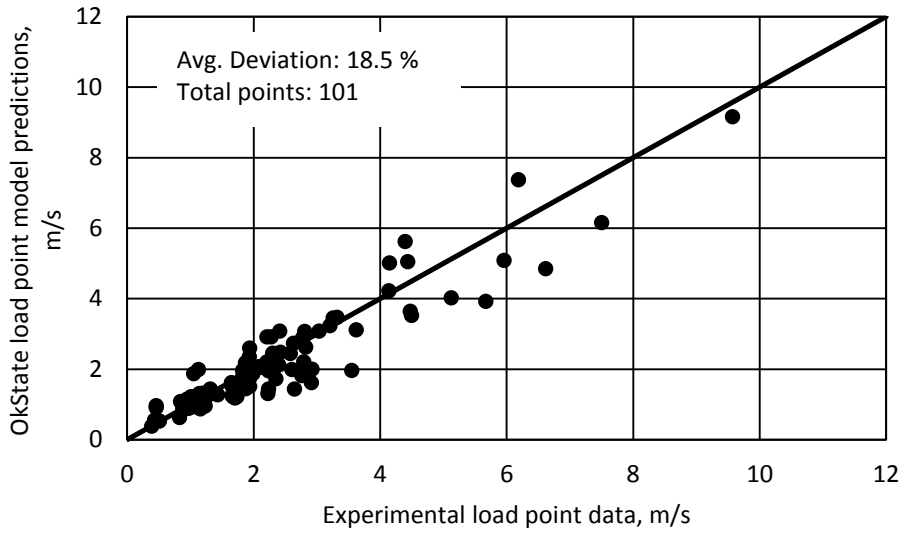

Fig. 3.10. Parity plot of OkState liquid holdup load point model predictions vs experimental liquid holdup load point data

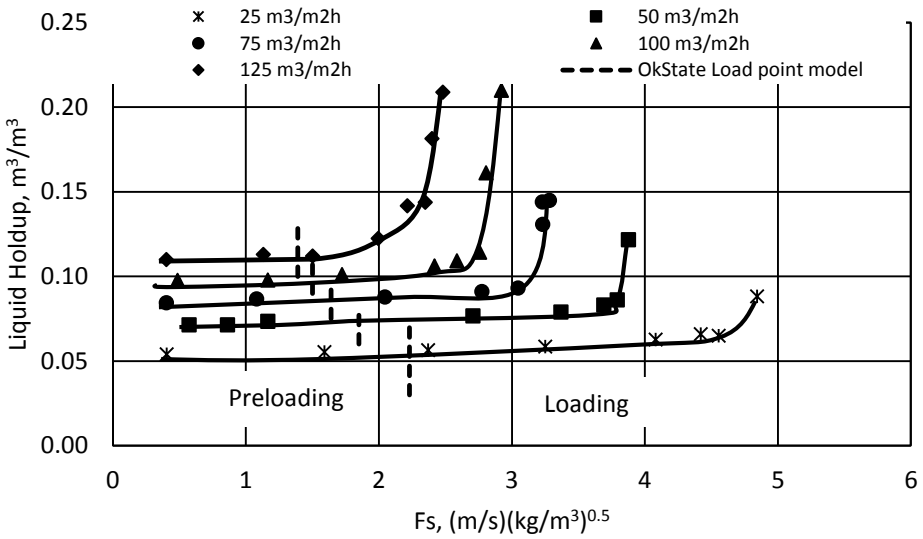

Fig. 3.11. Liquid holdup Experimental data and OkState load point model predictions for Sulzer Mellapak 250 X packings as a function of liquid flow rates and f factor. liquid holdup of (Sulzer Mellpak 250X data at different liquid flow rates [31], air/water, 1 bar)

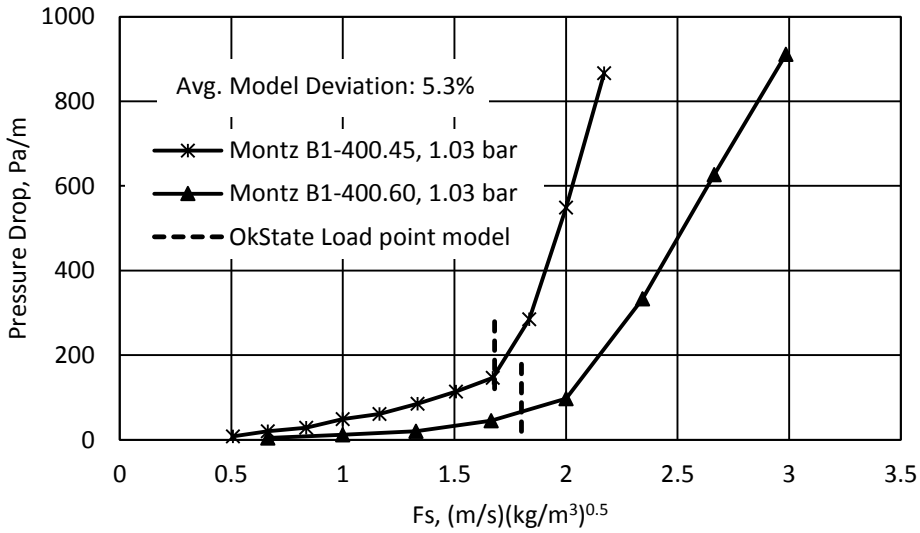

Fig. 3.12. Experimental pressure drop data as a function of vapor flowrate and corrugation angles and OkState load point model predictions (Montz B1-400.45 and B1-400.60, C6/C7, 1.03 bar, total reflux run)

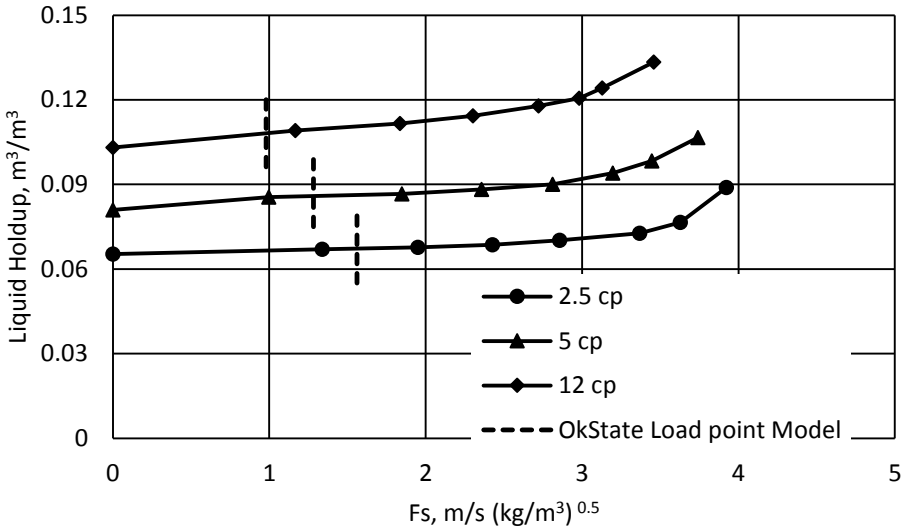

Fig. 3.13. Experimental liquid holdup data as a function of vapor flowrate and liquid viscosities and OkState load point model predictions (Montz B1-250M data, 1 bar pressure, air/water, 25 m^3/m^2hr [39])

In addition to the identification of load point, the main reason for developing the OkState load point model was to use in the model predictions of OkState liquid holdup load model. So the performance of the OkState liquid holdup load model was evaluated by reproducing the parity plots 3 and 4 using the OkState load point model predictions instead of using experimental data (Fig. 3.14 and 3.15). From the parity plots 3.14 and 3.15, the difference between overall error of OkState liquid holdup model predictions obtained by OkState load point model and the experimental load point data was less than 1%. The OkState load point model and the OkState liquid holdup models can be utilized while developing the models for pressure drop and HETP in the loading region of structured packed columns. In addition, both of these models can be further improved by collecting additional experimental data in the loading region for different systems using various packings.

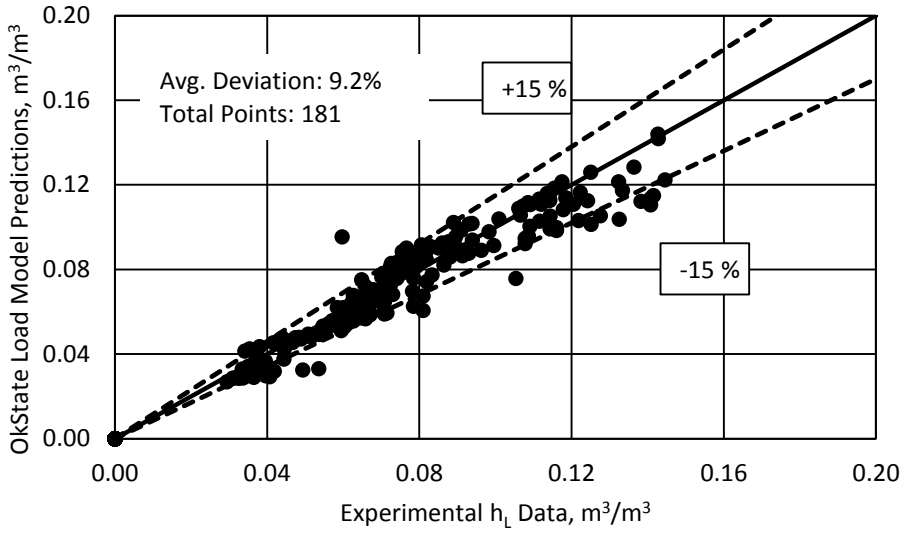

Fig. 3.14. OkState liquid holdup load model (eqn. 3.11) predictions obtained using both OkState liquid holdup preload and OkState load point models vs experimental liquid holdup loading data

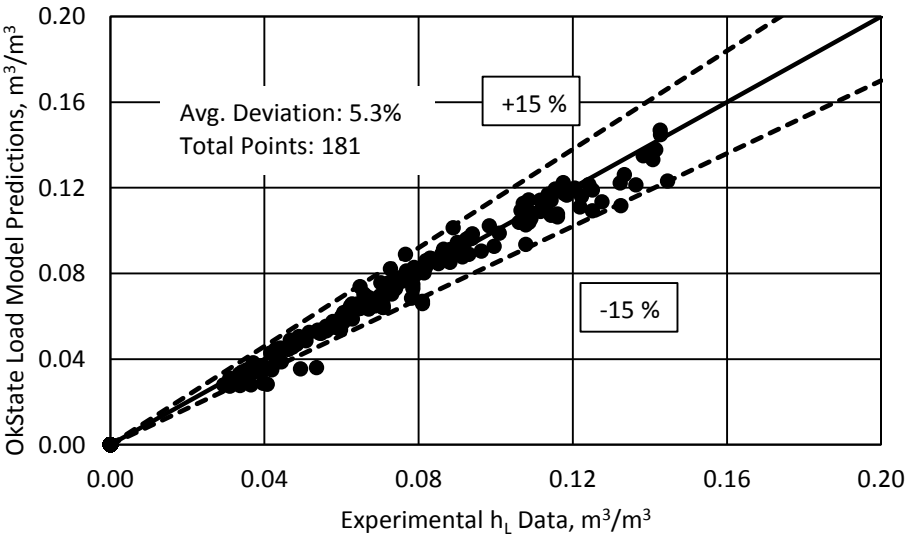

Fig. 3.15. OkState liquid holdup load model (eqn. 3.11) predictions obtained using both experimental liquid holdup preloading data and OkState load point model vs experimental liquid holdup loading data

3.5. Conclusion

Anew load point model developed using packing geometric area and void fraction. The performance of this new model was better than other load point models available in literature for a wide range of operating conditions. Moreover, the newly developed OkState load point model was used in model predictions of OkState liquid holdup load model.

The newly developed OkState liquid holdup load model relies on readily available packing geometrical area and void fraction to capture the experimental trend in the loading region, which makes it easier to apply for newly developed packings. In addition, this was the only model in the literature capturing the vapor velocity effect on liquid holdup for different packings over a wide range of operating conditions with an overall error of less than 10%. However, the experimental data utilized in model development was obtained for air/water test system. Further, collecting the experimental data from other test systems will help in understanding the effect of surface tension and vapor viscosity that in turn helps in refining the model further.

Acknowledgement:

We would like to thank Sravanthi Vupputuri, for her help in completing the present work and in preparing the manuscript.

We would also like to thank Dr. Tony Cai and Mike Resetarits from FRI, for their financial support and supervision for part of this work.

Example Problem:

1. An air/water column is being operated at atmospheric conditions using Mellapak 250Y. Please calculate the liquid holdup when the column has a constant liquid flow rate of 32 m^3/m^2h and vapor flow rates of 1.95 m/s and 2.81 m/s. The load point for the present operating condition is 2.21 m/s. Please use properties below for the calculations:

Water Density	=	1000 kg/m^3
Water Viscosity	=	1 cp
Air Density	=	1.3 kg/m^3
Packing Area (a)	=	250 m^2/m^3
Void fraction (ε)	=	97.5 m^3/m^3
Corrugation angle	=	45

Ans: Given, Liquid velocity U_L = 0.0089 m /s

Load point velocity $U_{G,\text{ Load point}}$ = 2.21 m/s

- At U_G = 1.95 m/s

  Since $U_G < U_{G,\text{ Load point}}$, the region of operation is preloading. So using eqn. 3.8 for liquid holdup calculation.

  From eqn. 3.6,

$$Re = \frac{1000\frac{kg}{m^3} \times 0.0089\frac{m}{s}}{250\frac{m^2}{m^3} \times \left(\frac{1}{1000}\right)\frac{Pa}{s}} = 35.6$$

$$h_{L,preload} = 0.114 \frac{250^{1.23}\ 35.6^{0.41}}{(1-(97.5/100))^{0.28}} \left(\frac{\left(\frac{1}{1000}\right)^2}{1000^2 \times 9.81 \times \sin 45} \right)^{1/3}$$

$= 0.0647\ m^3/m^3$

Actual experimental liquid holdup = 0.0642 m^3/m^3

Error, % = $abs\left(\frac{0.0647-0.0642}{0.0642}\right) \times 100 = 0.7\%$

Note: In OkState liquid holdup preload model, if the exponent of the viscosity term $\left[\left(\frac{\mu_L^2}{\rho^2\ g \sin\theta}\right)^{\frac{1}{3}}\right]$ is approximated as 0.33 instead of (1/3), it reduces the overall performance.

- At U_G = 2.81 m/s

  Since $U_G > U_{G,\text{ Load point,}}$ the region of operation is loading. So using eqn. 3.11 for liquid holdup calculation. But eqn. 3.11 requires preloading liquid holdup, since the liquid load rate is constant the preloading liquid holdup also remains constant. So preloading liquid holdup calculated at U_G of 1.95 m/s can be used here,

  From above calculation,

  $$h_{L,preload} = 0.0647\ m^3/m^3$$

  From eqn. 3.11,

  $$h_{L,load} = 0.0647 + (1.68\ 10^{-6}) \times \left(0.0089 \times \sqrt{1000}\right)^{0.671} \times (250)^{1.15} \times$$

$$\left[\left(\frac{2.81}{\left(\frac{97.5}{100}\right)\left(1-h_{L,load}\right)\sin 45}\sqrt{1.3}\right)^{1+\frac{h_{L,load}}{0.0647}}-\left(\frac{2.21}{\left(\frac{97.5}{100}\right)\left(1-0.0647\right)\sin 45}\sqrt{1.3}\right)^{2}\right]$$

Solving the above equation using algorithm from 2.2.1.

- Rearrange the above equation

$$\left\{0.0647+(1.68\,10^{-6})\times\left(0.0089\times\sqrt{1000}\right)^{0.671}\times(250)^{1.15}\right.$$

$$\times\left[\left(\frac{2.81}{\left(\frac{97.5}{100}\right)\left(1-h_{L,load}\right)\sin 45}\sqrt{1.3}\right)^{1+\frac{h_{L,load}}{0.0647}}\right.$$

$$\left.\left.-\left(\frac{2.21}{\left(\frac{97.5}{100}\right)\left(1-0.0647\right)\sin 45}\sqrt{1.3}\right)^{2}\right]\right\}-h_{L,load}=0$$

- Take initial guess for $h_{L,load}$ as $h_{L,preload}$, which is 0.0647 m^3/m^3
- Use excel solver or any line search algorithm by applying a constraint $h_{L,load} > h_{L,pre}$

The final solution is $h_{L,load}$ = 0.0702 m^3/m^3

Actual experimental liquid holdup = 0.0724 m^3/m^3

Error, % = $abs\left(\frac{0.0724-0.0702}{0.0724}\right)\times 100$ = 3.04%

CHAPTER IV

4. DEVELOPMENT AND EVALUATION OF LIQUID HOLDUP AND FLOODING VELOCITY MODELS TO IDENTIFY FLOODING REGION FOR A SHEET METAL STRUCTURED PACKING. PART III

Abstract:

Identification of a flooding is necessary for efficient design and safe operation of the column. Flooding can be identified with the help of flooding velocity model, liquid holdup flooding model, or pressure drop flooding model developed for the respective packings. In the open literature, only few theoretical models were available to identify the flooding for a sheet metal structured packing. However, the available models need packing specific constants for model predictions and did not account for the effect of corrugation angle. Analyzing the performance of those literature theoretical models using the experimental liquid holdup flooding data and flooding velocity data has shown a clear necessity for developing new flooding velocity and liquid holdup flooding models for a structured packed column. Therefore, new flooding velocity and liquid holdup models were developed for sheet metal structured packing in the flooding region using corrugation angle, packing surface area, and void fraction as the main model parameters. The most important features of the newly developed models were that they did not require any packing specific constants for

model predictions. Further, the new models were predicting the experimental database with minimum error.

4.1. Introduction

Flooding is one of the most important concepts in countercurrent vapor liquid flow operations [2, 27, 28, 53]. Flood point signifies the operating limit, and is a necessary term in design of equipment. Flood point has not been clearly defined yet for a structured packed column [2]. However, the most widely used interpretation is:

"A point at which sudden loss in mass transfer efficiency and exponential increase in liquid holdup and pressure drop occur inside a column."

Fig. 4.1, 4.2, and 4.3 illustrate the flooding region in structured packings for air/water and C6/C7 systems using experimental data. In Fig. 4.1, experimental liquid holdup data was plotted against vapor flow rate for Mellapak 250X and 250Y packings. This data showed an exponential increase in liquid hold up when the column started to approach flood point. Similarly, experimental pressure drop data obtained using Montz B1-250.45 and Montz B1-250.60 was plotted against vapor flow rate (Fig. 4.2). Consistent with earlier observations, an exponential increase in pressure drop was observed when approaching the flooding region. The loss of efficiency due to the exponential increase in liquid holdup and pressure drop can be observed by plotting the HETP data obtained at FRI using Mellapak 250Y packing (Fig. 4.3). These observations strongly support the above definition for flooding, which is a good approximation of the behavior taking place inside a structured packed distillation column at flooding region.

Flood point can be identified with the help of a flooding velocity model, a liquid holdup flooding model, or a pressure drop flooding model when the vapor velocity, liquid holdup, and pressure drop are greater than their respective model predictions. Further, the liquid holdup flooding model is also necessary to develop the flooding velocity model, since the latter will be influenced by the liquid holdup in the column. In addition, a thorough understanding and identification of flood point is necessary to calculate the diameter of the column, since a majority of the columns will be sized with an assumption of 70 – 80% flood point operation. Identification of flood point also helps in predicting the flow behavior and operation of the column, which in turn improves the overall efficiency and the safety of the column. Therefore, in the present work the focus will be on the liquid holdup flooding model and flooding velocity model. So a brief discussion of the available literature models for liquid holdup and flooding velocity was presented below.

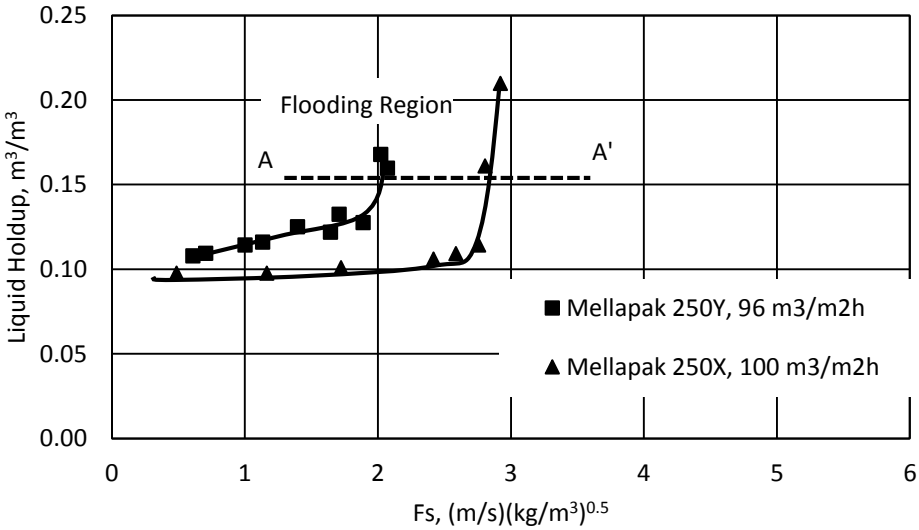

Fig. 4.1. Experimental liquid holdup data obtained using Mellapak 250X and 250Y packings, air/water, 1bar [31]

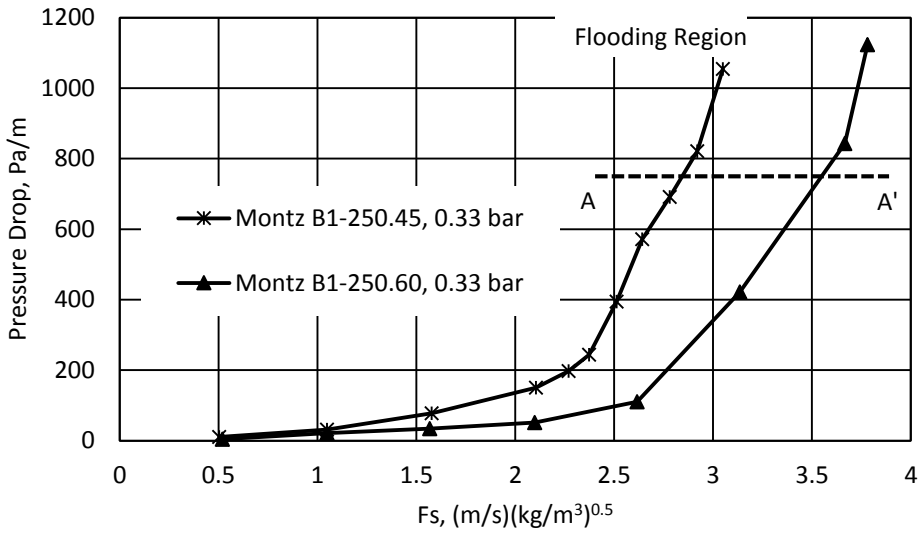

Fig. 4.2. Experimental pressure drop of packed column operation using the packings Montz B1-250.45 and Montz B1-250.60, C6/C7 system, 0.33 bar, and total reflux runs [47]

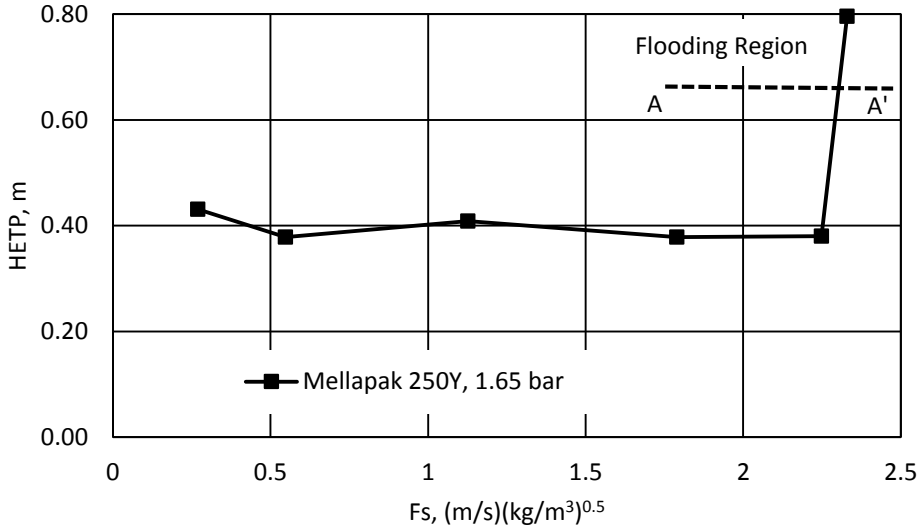

Fig. 4.3. Experimental HETP data measured using industrial sized FRI column for Mellapak 250Y, C6/C7, 1.65 bar, and total reflux runs [54]

Flood point can be obtained either through charts or theoretical models. Sherwood (1938) [55] type charts have been more popular in estimating the flood point. Numerous researchers (Eckert [1975] [56], Kister [1991, 1992] [2, 57], Leva, [1992] [58]) have developed different

versions of the Sherwood charts over the years, with the most recent and popular version being that of Kister (1992) [2]. However, the charts were more readily available for random packings compared to structured packings. Therefore, a good theoretical model is necessary for estimating flood point in structured packings. In addition, having a model in equation form is useful for simulations on a computer and for easy and accurate interpretations for new packings.

Previously, theoretical models that were developed for random packings were adapted to structured packings. Billet (1999) [16], Mackowiak (1990) [59], and Brunazzi (2008) [60] models were among those, however, the lack of packing specific constants for structured packings is the major limitation for this approach. To avoid these downsides, Lockett (1995) [61] and Spiegel (1987) [62] developed flooding velocity models for structured packed columns using a Wallis - type equation. Further, Locket showed that the Wallis type equation can be easily applied to develop flooding velocity models for various structured packed columns. The downside of the Lockett model was that it was developed only for Y- type packings (45° corrugation angle), and does not account for the effect of X- type packings (60° corrugation angle) on the flooding. In contrast to Lockett's approach, Kuzniewska (1999) [63] used dimensional analysis for developing a flooding velocity model. The Kuzniewska model was the only model in the literature developed for both random and structured packings without the necessity of packing specific constants for model predictions. However, this model also did not account for the effect of corrugation angle on the flooding velocity. In addition to corrugation angle, liquid hold up also shows a significant effect on flood point and none of the previous models were accounting for this effect. Although a few models such as the Mackowiak [59] model accounted for liquid holdup, dependency on packing specific constants for model predictions was the major limitation.

In the present study, the performance of the available literature flooding velocity models were evaluated using the experimental flooding velocity database assembled from the open literature. The results showed that the performance of the literature models was limited due to the lack of consideration of corrugation angle effects and packing specific constants (please refer Table 4.2 and Appendix I).

Compared to flooding velocity models, availability of liquid holdup flooding models in literature was very limited. To our knowledge, there were only two liquid holdup flooding models that were developed by Billet (1999) [16] and Mackowiak (1990) [59]. However, the Billet (1999) model required packing specific constants for model predictions which limited the usability of the model. On the other hand, the Mackowiak (1990) model did not include any packing dimensions in the model development. Therefore, the performance of the Mackowiak model was not satisfactory when evaluated using the experimental literature data for sheet metal structured packing (please refer Appendix H). This was an expected result, since both of these models were not developed particularly for structured packing.

From the above observations, there is a clear need for development of liquid holdup flooding and flooding velocity models for sheet metal structured packing columns. In the present study, a liquid holdup flooding model was developed first, and then it was utilized to develop a flooding velocity model.

4.2. Model Development

Flooding in a structured packed column can be either due to liquid or vapor flow. Increased liquid flow rates in a structured packed column increases liquid film thickness over the packing surface. Subsequently, increased film thickness fills the space between packing metal plates and prevents

the vapor flow. This causes inoperability of the structured packed column at high liquid flow rates. However, the typical flooding encountered in the industrial structured packed column is due to vapor flow. At flood point, the vapor flow pushes back the liquid flowing down the column and increases the liquid film thickness**,** which in turn fills the entire packed bed. The velocity with which the vapor pushes back the liquid is necessary to identify the flood point in a structured column. Therefore, developing a model to determine the flooding vapor velocity is essential for structured packed columns. However, it is important to develop a liquid holdup flooding model before developing a flooding vapor velocity model**,** as first influences the later.

4.2.1. Liquid Holdup flooding model

As discussed in our previous article [64], liquid holdup and film thickness in a structured packed column increases with increasing vapor flow rate after the load point. When the column is close to the flood point, the liquid film thickness reaches a critical value which can be easily influenced and supported by the countercurrent vapor flow. A model to estimate this critical liquid film thickness will help in developing the liquid holdup model at flood point, since liquid holdup accounts for the liquid film formed on the packing surface.

Recently**,** Ruan [45] showed that the critical liquid film thickness at flood point can be related to the preloading liquid film thickness using the relation below (equation 4.1).

$$\delta_c = 1.587\ \delta_A \tag{4.1}$$

Where,

δ_c = Critical film thickness $= \left(\frac{3\ \mu_L^2\ Re}{\rho_L^2 g \sin\theta}\right)^{\frac{1}{3}}$

δ_A = Preloading film thickness = $\left(\frac{3\,\mu_L^2\,Re}{4\,\rho_L^2 g \sin\theta}\right)^{\frac{1}{3}}$

In the present model development the concept proposed by Ruan was adapted to relate the critical liquid holdup at the flood point to the liquid holdup at the preloading region:

$$h_{L,fl} = C\ h_{L,pre} \tag{4.2}$$

Where,

$$h_{L,pre} = Preloading\ liquid\ holdup\ model = 0.114\ \frac{a^{1.23}\ Re^{0.41}}{(1-\varepsilon)^{0.28}}\ \left(\frac{\mu_L^2}{\rho_L^2\ g \sin\theta}\right)^{\frac{1}{3}} \tag{4.3}$$

However, the geometry of a structured packed column is much more complex than the scenario considered by Ruan (flat plate), and these geometric variations (packing geometric area and void fraction) should be taken into account to develop the liquid holdup model at the flood point. Therefore, equation 4.3 was modified to consider the geometric variations

$$h_{L,fl} = C_1\ \frac{a^{C_2}\ Re^{0.41}}{(1-\varepsilon)^{C_3}}\ \left(\frac{\mu_L^2}{\rho_L^2\ g \sin\theta}\right)^{\frac{1}{3}} \tag{4.4}$$

The constants $C_1, C_2,$ and C_3 were obtained by regressing the model using experimental liquid holdup data in the flooding region. The final form of the equation is

$$h_{L,fl} = 2.0\ \frac{a^{0.88}\ Re^{0.41}}{(1-\varepsilon)^{0.15}}\ \left(\frac{\mu_L^2}{\rho_L^2\ g \sin\theta}\right)^{\frac{1}{3}} \tag{4.5}$$

The above model predicts the critical liquid holdup at the flood point which helps in evaluating the region of operation based on the experimental liquid holdup data. If the operational liquid holdup is greater than the predicted liquid holdup, then the column can be considered to be

either in or close to flooded region. The focus of the present work was to identify the flood point and we were not interested in predicting the exponential increase of liquid holdup with vapor flow rate in the flooding region.

Henceforth, the newly developed liquid holdup flood model (equation 4.5) will be referred to as the "OkState liquid holdup flooding model".

4.2.2. Flooding velocity model

One of the popular methods to estimate the flooding velocities of a counter current vapor and liquid operation was by utilizing the Wallis equation [65]. In addition, Lockett [61, 66] showed that the Wallis equation did a good job in estimating flooding velocity for a structured packed column. Therefore, the Wallis equation was utilized to develop the present flooding velocity model. The Wallis equation correlates the gas flux with the liquid flux under the flooding conditions as show in equation 4.6.

$$j_G^{*\frac{1}{2}} + m\, j_L^{*\frac{1}{2}} = c \tag{4.6}$$

m and c are constants obtained using the experimental data. J_G^* and J_L^* are dimensionless fluxes of gas and liquid, respectively. These fluxes can be calculated using the equation 4.7 and 4.8.

$$j_G^* = \frac{\rho_G^{\frac{1}{2}}\, U_G}{[g\, D\, (\rho_L - \rho_G)]^{\frac{1}{2}}} \tag{4.7}$$

$$j_L^* = \frac{\rho_L^{\frac{1}{2}}\, U_L}{[g\, D\, (\rho_L - \rho_G)]^{\frac{1}{2}}} \tag{4.8}$$

U_G and U_L are the superficial velocities of vapor and liquid in the column. D is the diameter of the test section and for structured packed column and it can be calculated using equation 4.9.

$$d_e = \frac{4\,\varepsilon}{a} \tag{4.9}$$

The liquid flux j_L can be neglected at the flood point because of negligible liquid flow in a structured packed column. Hence equation 4.6 can be written as

$$j_G^{*\frac{1}{2}} = c \tag{4.10}$$

From Lockett [61], c is a function of viscosity (ml) and packing surface area (a).

$$j_G^{*\frac{1}{2}} = c\frac{a^{c_1}}{\mu_L^{c_2}} \tag{4.11}$$

Apart from these**,** the flooding velocity also depends on void fraction (ε), surface tension (σ), and the liquid holdup (1-$h_{L,fl}$) at flooding. So equation 4.11 becomes

$$j_G^{*\frac{1}{2}} = \frac{c_1\, d_e^{c_2}\mu^{c_3}}{\sigma^{c_4}}\left(1 - h_{L,fl}\right) \tag{4.12}$$

Substituting equation 4.7 into 4.12,

$$\frac{\rho_G^{\frac{1}{2}}\, U_{G,fl}}{[g\; d_e\; (\rho_L - \;\rho_G)]^{\frac{1}{2}}} = \frac{c_1\, d_e^{c_2}\mu^{c_3}}{\sigma^{c_4}}\left(1 - h_{L,fl}\right)^2 \tag{4.13}$$

U_G is a function of the liquid holdup at the flooding, which can be calculated using the equation 4.14.

$$U_{G,fl} = \frac{u_{G,fl}}{\varepsilon\left(1 - h_{L,fl}\right)\sin\theta} \tag{4.14}$$

Substituting equation 4.14 into equation 4.13 and rearranging, the final expression for flooding velocity is

$$u_{G,fl} = \frac{c_1 \, d_e^{c_2} \mu^{c_3} \, \sin\theta}{\sigma^{c_4}} \left(1 - h_{L,fl}\right)^3 \left(\frac{\rho_L - \rho_G}{\rho_G} \, g\right)^{0.5} \qquad (4.15)$$

The constants c1, c2, c3, and c4 were obtained by regressing the model using the assembled literature database. The final flooding velocity model is

$$u_{G,fl} = 0.695 \, \frac{d_e^{0.36} \mu^{0.25} \, \sin\theta}{\sigma^{0.25}} \left(1 - h_{L,fl}\right)^3 \left(\frac{\rho_L - \rho_G}{\rho_G} \, g\right)^{0.5} \qquad (4.16)$$

From this point on**,** the newly developed flooding velocity model (equation 4.15) will be referred to as "OkState flooding velocity model". The newly developed OkState liquid holdup flooding model and OkState flooding velocity model do not require any packing specific constants, and the variations between different packings was accounted by using packing geometric area and void fraction, which are readily available in the open literature. The OkState flooding velocity model was developed using the OkState liquid holdup flooding model, the first liquid holdup flooding model developed for structured packed columns.

4.3. Literature Database

A database of experimental liquid holdup flooding data was assembled from the open literature [31, 39, 40]. A more detailed discussion of the database was presented in our previous article [48]. The experimental literature liquid holdup data was screened as liquid holdup data at flooding region when liquid holdup was exponentially increasing with vapor flow rate. The available test systems in the database were limited to air/water, air/water/sucrose, and

air/water/MEA. A total of 6 packings were considered for model development including the popular X and Y type packing configurations.

Table 4.1. Variable ranges describing the Flooding velocity database

Variable	Range
Operating pressure (bar)	0.033 – 4.14
Liquid density (kg/m3)	561 – 1000
Vapor density(kg/m3)	0.14 – 13.14
Liquid velocity (m/s)	0.0011 – 0.049
Vapor velocity (m/s)	0.39 – 9.74
Liquid viscosity (Pa.s)	0.0001 – 0.0025
Vapor viscosty (Pa.s)	0.000006 – 0.000686
Surface tension (N/m)	0.08 – 0.725

Similar to the experimental liquid holdup flooding database, a wide database of flooding velocity data was also assembled from HETP , pressure drop, and liquid holdup experimental data. A more detailed discussion of these databases was presented in our earlier articles [50, 51]. Flood point was obtained from the experimental data with exponential liquid hold up and pressure drop increase. The assembled database consists of a wide range of operating conditions, which are summarized in Table 4.1. These tests were conducted using the air/water, cyclohexane/n-heptane, chlorobenzene/ethylbenzene, iso-octane/toluene, m-xylene/p-xylene, and methanol/water test systems. Apart from the above conditions, the database was also collected for different types of structured packings with packing surface area between 55 to 500 m^2/m^3, void fraction between 90 to 98.9, and corrugation angles of 45 & 60^o. In addition to the above mentioned data, experimental FRI data was assembled from the open literature to validate the performance of the newly developed model for an industrial sized column (1.2 m diameter).

There were few packings in the literature without any packing geometry information. These packings were excluded from the main work and the performance of the literature models for these packings was presented separately in Appendix J.

4.4. Results and Discussion

4.4.1. OkState liquid holdup flooding model

An overall performance of the newly developed OkState liquid holdup flooding model can be seen in Fig. 4.4. The model predictions were equally spread out and doing a good job in capturing the behavior of experimental data. The model has an overall mean absolute relative error (MARE) of 13.1% with a standard deviation of 10.7%. MARE was calculated using the below expression,

$$MARE,\ \% = \frac{(Measured\ Holdup\ - Predicted\ Holdup)}{(Measured\ Holdup)}\ X\ 100 \tag{4.17}$$

The OkState liquid holdup flooding model was developed to identify the start of the flooding region**,** and does not account for the exponential increase in liquid holdup with the vapor flow rate in the flooding region. Due to this reason, there were higher deviations in model predictions for a few data points past the flood point. To properly evaluate the performance of the newly developed model, individual plots were created to see how well the new model is capturing the flood point for different liquid flow rates and packings (Figs. 4.5, 4.6, and 4.7).

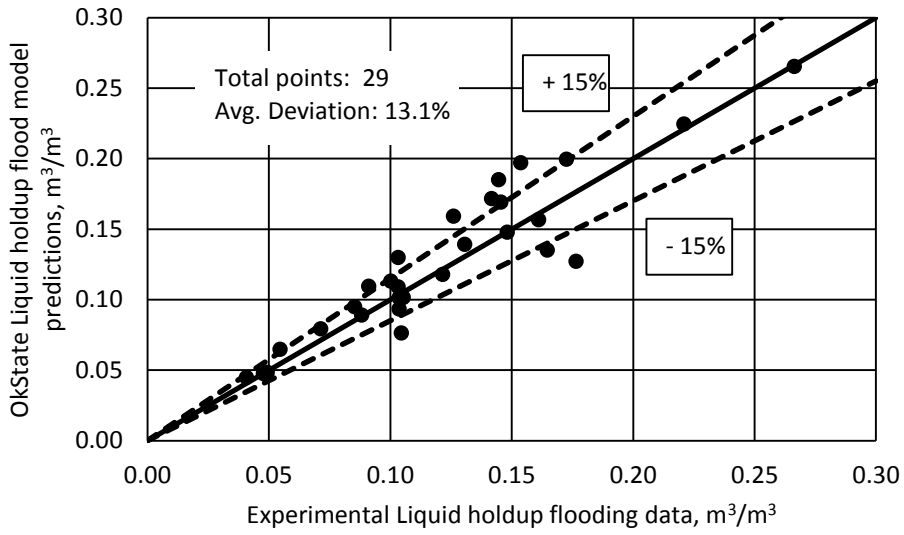

Fig. 4.4. Parity plot for OkState liquid hold up flood model predictions using experimental liquid holdup flood data

OkState liquid holdup flooding model predictions and the experimental liquid holdup data of Mellapak 250X and 250Y packings obtained using air/water test system at atmospheric conditions for various liquid load rates were plotted (Figs. 4.5 and 4.6). Based on experimental data behavior, the figures were divided into different regions of operations (preloading, loading, and flooding). The plots showed that the newly developed model has an overall error of less than 6% in capturing the beginning of the flooding region. Moreover, it is also accounting for the liquid load effect on the flooding. Average model prediction error was higher for Mellapak 250Y (6%) compared to Mellapak 250X (3%), due to the lack of experimental liquid holdup data at the flood point for Mellapak 250Y at 64 m^2/m^3h load. So from both Fig. 4.5 and Fig. 4.6, it can be observed that the newly developed model was properly capturing the effect of corrugation angle and liquid load rates on the experimental liquid holdup flooding data.

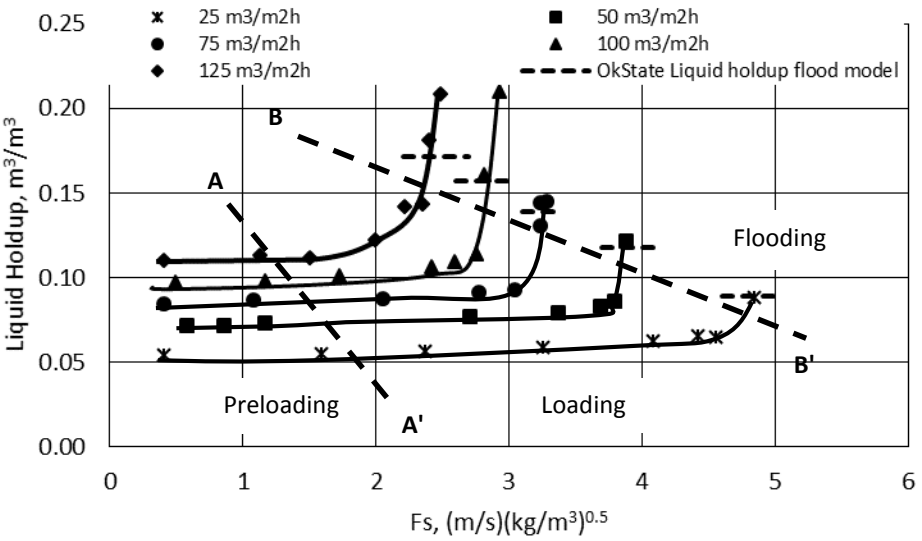

Fig. 4.5. OkState liquid holdup flooding model predictions for experimental liquid holdup data of Mellapak 250X, air/water, 1 bar [31]

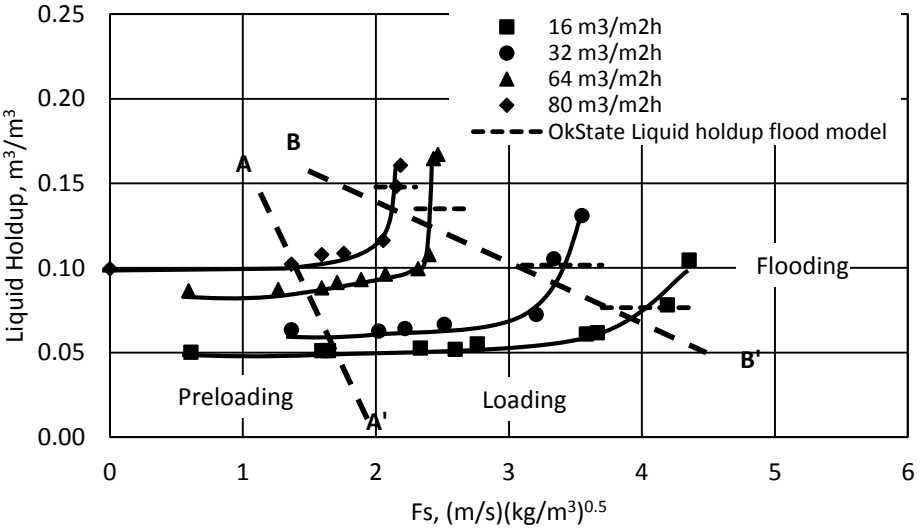

Fig. 4.6. OkState liquid holdup flooding model predictions for experimental liquid holdup data of Mellapak 250Y, air/water, 1 bar [31]

Fig. 4.7 shows the experimental liquid holdup flooding data for Montz B1-250 packing tested at atmospheric conditions using an air/water test system. The data was collected at a liquid load rate of 30 m^3/m^2h. As shown in figure 4.7, the newly developed OkState liquid holdup flooding model predicted a constant critical liquid holdup value based on the liquid load rate,

irrespective of the vapor flow rate. This value will be useful to identify the flooding region based on experimental liquid holdup data. At the experimental liquid holdup value greater than the critical value predicted by the OkState liquid holdup flooding model, the system was considered to be in or close to flooding region. Plots 5, 6, and7 showed that the model was doing a good job in identifying the start of the flooding region. Obtaining the data for other test systems will help in evaluating and improving the performance of the present model and also to account for the effect of viscosity and surface tension.

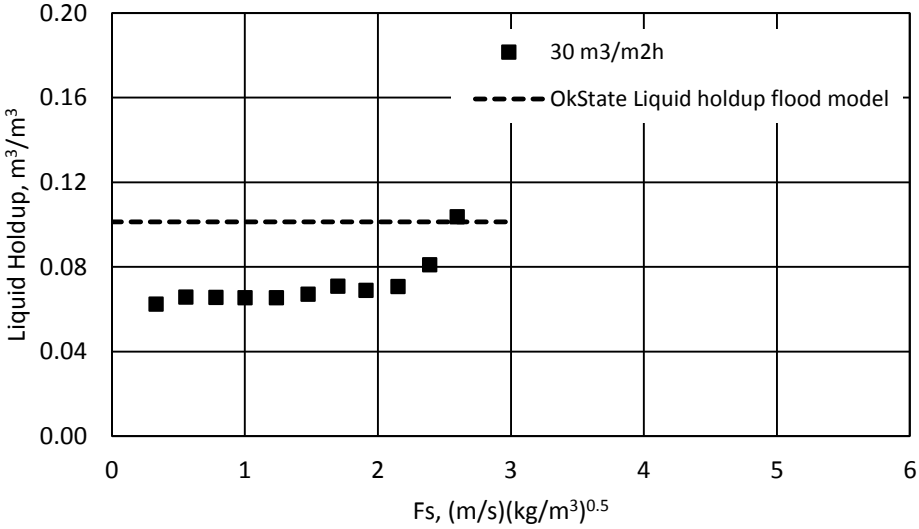

Fig. 4.7. OkState liquid holdup flooding model predictions for experimental liquid holdup data of Montz B1-250, air/water, 1 bar [40]

4.4.2. OkState flood velocity model

Table 4.2. Summary of literature flood velocity model performance using experimental flood velocity data

Model	Average Mean Absolute Relative Error, %
OkState	12.2
Lockett	21.9
Kuzniewska	24.8

$$MARE,\ \% = \frac{(Measured\ Flooding\ velocity\ -Predicted\ looding\ velocity)}{(Measured\ looding\ velocity)}\ X\ 100 \qquad (4.18)$$

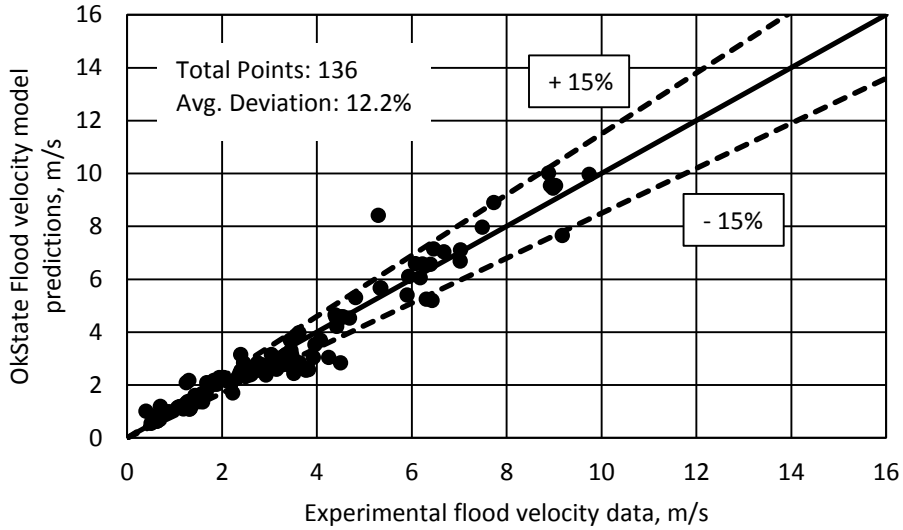

Fig. 4.8. Parity plot for OkState flood velocity model predictions using experimental flooding velocity data

Fig. 4.8 shows the parity plot for the newly developed OkState flooding velocity model using experimental flood velocity data. From Table 4.2 and Fig. 4.8, the model has a MARE of 12.2% with a standard deviation of 16.8%. Out of the 136 experimental points, more than 80% of the points lie in between the 15% deviation lines. It can be observed from the parity plot that the model is conservative in predictions. Further, similar to the liquid holdup flooding data, the flooding velocity data was also obtained from discrete experimental data of pressure drop, HETP and liquid holdup. Therefore, some of the data points were past the flood point and those points were chosen because of unavailability of data points at the beginning of the flooding region. There was a chance that the points selected past flood point could reduce the performance of the newly developed OkState flooding velocity model. So the performance of the OkState flooding velocity model was

further tested using FRI test data and few other data points that were not considered in the model development.

Figs. 4.9, 4.10, 4.11 and 4.12 show the experimental HETP data obtained using the FRI test facility, whose column operation was close to the industrial column operation. The tests were conducted using o/p-xylene low pressure system, cyclohexane/n-heptane medium pressure system, and i-/n/butane high pressure system. All the tests were total reflux runs with pressures varying between 0.13 to 11.4 bar. All these plots showed that the OkState flooding velocity model did a good job in identifying the flood point by capturing the effect of different systems and operating pressure on flood point. The average deviation of the present model tested using FRI experimental data was less than 10%. Also, the model predictions were conservative compared to experimental data.

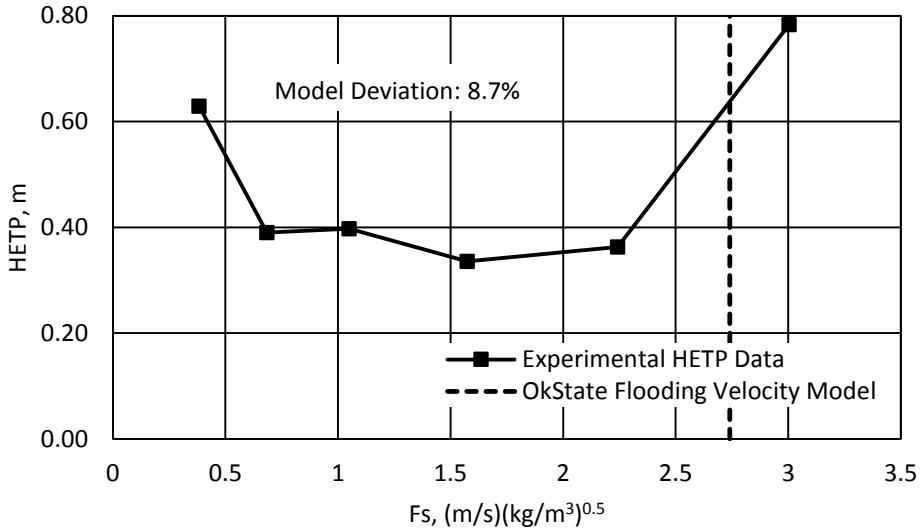

Fig. 4.9. OkState flooding velocity model prediction for experimental HETP data of Mellapak 250Y tested at FRI, o/p xylene, 0.13 bar [54]

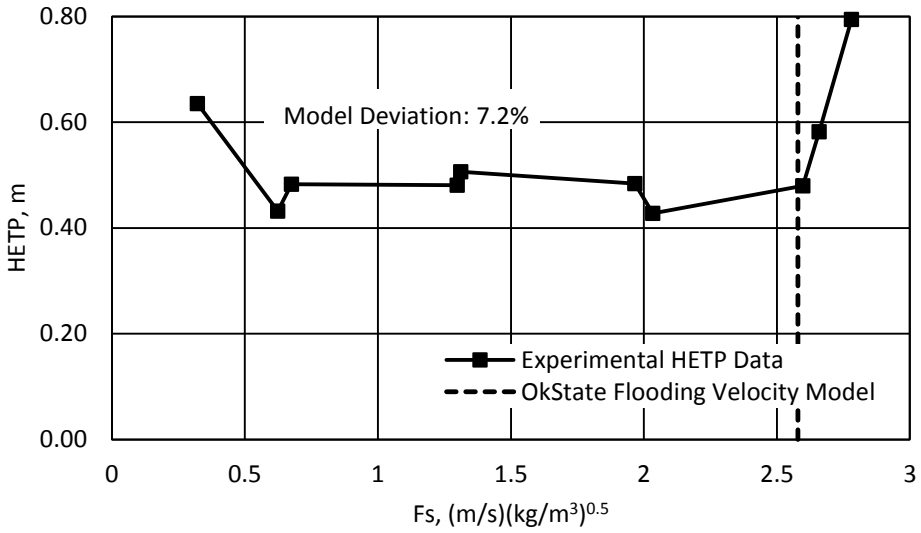

Fig. 4.10. OkState flooding velocity model prediction for experimental HETP data of Mellapak 250Y tested at FRI, C6/C7, 0.34 bar, and total reflux [54]

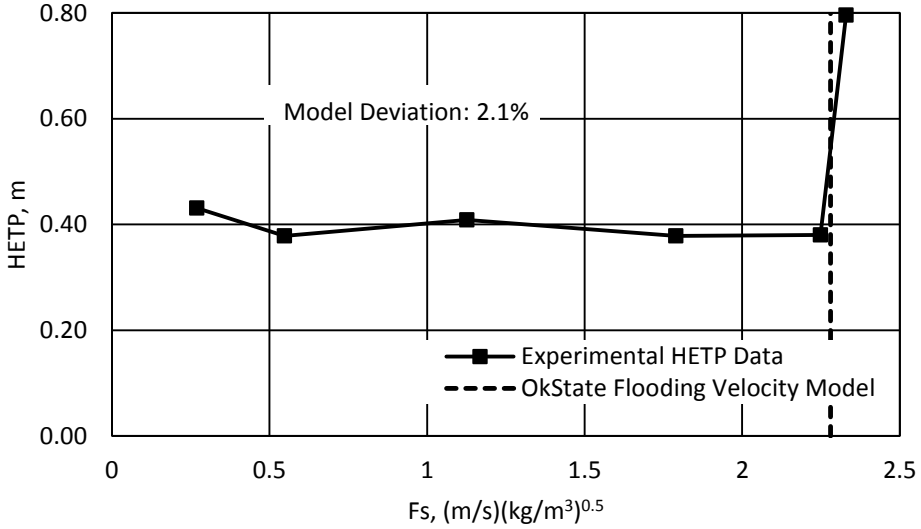

Fig. 4.11. OkState flooding velocity model prediction for experimental HETP data of Mellapak 250Y tested at FRI, C6/C7, 1.65 bar, and total reflux [54]

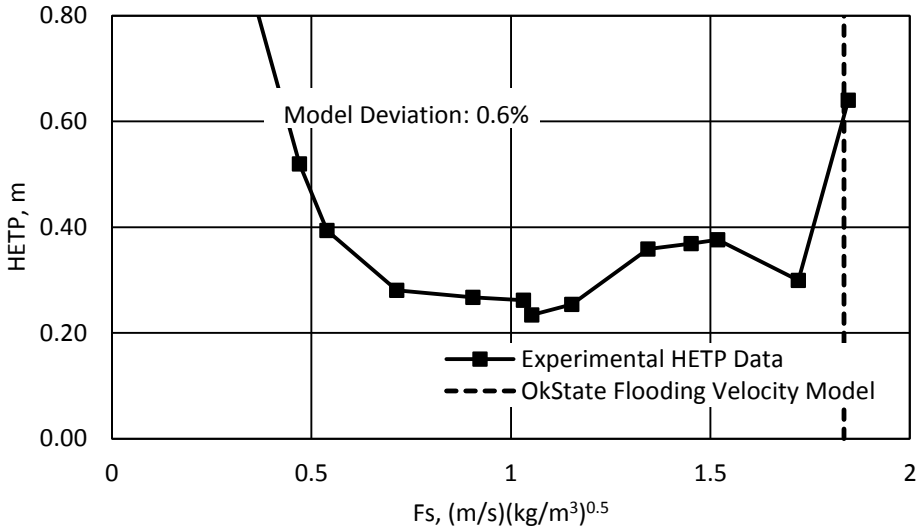

Fig. 4.12. OkState flooding velocity model prediction for experimental HETP data of Mellapak 250Y tested at FRI, i/n-butane, 11.4 bar, and total reflux [54]

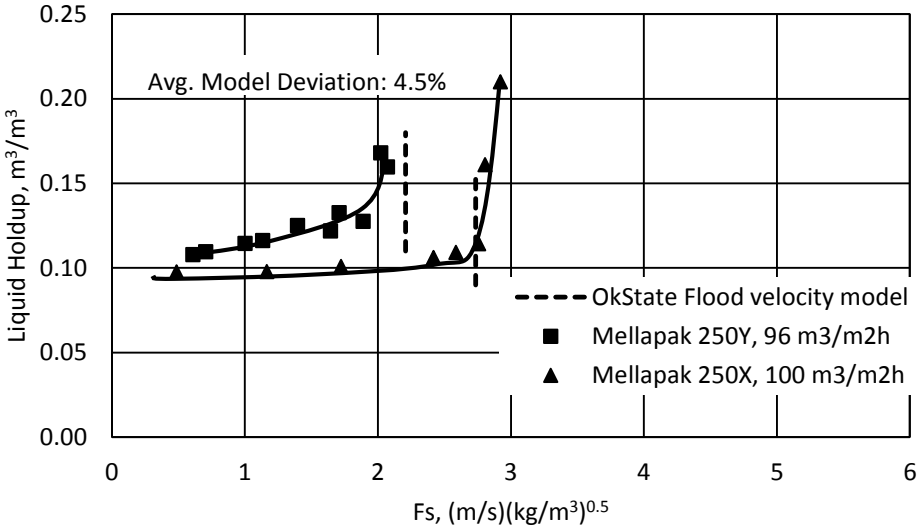

Fig. 4.13. OkState flooding velocity model prediction for experimental liquid holdup data obtained using the packings Mellapak 250Y and 250X, air/water, 1 bar [31]

The performance of the newly developed OkState flooding velocity model was validated using the liquid holdup experimental data. Fig. 4.13 shows the experimental liquid holdup data obtained for Mellapak 250Y and 250X packings using an air/water test system at different liquid load rates. In addition to the experimental data, OkState flooding velocity model predictions were

also plotted in the same figure. As shown in Fig. 4.13**,** the OkState Flooding velocity model was identifying the flood point really well for both 250Y and 250X with an average deviation of 4.5%. The effect of corrugation angle on flood point was also shown in the figure. The present model was also capturing the effect of corrugation angle on flood velocity.

The OkState flooding velocity model predictions were also plotted for experimental pressure drop data in Fig. 4.14. This experimental data was obtained using cyclohexane/n-heptane system at 0.33 bar for a total reflux condition. The packings tested were Montz B1-250.45 and B1-250.60. The model predictions have an average deviation of 8.3% from the experimental data. Further, the model predictions were also conservative.

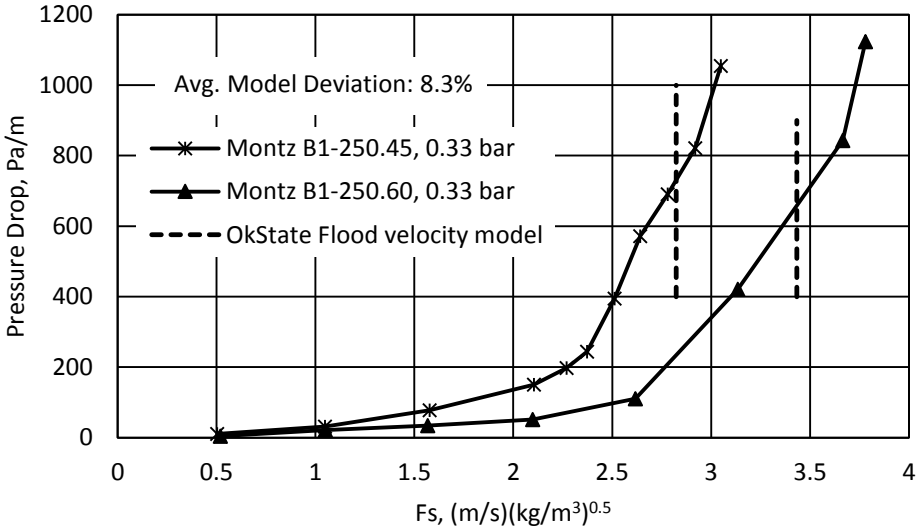

Fig. 4.14. Experimental pressure drop data using Montz B1-250.45 and B1-250.60, C6/C7 system, 0.33 bar, and total reflux condition [47]

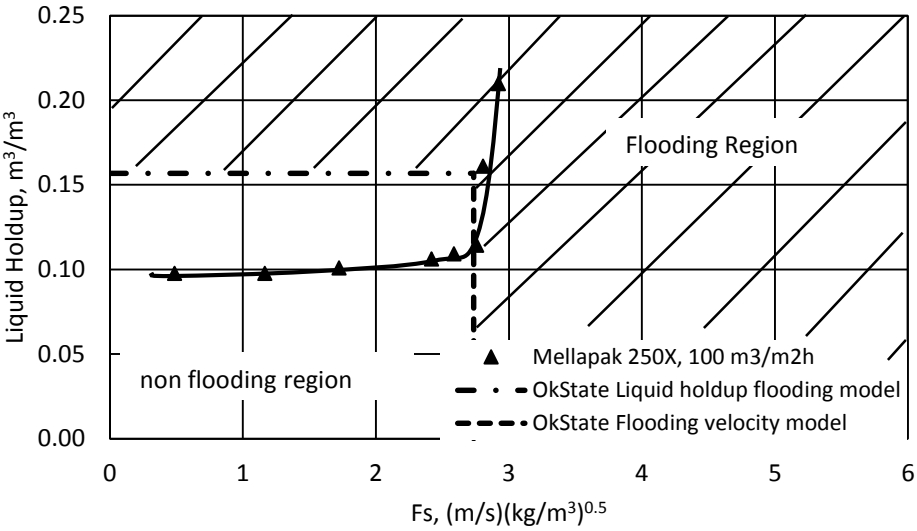

Fig. 4.15. Flooding region surface obtained using OkState liquid holdup flooding model and OkState flood velocity model for experimental Liquid holdup data obtained using Mellapak 250X packing, air/water, and 1 bar [31]

From the above results, it can be observed that the OkState liquid holdup flooding model and OkState flooding velocity model were identifying the flood point for different packings with reasonable error. A much better approach to identify flooding**,** however**,** is to combine the predictions from the above models. This will generate a surface in which flooding might occur. For example, Fig. 4.15 shows the experimental liquid holdup data for Mellapak 250X packing obtained at atmospheric conditions. In this figure, by combining the predictions of the OkState liquid holdup flooding model and OkState flooding velocity model, a safe operating region and flooding regions was identified. Often times it is difficult to identify the exact flood point for different operations, so when the experimental data falls in the shaded region**,** then the column can be considered to be flooded. This approach can be very valuable for column design and especially for troubleshooting.

4.5. Conclusion

The new OkState liquid holdup flooding model was correctly predicting the critical liquid holdup value, with an average deviation of 13% that can be used to identify the flooding based on the experimental liquid holdup data. However, the data was only available for an air/water test system. Obtaining additional test data from different test systems will definitely help in improving the performance of the present model for capturing the effects of viscosity and surface tension.

The new OkState flood velocity model was doing a good job in capturing the effect of corrugation angle, operating pressure and operating system on the flood point. Unlike other model, the OkState flooding velocity model captures the variations in different packings using the packing surface area, void fraction, and corrugation angle of the packing, thereby taking their effects into consideration. Moreover, The OkState flooding velocity model was predicting the flood point for an industrial sized FRI column data without any need of packing specific constants.

Example Problem:

1. A packed column using Mellapak 250X structured packing is being operated under atmospheric conditions with a liquid load of 100 m3/m2h. Check whether the column is flooded or not when the measured liquid holdup of the column is 0.21 m3/m3 and the vapor velocity of the column is 2.56 m/s. Use below properties for the calculations:

Water Density	=	1000 kg/m^3
Water Viscosity	=	1 cp
Air Density	=	1.3 kg/m^3
Packing Area (a)	=	250 m^2/m^3
Void fraction (ε)	=	98 m^3/m^3
Corrugation angle	=	60
Surface tension	=	0.072 N/m

Ans: a. Liquid holdup value at flooding:

First calculating the critical liquid holdup using OkState liquid holdup flooding model (equation 4.5).

$$h_{L,fl} = 2.0 \ \frac{a^{0.88}\, Re^{0.41}}{(1-\varepsilon)^{0.15}} \left(\frac{\mu_L^2}{\rho^2\, g \sin\theta}\right)^{\frac{1}{3}}$$

Where,

$$Re = \frac{u_L \rho_L}{a\, \mu_L} = \frac{\left(\frac{100}{3600}\right)\left(\frac{m}{s}\right)\ 1000\ \left(\frac{kg}{m^3}\right)}{250\ \left(\frac{m^2}{m^3}\right)\ \left(\frac{1}{1000}\right)\ (Pa.s)} = 111.11$$

$$h_{L,fl} = 2.0 \ \frac{250^{0.88} \ 111.11^{0.41}}{(1\text{-}0.98)^{0.15}} \ \left(\frac{(1/1000)^2}{1000^2 \ 9.81 \sin 60}\right)^{\frac{1}{3}} = 0.157 \ m^3/m^3$$

Since the experimental liquid holdup ($h_{L,\text{exp}}$ = 0.21 m3/m3) is greater than the model predicted critical value of $0.157 \ m^3/m^3$. The column is flooded based on the experimental liquid holdup data.

b. Flood point vapor velocity:

Flood point vapor velocity can be calculated using the OkState flooding velocity model (equation 4.16).

$$u_{G,fl} = \ 0.695 \ \frac{d_e^{0.36} \mu^{0.25} \ \sin\theta}{\sigma^{0.25}} \left(1 - h_{L,fl}\right)^3 \ \left(\frac{\rho_L - \rho_G}{\rho_G} \ g\right)^{0.5}$$

Where,

$$d_e = \frac{4 \ \varepsilon}{a} = \frac{4 \ \times \ 0.98}{250} = \ 0.01568 \ m$$

$$u_{G,fl} = \ 0.695 \ \frac{(0.01568)^{0.36} \left(\frac{1}{1000}\right)^{0.25} \ \sin 60}{0.072^{0.25}} \ (1 - 0.157)^3 \ \left(\frac{1000 - 1.3}{1.3} \ 9.81\right)^{0.5}$$

$$u_{G,fl} = 2.40 \ m/s$$

Since the vapor velocity of the column (u_G = 2.56 m/s) is greater than the OkState flooding velocity model predictions. The column is considered to be flooded.

CHAPTER V

5. SUMMARY AND CONCLUSIONS

In this chapter the major findings and contributions of this work are discussed; conclusions, and directions for future work are presented.

5.1. Major findings

The contributions and major findings are summarized below:

- A new liquid holdup preloading model was developed for a sheet metal structured packing with the following features:
    - It has a simple model structure, which is based on a liquid film thickness model.
    - It predicts the liquid holdup over a wide range of liquid flow rates.
- A new liquid holdup loading model was developed with the following features:
    - It incorporates the effect of vapor velocity on the liquid holdup in the loading region.
    - It relies on simple kinetic energy term as the main model parameter.
- A new liquid holdup flood model was developed with the following features:
    - It is based on the liquid film model.
    - It is the first liquid holdup model developed for a structured packed column.

- A new flooding velocity model was developed with the following features:
    - It is based on the Wallis type model for a counter current vapor and liquid flow.
    - It uses liquid holdup term as a main model parameter.
    - It is simple compared to other literature flood models.
- In addition all the models that were developed have the following advantages:
    - They do not rely on any packing specific constants for model predictions.
    - They only rely on the packing geometrical area, void fraction, and physical properties for model prediction.
    - The present models were developed using a wider experimental database than any other literature models.

5.2. Conclusions

The current OkState preloading liquid holdup model was developed on the basis of a film model with an overall deviation of 5%. This again reiterates the point that structured packings are film contacting devices and a good liquid film thickness model accounting for the effect of various complex surfaces will help to improve the overall understanding of the packed column. In addition, the liquid holdup model also showed that packing geometric surface area and packing void fraction are sufficient to identify the effect of different packings on experimental data.

The new OkState loading liquid holdup model was the only literature model that was properly capturing the vapor flow rate effect on the liquid holdup. In addition, this model does not rely on any packing specific constants to capture this behavior. Also, a new OkState loading point model was developed to support the OkState loading liquid holdup model predictions. These

models are the first literature models developed using a wide experimental structured packing data. Furthermore, the complexity of these models can be attributed to the complexity of the loading region.

The OkState liquid holdup flood model was the first liquid holdup model developed in the flooding region for a structured packed column. In addition, this model relies on the readily available packing information, such as packing geometrical area and packing void fraction for model predictions. An important thing to note about this model is that it specifies the upper safe operating limit for structure packing experimental liquid holdup data.

In addition to the liquid holdup models, a new OkState flooding velocity model was also developed in the present work using the Wallis type equation. This model is also a necessary model for a structured packed column because a majority of the literature flooding models were adopted from the random packing columns. This was limiting the overall performance of the literature flooding velocity models. However, the new OkState model was properly accounting for the effect of operating conditions and packing variations compared to other literature models. Another significant point is that the new OkState model is simple and requires less information when compared to other literature models.

Overall, in the present work performance of the literature liquid holdup, load point and flood point models were evaluated using experimental literature data. In addition, new models were developed for liquid holdup in preloading, loading, and flooding region, as well as new load and flood point models.

5.3. Future work

Experimental data is needed for systems other than air/water to account for the proper effect of physical properties on the liquid holdup. Data is especially needed in the loading region to identify the effect of vapor viscosity and surface tension on the liquid holdup. In addition, the data collected on commercial scale columns will be valuable to identify the effect of vapor and liquid flow rates on liquid holdup.

Furthermore, current models were developed using third generation structured packing data. New fourth generation structured packings are now available from the packing manufacturers, so experimental data from the fourth generation packings will be valuable for evaluating the newly developed models and in identifying the differences in liquid holdup behavior in different regions of operations.

For a structured packed column, in addition to the liquid holdup and flooding velocity models, there is also a need for a new pressure drop model. Similar to the liquid holdup models, pressure drop models should be developed for each region operation. In addition, pressure drop model is also a strong function of liquid holdup model similar to flooding velocity model. Therefore, the newly developed liquid holdup models should be incorporated in the pressure drop model. Furthermore, the newly developed load point and flooding velocity models will help in identifying different regions of operation.

In addition, new volumetric mass transfer coefficient models are also necessary for HETP model predictions and rate based modeling of a structured packed column. However, the following gaps need to be addressed first before developing new volumetric mass transfer coefficient models:

- Need of volumetric mass transfer coefficient data for a distillation system

- Need of structured packing distillation concentration profile data

In addition, liquid holdup model terms also need to be incorporated into the volumetric mass transfer coefficient models to improve their performance.

REFERENCES

1. Lockett, M.J., *Distillation tray fundamentals.* 1986.
2. Kister, H.Z., *Distillation Design*. 1992: McGraw-Hill.
3. Kunesh, J.G., et al., *Distillation: still towering over other options.* Chemical engineering progress, 1995. **91**(10): p. 43-54.
4. Porter, K.E., *Why research is needed in distillation.* Chemical Engineering Research and Design, 1995. **73**(A4): p. 357-362.
5. Lucia, A. *The Long and the Short of Energy Consumption in Distillation*. in *AICHE*. 2007.
6. Schultes, M., *Raschig super-ring: a new fourth generation packing offers new advantages.* Chemical Engineering Research and Design, 2003. **81**(1): p. 48-57.
7. Chan, H. and J.R. Fair, *Prediction of point efficiencies on sieve trays. 1. Binary systems.* Industrial & Engineering Chemistry Process Design and Development, 1984. **23**(4): p. 814-819.
8. Garcia, J.A. and J.R. Fair, *A fundamental model for the prediction of distillation sieve tray efficiency. 1. Database development.* Industrial & Engineering Chemistry Research, 2000. **39**(6): p. 1809-1817.
9. Committee, A.I.o.C.E.R., *Bubble-Tray: Design Manual Prediction of Fractionation Efficiency*. 1958: American Institute of Chemical Engineers.
10. Vennavelli, A.N., J.R. Whiteley, and M.R. Resetarits, *New Fraction Jetting Model for Distillation Sieve Tray Efficiency Prediction.* Industrial & Engineering Chemistry Research, 2012. **51**(35): p. 11458-11462.
11. Wagner, I., J. Stichlmair, and J.R. Fair, *Mass transfer in beds of modern, high-efficiency random packings.* Industrial & engineering chemistry research, 1997. **36**(1): p. 227-237.
12. Wang, G.Q., X.G. Yuan, and K.T. Yu, *Review of Mass-Transfer Correlations for Packed Columns**. Industrial & Engineering Chemistry Research, 2005. **44**(23): p. 8715-8729.
13. Sherwood, T.K. and F.L. Holloway, *Performance of packed towers-liquid film data for several packings.* Trans Am. Inst. Chem. Engrs, 1940. **36**: p. 39-70.
14. Shulman, H.L. and J.J. DeGouff, *Mass Transfer Coefficients and Interfacial Areas for 1-Inch Raschig Rings.* Industrial & Engineering Chemistry, 1952. **44**(8): p. 1915-1922.
15. Cornell, D., W. Knapp, and J. Fair, *Mass transfer efficiency packed columns part 1.* Chem. Eng. Prog, 1960. **56**(8): p. 68.
16. Billet, R. and M. Schultes, *Prediction of Mass Transfer Columns with Dumped and Arranged Packings: Updated Summary of the Calculation Method of Billet*

and Schultes. Chemical Engineering Research and Design, 1999. **77**(6): p. 498-504.
17. Stichlmair, J., Stemmer, A.,, *Influence of Maldistribution on Mass Transfer in Packed Columns.* I. Chem. Series, 1987. **104**: p. B213-B224.
18. Krishnamurthy, R. and R. Taylor, *A nonequilibrium stage model of multicomponent separation processes. Part III: The influence of unequal component-efficiencies in process design problems.* AIChE journal, 1985. **31**(12): p. 1973-1985.
19. Krishnamurthy, R. and R. Taylor, *A nonequilibrium stage model of multicomponent separation processes. Part II: Comparison with experiment.* AIChE Journal, 1985. **31**(3): p. 456-465.
20. Krishnamurthy, R. and R. Taylor, *A nonequilibrium stage model of multicomponent separation processes. Part I: Model description and method of solution.* AIChE Journal, 1985. **31**(3): p. 449-456.
21. Rocha, J.A., J.L. Bravo, and J.R. Fair, *Distillation columns containing structured packings: a comprehensive model for their performance. 1. Hydraulic models.* Industrial & Engineering Chemistry Research, 1993. **32**(4): p. 641-651.
22. Hanley, B., *On packed column hydraulics.* AIChE Journal, 2012. **58**(6): p. 1671-1682.
23. Mackowiak, J., *Fluid dynamics of packed columns*. Principles of the Fluid Dynamic Design of Columns for Gas/Liquid and Liquid/Liquid Systems, London, New York, 2010.
24. Hanley, B. and C.-C. Chen, *New mass-transfer correlations for packed towers.* AIChE Journal, 2011: p. n/a-n/a.
25. Olujic, Z., A.B. Kamerbeek, and J. de Graauw, *A corrugation geometry based model for efficiency of structured distillation packing.* Chemical Engineering and Processing, 1999. **38**(4-6): p. 683-695.
26. Adler, S., et al., *Vision 2020: Separations Roadmap.* American Institute of Chemical Engineers, New York, 2000.
27. Billet, R., *Packed towers in processing and environmental technology*. 1995: VCH.
28. Strigle, R.F., *Packed tower design and applications: random and structured packings*. 1994: Gulf Pub. Co.
29. Kolev, N., *Packed bed columns: for absorption, desorption, rectification and direct heat transfer*. 2006: Elsevier.
30. Iliuta, I. and F. Larachi, *Mechanistic Model for Structured-Packing-Containing Columns: Irrigated Pressure Drop, Liquid Holdup, and Packing Fractional Wetted Area.* Industrial & Engineering Chemistry Research, 2001. **40**(23): p. 5140-5146.
31. Suess, P. and L. Spiegel, *Hold-up of mellapak structured packings.* Chemical Engineering and Processing, 1992. **31**(2): p. 119-124.
32. Rocha, J.A., J.L. Bravo, and J.R. Fair, *Distillation Columns Containing Structured Packings: A Comprehensive Model for Their Performance. 2. Mass-Transfer Model.* Industrial & Engineering Chemistry Research, 1996. **35**(5): p. 1660-1667.

33. Olujic, Z., et al., *Predicting the efficiency of corrugated sheet structured packings with large specific surface area.* Chemical and Biochemical Engineering Quarterly, 2004. **18**(2): p. 89-96.
34. Olujic, Z., *Development of a complete simulation model for predicting the hydraulic and separation performance or distillation columns equipped with structured packings.* Chemical and Biochemical Engineering Quarterly, 1997. **11**(1): p. 31-46.
35. Olujic, Z., et al., *Stretching the Capacity of Structured Packings†.* Industrial & Engineering Chemistry Research, 2001. **40**(26): p. 6172-6180.
36. Nusselt, W., *Die Oberflachen-Kondensation des Wasserdampfes. 2.* Verein. Deutsch. Ing, 1916. **60**: p. 541-569.
37. Zhou, D., T. Gambaryan-Roisman, and P. Stephan, *Measurement of water falling film thickness to flat plate using confocal chromatic sensoring technique.* Experimental Thermal and Fluid Science, 2009. **33**(2): p. 273-283.
38. Lel, V., et al., *Local thickness and wave velocity measurement of wavy films with a chromatic confocal imaging method and a fluorescence intensity technique.* Experiments in fluids, 2005. **39**(5): p. 856-864.
39. Zakeri, A., A. Einbu, and H.F. Svendsen, *Experimental investigation of liquid holdup in structured packings.* Chemical Engineering Research and Design, 2012. **90**(5): p. 585-590.
40. Verschoof, H.-J., Z. Olujic, and J.R. Fair, *A General Correlation for Predicting the Loading Point of Corrugated Sheet Structured Packings.* Industrial & Engineering Chemistry Research, 1999. **38**(10): p. 3663-3669.
41. Alix, P. and L. Raynal, *Liquid distribution and liquid hold-up in modern high capacity packings.* Chemical Engineering Research and Design, 2008. **86**(6): p. 585-591.
42. Mackowiak, J., *Pressure drop in irrigated packed columns.* Chemical Engineering and Processing: Process Intensification, 1991. **29**(2): p. 93-105.
43. Stichlmair, J., J.L. Bravo, and J.R. Fair, *General model for prediction of pressure drop and capacity of countercurrent gas/liquid packed columns.* Gas Separation & Purification, 1989. **3**(1): p. 19-28.
44. Valenz, L., F.J. Rejl, and V. Linek, *Gas and Liquid Axial Mixing in the Column Packed with Mellapak 250Y, Pall Rings 25, and Intalox Saddles 25 under Flow Conditions Prevailing in Distillation Columns.* Industrial & Engineering Chemistry Research, 2010. **49**(20): p. 10016-10025.
45. Ruan, B., H. Li, and Q. Wang. *Theoretical analysis on film thickness of intertube falling-film flow with a countercurrent gas flow*. in *ASME 2011 International Mechanical Engineering Congress and Exposition*. 2011. American Society of Mechanical Engineers.
46. Roy, R. and S. Jain, *A study of thin water film flow down an inclined plate without and with countercurrent air flow.* Experiments in fluids, 1989. **7**(5): p. 318-328.
47. Olujic, Z., A.F. Seibert, and J.R. Fair, *Influence of corrugation geometry on the performance of structured packings: an experimental study.* Chemical Engineering and Processing, 2000. **39**(4): p. 335-342.

48. Anil Krishna Jammula., R.W., *Development and Evaluation of Liquid Holdup Models in Preloading Region for a Sheet Metal Structured Packing. Part I.* Chemical Engineering Research and Design, 2015.
49. Anil Krishna Jammula., R.W., *Development and Evaluation of Liquid Holdup and Flooding Velocity Models to Identify Flooding Region for a Sheet Metal Structured Packing. Part III.* Chemical Engineering Research and Design, 2015.
50. Anil Krishna Jammula. Rob Whiteley., T.C., Mike Resetarits.,, *Performance Comparison of Structured Packing HETP Correlations*, in *AIChE Spring Meeting*. 2012: Houston, TX.
51. Anil Krishna Jammula., R.W., Tony Cai., Mike Resetarits.,. *Performance comarison of literature liquid holdup and pressure drop correlations*. in *AIChE Spring Meeting*. 2013. San Antonion, TX.
52. Gualito, J.J., et al., *Design Method for Distillation Columns Filled with Metallic, Ceramic, or Plastic Structured Packings.* Industrial & Engineering Chemistry Research, 1997. **36**(5): p. 1747-1757.
53. Zapke, A. and D. Kröger, *Countercurrent gas–liquid flow in inclined and vertical ducts—I: Flow patterns, pressure drop characteristics and flooding.* International journal of multiphase flow, 2000. **26**(9): p. 1439-1455.
54. Fitz, C.W., J.G. Kunesh, and A. Shariat, *Performance of Structured Packing in a Commercial-Scale Column at Pressures of 0.02−27.6 bar.* Industrial & Engineering Chemistry Research, 1998. **38**(2): p. 512-518.
55. Sherwood, T., G. Shipley, and F. Holloway, *Flooding velocities in packed columns.* Industrial & Engineering Chemistry, 1938. **30**(7): p. 765-769.
56. Eckert, J., *How tower packings behave.* Chemical Engineering, 1975. **82**(8): p. 70-76.
57. Kister, H. and D. Gill, *Predict Flood Point and Pressure-Drop for Modern Random Packings.* Chemical Engineering Progress, 1991. **87**(2): p. 32-42.
58. LEVA, M., *Reconsider packed-tower pressure-drop correlations.* Chemical engineering progress, 1992. **88**(1): p. 65-72.
59. Maćkowiak, J., *Determination of flooding gas velocity and liquid hold-up at flooding in packed columns for gas/liquid systems.* Chemical Engineering & Technology, 1990. **13**(1): p. 184-196.
60. Brunazzi, E., R. Macías-Salinas, and A. Viva, *CALCULATION PROCEDURE FOR FLOODING IN PACKED COLUMNS USING A CHANNEL MODEL.* Chemical Engineering Communications, 2008. **196**(3): p. 330-341.
61. Lockett, M.J., *FLOODING OF ROTATING STRUCTURED PACKING AND ITS APPLICATION TO CONVENTIONAL PACKED-COLUMNS.* Chemical engineering research & design, 1995. **73**(A4): p. 379-384.
62. Spiegel, L., Meier, W.,, *Correlations of the performance Characteristics of the Various MELLAPAK Types.* I. Chem. E. Symposium Series, 1987. **104**: p. A203-A215.
63. Kuźniewska-lach, I., *Estimation of phase velocities at flooding point in packed columns for any gas/liquid system.* The Canadian Journal of Chemical Engineering, 1999. **77**(3): p. 439-446.

64. Anil Krishna Jammula., R.W., *Development and Evaluation of Liquid Holdup and Load Point Models in Loading Region for a Sheet Metal Structured Packing. Part II.* Chemical Engineering Research and Design, 2015.
65. Wallis, G.B., *One-dimensional two-phase flow.* 1969.
66. Lockett, M., R. Victor, and J. Billingham. *Structured packing flooding: its measurement and prediction*. in *INSTITUTION OF CHEMICAL ENGINEERS SYMPOSIUM SERIES*. 2006. Institution of Chemical Engineers; 1999.
67. Macías-Salinas, R. and J.R. Fair, *Axial mixing in modern packings, gas and liquid phases: I. Single-phase flow.* AIChE Journal, 1999. **45**(2): p. 222-239.
68. Pondebat, C.P., J. L. Huor, M. H. Prevost, M., *Hydrodynamics of a gas-liquid column equipped with a structured packing.* INSTITUTION OF CHEMICAL ENGINEERS SYMPOSIUM SERIES, 1992. **VOL 128/2**: p. pages B253.

APPENDICES

A. Preloading Literature Models performance using experimental liquid holdup preloading data (Table 2.1)

A.1. Alix-1 Model [41]:

$$h_L = h_{L_0} + K^P \frac{\Gamma}{\rho_L} \left(\frac{\mu_L}{\mu_w}\right)^{\frac{1}{3}}$$

$$\Gamma = \rho_L \frac{V_{SL}}{a_g}$$

$$K^P = 691\ [s\ m^{-2}]$$

$$h_{L_0} = 6.3\%$$

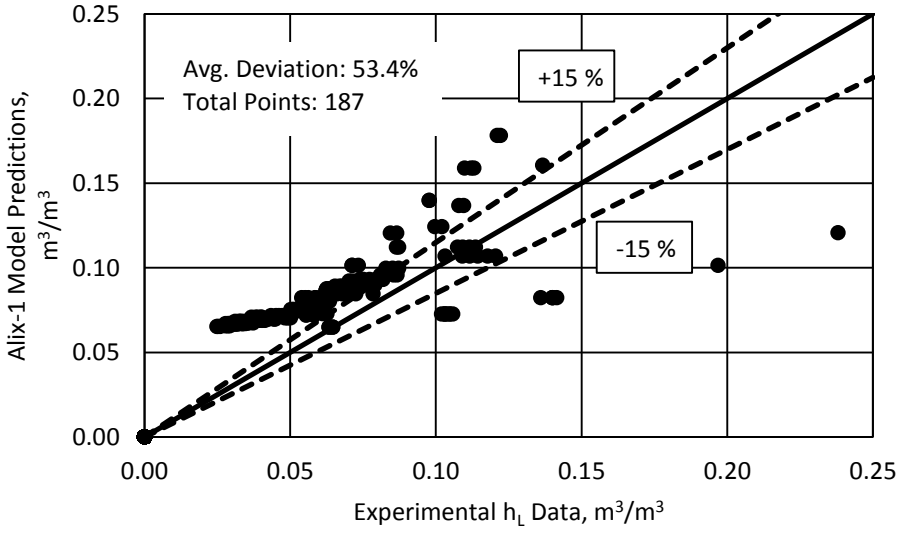

Fig. A.1. Alix-1 preloading model predictions vs experimental liquid holdup preloading data

A.2. Alix-2 Model [41]:

$$h_L = h_{L_0} + C_1 \Gamma^{0.4} \left(\frac{\mu_L}{\mu_w}\right)^{\frac{1}{3}}$$

$$Re_L = \frac{4\Gamma}{\mu_L} = \frac{4\,\rho_L V_{SL}}{a_g \mu_L}$$

$$C_1 = 0.2683\ [s\,m^{-2}]$$

$$Re_{L_0} = \frac{4\,\Gamma_0}{\mu_L} = 800$$

$$h_{L_0} = 0.032\,\frac{\Gamma}{\Gamma_0}\ for\ Re_L \le Re_{L_0}$$

$$h_{L_0} = 0.032\ for\ Re_L > Re_{L_0}$$

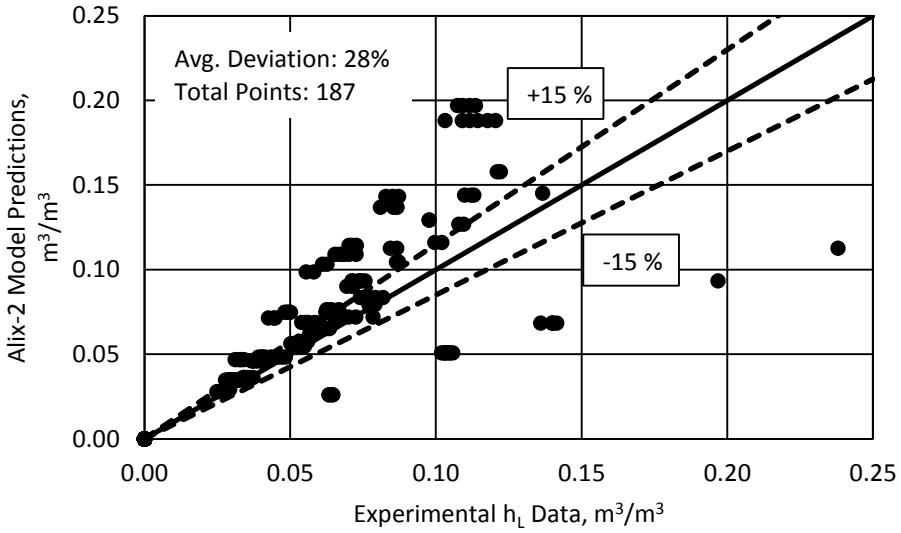

Fig. A.2. Alix-2 preloading model predictions vs experimental liquid holdup preloading data

A.3. Delft Model [25, 33-35]:

$$\alpha_L = arctan\left[\frac{cos\,(90-\alpha)}{\sin(90-\alpha)\cos\left[arctan\left(\frac{b}{2h}\right)\right]}\right]$$

$$\delta = \left(\frac{3\,\mu_L\,u_{Ls}}{\rho_L g\,a_P \sin\alpha_L}\right)^{\frac{1}{3}}$$

$$h_L = \delta\,a_P$$

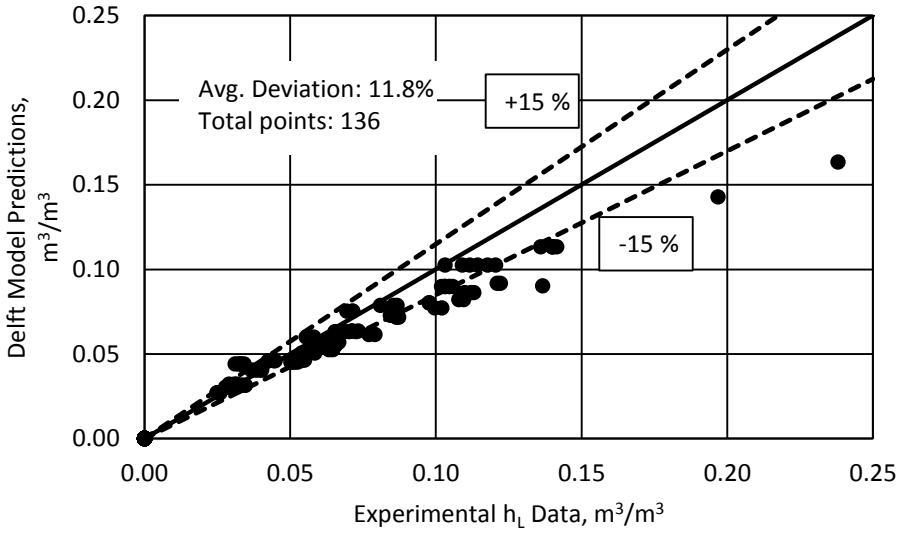

Fig. A.3. Delft preloading model predictions vs experimental liquid holdup preloading data

A.4. Gualito Model [52]:

$$\left(\frac{\Delta P}{\Delta Z}\right)_{dry} = \left(\frac{\rho_G}{\rho_{(air,1\ bar)}}\right)^{0.4}\left(\frac{0.177\ \rho_G U_{GS}^2}{S\ \epsilon^2(\sin\theta)^2} + \frac{88.77\ u_G U_{GS}}{S^2\epsilon\sin\theta}\right)$$

$$F_t = \frac{a_e}{a_p} = \frac{(We_L Fr_L)^{0.15} 29.12\ S^{0.36}}{Re_L^{0.2}\ \epsilon^{0.6}(1-0.93\cos\gamma)(\sin\theta)^{0.3}}$$

$$\left(\frac{\Delta P}{\Delta Z}\right)_{flood} = 1500 + 65000\ U_{LS}$$

Solve below equations,

$$h_L = \left[\frac{4\ F_t}{S}\right]^{\frac{2}{3}}\left\{\frac{3\ \mu_L U_{Ls}}{\rho_L\epsilon\sin\theta\left[\left(\frac{\rho_L-\rho_G}{\rho_L}\right)\left(1-\frac{\left(\frac{\Delta P}{\Delta Z}\right)_{new}}{\left(\frac{\Delta P}{\Delta Z}\right)_{flood}}\right)\right]}\right\}^{\frac{1}{3}}$$

$$\frac{\Delta P}{\Delta Z} = \frac{\left(\frac{\Delta P}{\Delta Z}\right)_{dry}}{[1-(0.614+71.35\ S)h_L]^5}$$

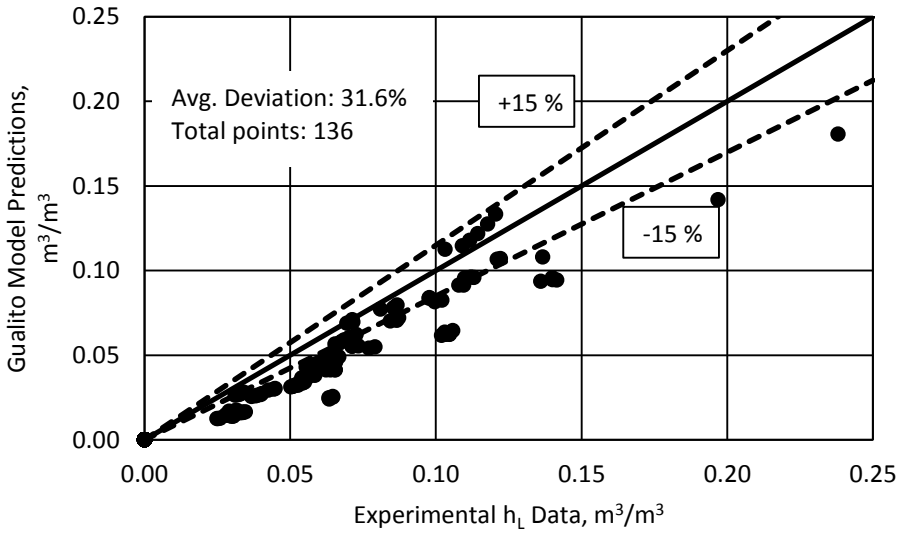

Fig. A.4. Gualito preloading model predictions vs experimental liquid holdup preloading data

A.5. Macias Model [67]:

$$d_{eq} = Bh\left[\frac{1}{B+2S}+\frac{1}{2S}\right]$$

$$Fi = \frac{Fr}{Re} = \frac{\left(\frac{v_s^2}{g\ d_{eq}}\right)}{\frac{v_s d_{eq}\rho}{\eta}}$$

$$H_t = 0.05557\ Fi^{0.3165}\left(\frac{3}{\sin^2\emptyset}\right)^{0.8767}\left(d_{eq}\ a_p\right)^{2.405}$$

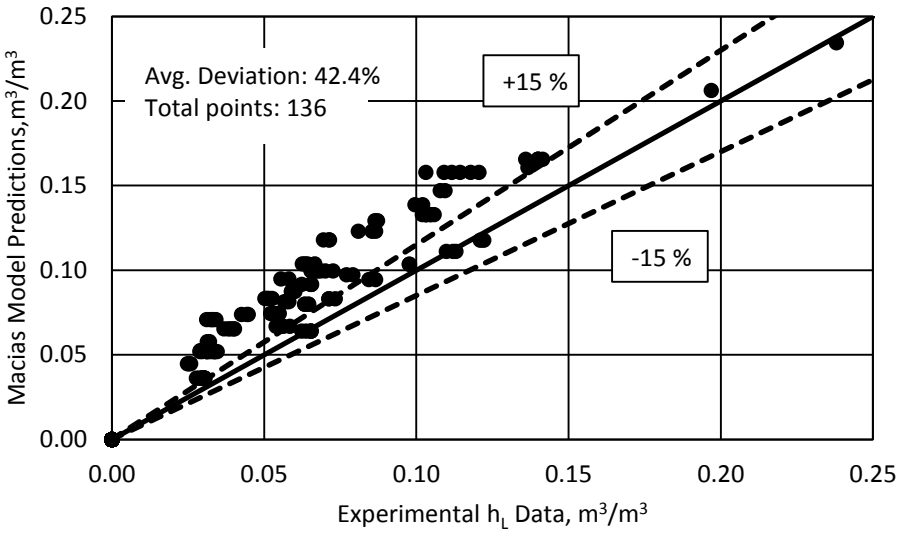

Fig. A.5. Macias preloading model predictions vs experimental liquid holdup preloading data

A.6. Mackowiak-2 Model [42]:

$$h_L = 0.465 \left(\frac{u_L^2 a}{g}\right)^{\frac{1}{3}}$$

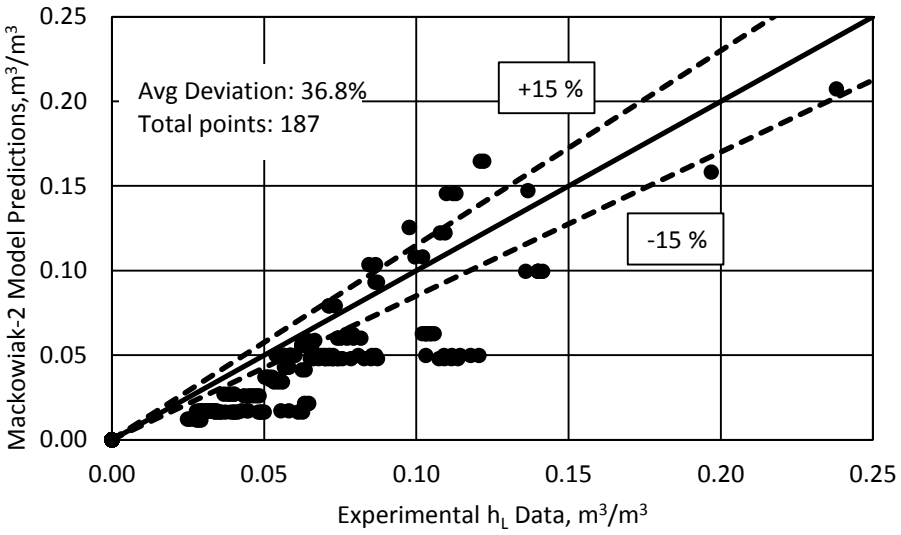

Fig. A.6. Mackowiak-2 preloading model predictions vs experimental liquid holdup preloading data

A.7. Mackowiak Model [23]:

$$d_P = \frac{6\,(1-\varepsilon)}{a}$$

$$B_L = \left(\frac{\mu_L}{g^2 \rho_L}\right)^{\frac{1}{3}} \left(\frac{u_L}{\varepsilon}\right) \left(\frac{1-\varepsilon}{\varepsilon\, d_P}\right)$$

$$h_L = 2.2\, B_L^{0.5}$$

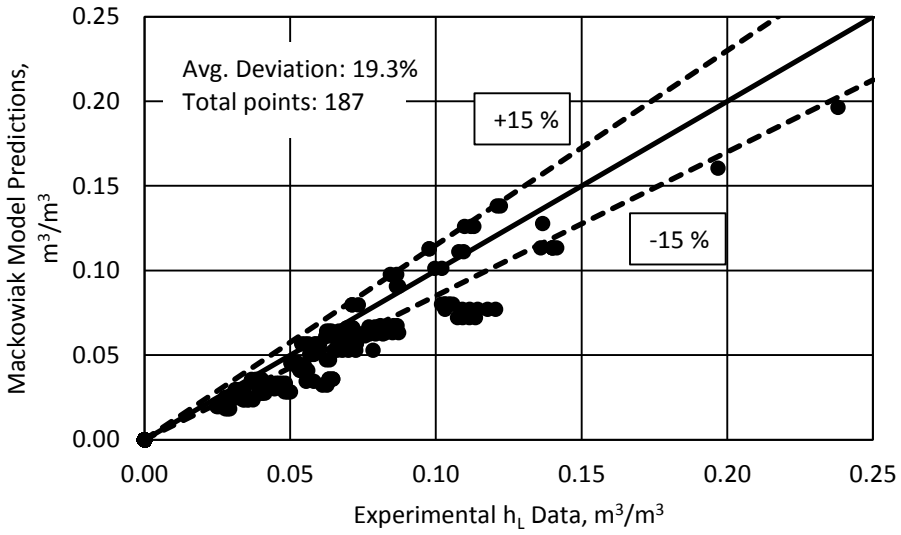

Fig. A.7. Mackowiak-2 preloading model predictions vs experimental liquid holdup preloading data

A.8. Pondebat Model [68]:

$$h_L = K_3 \left[\frac{\mu_L}{\rho_L v_{Water}}\right]^{A_5} u_L^{A_6} \exp(K_4\, u_V\, \rho_G^{0.5})$$

$$u_{L,Eff} = \left[\frac{3\, u_L}{2\, Per}\right] \left[\frac{(g\, Per)}{3\, \nu_L\, u_L}\right]^{\frac{1}{3}}$$

$$Per = \frac{4\, S + B}{B\, h}$$

If $u_{L,Eff} \leq 0.255$, $K_3 = 0.38548$, $A_5 = 0.17954$, $A_6 = 0.36739$, $K_4 = 0.02048$

If $0.255 \leq u_{L,Eff} \leq 0.36$, $K_3 = 1.0467$, $A_5 = 0.056825$, $A_6 = 0.5867$, $K_4 = 0.03956$

If $u_{L,Eff} \geq 0.255$, $K_3 = 1.8229$, $A_5 = -0.04219$, $A_6 = 0.7191$, $K_4 = 0.04258$

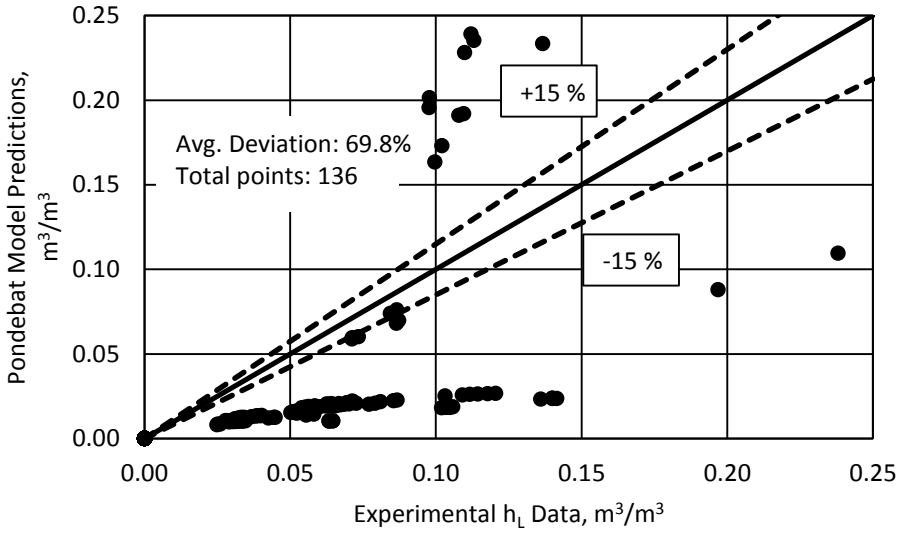

Fig. A.8. Pondebat preloading model predictions vs experimental liquid holdup preloading data

A.9. Spiegel Model [31]:

$$h_L = \left(c\, a_d^{0.83}\, u_L^x \left(\frac{\mu_L}{\mu_{Water}}\right)^{0.25} \right)$$

$$c = 0.0169\ and\ x = 0.37\ if\ u_L < 40$$

$$c = 0.0075\ and\ x = 0.59\ if\ u_L > 40$$

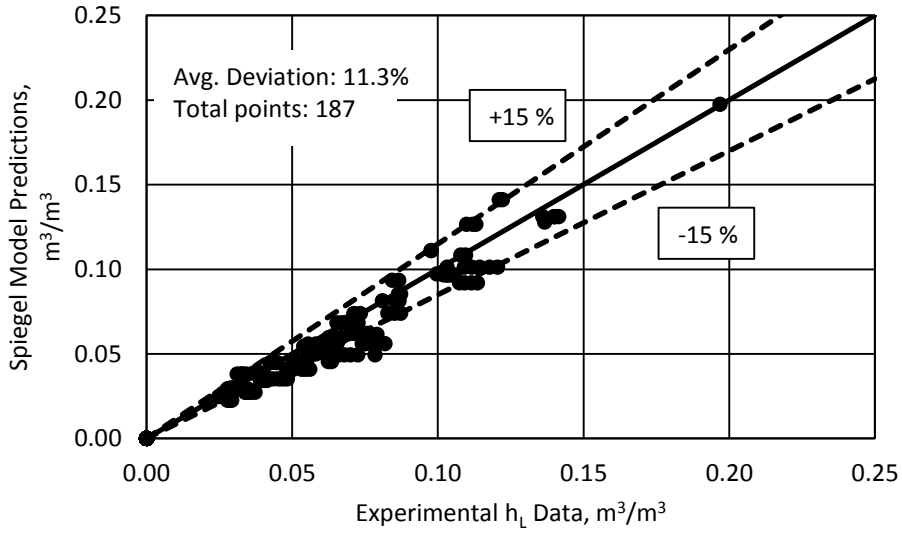

Fig. A.9. Spiegel preloading model predictions vs experimental liquid holdup preloading data

A.10. SRP Model [21]:

$$\left(\frac{\Delta P}{\Delta Z}\right)_{dry} = \left(\frac{\rho_G}{\rho_{(air,1\ bar)}}\right)^{0.4}\left(\frac{0.177\ \rho_G U_{GS}^2}{S\ \epsilon^2(\sin\theta)^2} + \frac{88.77\ u_G U_{GS}}{S^2\epsilon\sin\theta}\right)$$

$$F_t = \frac{a_e}{a_p} = \frac{(We_L Fr_L)^{0.15} 29.12\ S^{0.36}}{Re_L^{0.2}\ \epsilon^{0.6}(1-0.93\cos\gamma)(\sin\theta)^{0.3}}$$

Solve the below equations,

$$h_L = \left[\frac{4\ F_t}{S}\right]^{\frac{2}{3}}\left\{\frac{3\ \mu_L U_{Ls}}{\rho_L\epsilon\sin\theta\left[\left(\frac{\rho_L-\rho_G}{\rho_L}\right)\left(1-\frac{\left(\frac{\Delta P}{\Delta Z}\right)_{new}}{\left(\frac{\Delta P}{\Delta Z}\right)_{flood}}\right)\right]}\right\}^{\frac{1}{3}}$$

$$\frac{\Delta P}{\Delta Z} = \frac{\left(\frac{\Delta P}{\Delta Z}\right)_{dry}}{[1-(0.614+71.35\ S)h_L]^5}$$

$$\left(\frac{\Delta P}{\Delta Z}\right)_{flood} = 1025\ Pa/m$$

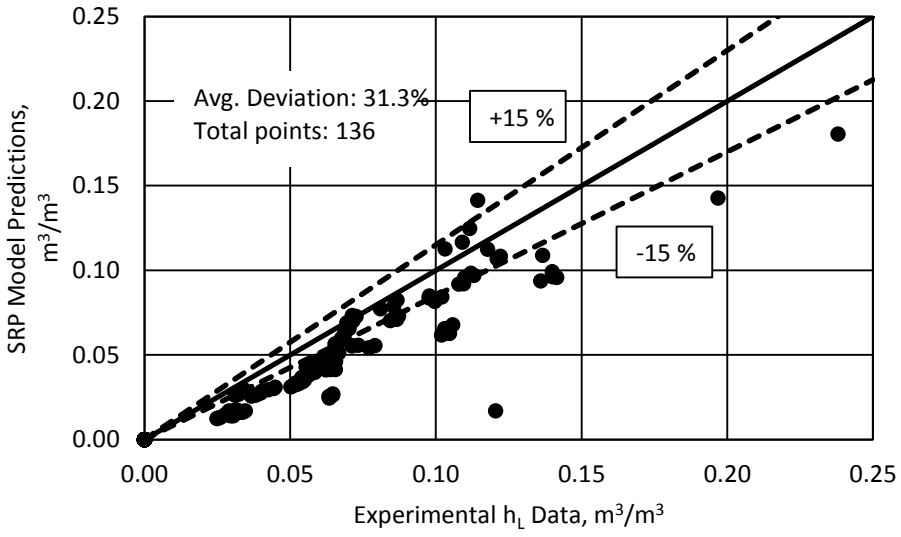

Fig. A.10. SRP preloading model predictions vs experimental liquid holdup preloading data

A.11. Stichlmair Model [43]:

$$h_L = 0.555 \left(U_L^2 \frac{a}{g\, \varepsilon^{4.65}} \right)^{\frac{1}{3}}$$

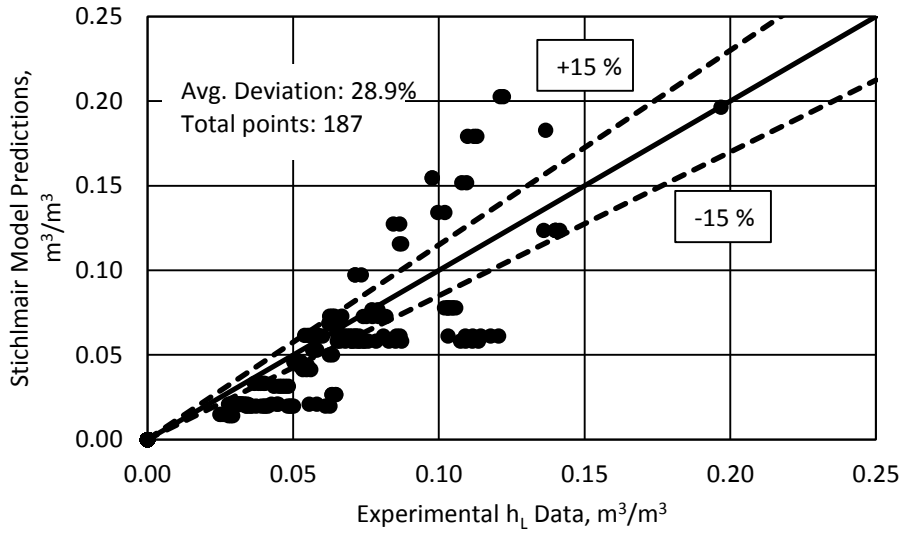

Fig. A.11. Stichlmair preloading model predictions vs experimental liquid holdup preloading data

A.12. Valenz Model [44]:

$$h_L = 0.6844\, Fi^{0.5296} \left(\frac{3}{\sin^2 \alpha}\right)^{0.877} \left(d_{eq} a_p\right)^{2.405}$$

$$Fi = \frac{\eta_L u_L}{d_{eq}^2 \rho_L g}$$

$$d_{eq} = Bh \left[\frac{1}{B + 2S} + \frac{1}{2S}\right]$$

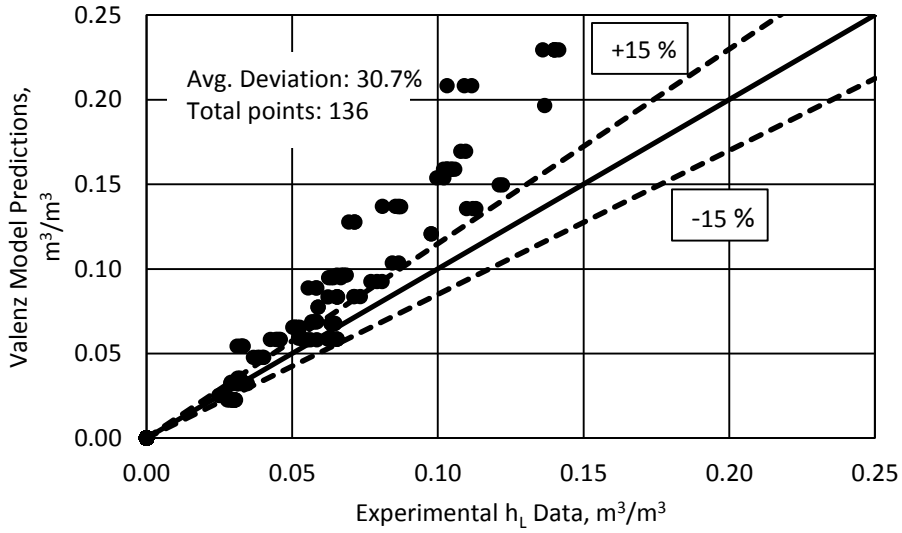

Fig. A.12. Valenz preloading model predictions vs experimental liquid holdup preloading data

B. Data without packing surface area information

Table B.1. Summary of packing data without packing surface area information

Database	Packing	Effective area, (Approximated) m2/m3	Void fraction, ε	s, mm	Preloading	Loading	System
Koch [21]	Gempak 1A	115	96	36	8	7	Air/Water
	Gempak2A	220	95	18	6	7	
	Gempak 4A	453	91	9	5	11	
	Flexipac 1	453	91	9	5	10	
	Flexipac 2	220	95	18	9	15	
	Flexipac 3	115	96	36	15	13	
	Flexipac 4	55	98	72	16	12	
Total Points					64	75	

Table B.2. Summary of literature holdup model performance using experimental liquid holdup data (with approximated packing surface area) in preloading region

Database	Packing	Mean Absolute Relative Error, %								
		OkState Model (Eqn. 2.8)	Alix [41]	Billet [16]	Delft [33]	Mackowiak [42]	Spiegel [31]	SRP [21]	Stichlmair [43]	Valenz [44]
Koch [21]	Gempak 1A	**25.6**	359.3	NA	NA	86.5	35.9	37.7	155.3	70.3
	Gempak2A	**9.3**	82.3	NA	NA	42.5	24.6	9.5	73.7	75.1
	Gempak 4A	19.7	**10.8**	NA	NA	62.0	81.4	39.4	101.0	136.8
	Flexipac 1	**3.9**	20.4	NA	NA	23.2	34.0	5.2	26.5	124.5
	Flexipac 2	9.3	64.7	NA	NA	31.3	16.4	**4.9**	66.0	62.9
	Flexipac 3	**15.1**	308.5	NA	NA	68.9	24.5	28.8	138.0	56.6
	Flexipac 4	13.4	545.5	NA	NA	33.7	21.2	**2.3**	112.3	21.0
Average Deviation		**14.1**	272.8	NA	NA	50.4	29.1	17.1	106.0	63.6

- Lowest error for each packing were bolded
- Billet model error was reported only for the packing with packing specific constants and the ones without them were written as NA
- For models requiring packing dimension information, error was displayed as NA when the packing dimension information was not available

$$MARE,\ \% = \frac{(Measured\ Holdup\ -\ Predicted\ Holdup)}{(Measured\ Holdup)}\ X\ 100$$

B.1. Preloading Literature Models performance using experimental liquid holdup preloading data (Table B.1)

B.1.1. Alix-1 Model [41]:

$$h_L = h_{L_0} + K^P \frac{\Gamma}{\rho_L} \left(\frac{\mu_L}{\mu_w}\right)^{\frac{1}{3}}$$

$$\Gamma = \rho_L \frac{V_{SL}}{a_g}$$

$$K^P = 691\ [s\ m^{-2}]$$

$$h_{L_0} = 6.3\%$$

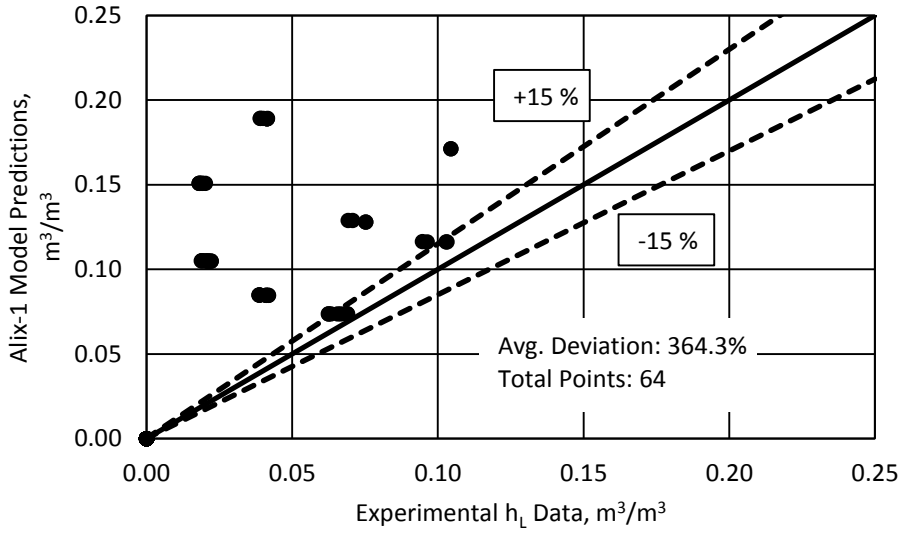

Fig. B.1.1. Alix-1 preloading model predictions vs experimental liquid holdup preloading data

B.1.2. Alix-2 Model [41]:

$$h_L = h_{L_0} + C_1 \Gamma^{0.4} \left(\frac{\mu_L}{\mu_w}\right)^{\frac{1}{3}}$$

$$Re_L = \frac{4\Gamma}{\mu_L} = \frac{4\,\rho_L V_{SL}}{a_g \mu_L}$$

$$C_1 = 0.2683\ [s\,m^{-2}]$$

$$Re_{L_0} = \frac{4\,\Gamma_0}{\mu_L} = 800$$

$$h_{L_0} = 0.032\,\frac{\Gamma}{\Gamma_0}\ for\ Re_L \le Re_{L_0}$$

$$h_{L_0} = 0.032\ for\ Re_L > Re_{L_0}$$

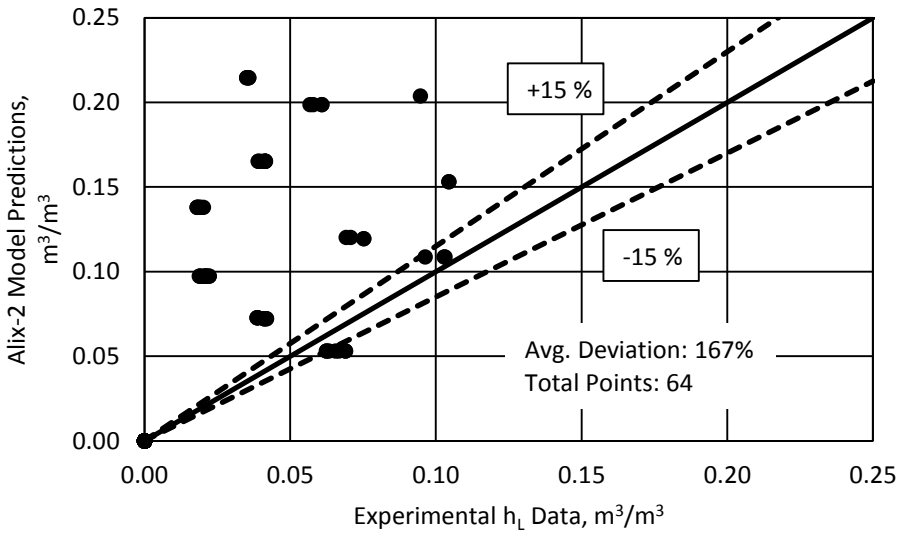

Fig. B.1.2. Alix-2 preloading model predictions vs experimental liquid holdup preloading data

B.1.3. Gualito Model [52]:

$$\left(\frac{\Delta P}{\Delta Z}\right)_{dry} = \left(\frac{\rho_G}{\rho_{(air,1\ bar)}}\right)^{0.4}\left(\frac{0.177\ \rho_G U_{GS}^2}{S\ \epsilon^2(\sin\theta)^2} + \frac{88.77\ u_G U_{GS}}{S^2\epsilon\sin\theta}\right)$$

$$F_t = \frac{a_e}{a_p} = \frac{(We_L Fr_L)^{0.15} 29.12\ S^{0.36}}{Re_L^{0.2}\ \epsilon^{0.6}(1-0.93\cos\gamma)(\sin\theta)^{0.3}}$$

$$\left(\frac{\Delta P}{\Delta Z}\right)_{flood} = 1500 + 65000\ U_{LS}$$

Solve below equations,

$$h_L = \left[\frac{4\ F_t}{S}\right]^{\frac{2}{3}}\left\{\frac{3\ \mu_L U_{Ls}}{\rho_L \epsilon\sin\theta\left[\left(\frac{\rho_L-\rho_G}{\rho_L}\right)\left(1-\frac{\left(\frac{\Delta P}{\Delta Z}\right)_{new}}{\left(\frac{\Delta P}{\Delta Z}\right)_{flood}}\right)\right]}\right\}^{\frac{1}{3}}$$

$$\frac{\Delta P}{\Delta Z} = \frac{\left(\frac{\Delta P}{\Delta Z}\right)_{dry}}{[1-(0.614+71.35\ S)h_L]^5}$$

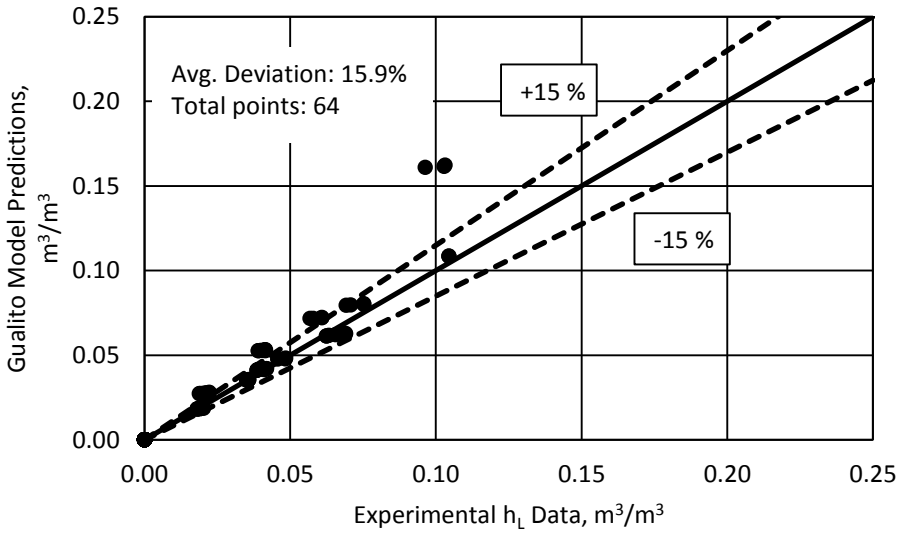

Fig. B.1.3. Gualito preloading model predictions vs experimental liquid holdup preloading data

B.1.4. Mackowiak-2 Model [42]:

$$h_L = 0.465 \left(\frac{u_L^2 a}{g}\right)^{\frac{1}{3}}$$

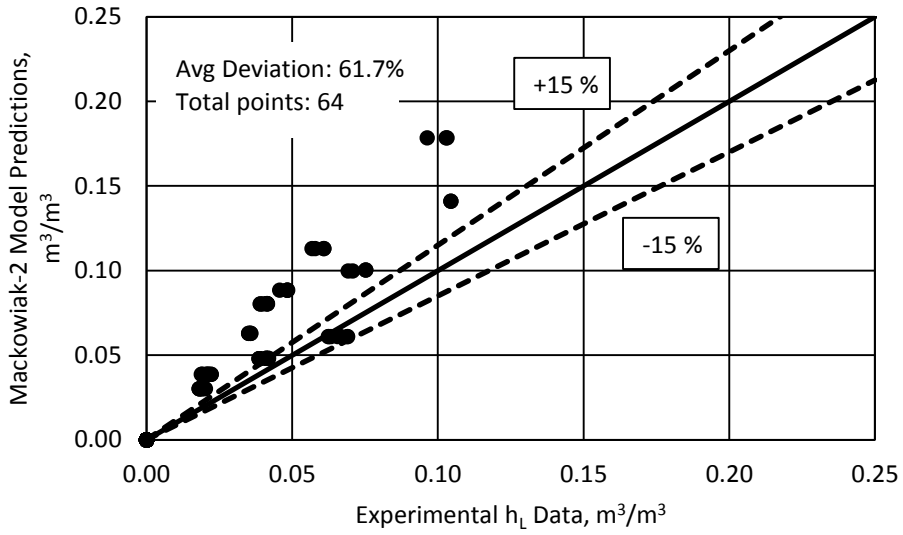

Fig. B.1.4. Mackowiak-2 preloading model predictions vs experimental liquid holdup preloading data

B.1.5. Mackowiak Model [23]:

$$d_P = \frac{6\,(1-\varepsilon)}{a}$$

$$B_L = \left(\frac{\mu_L}{g^2 \rho_L}\right)^{\frac{1}{3}} \left(\frac{u_L}{\varepsilon}\right) \left(\frac{1-\varepsilon}{\varepsilon\, d_P}\right)$$

$$h_L = 2.2\, B_L^{0.5}$$

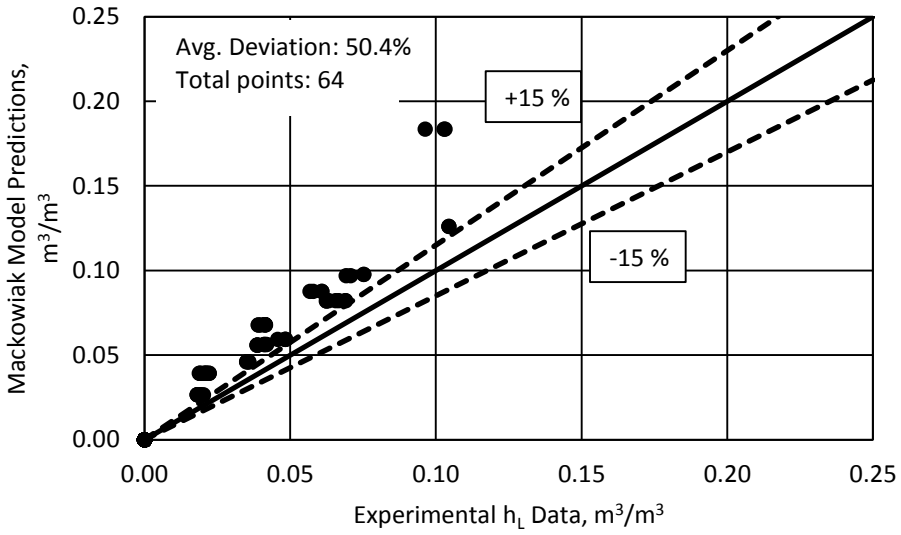

Fig. B.1.5. Mackowiak-2 preloading model predictions vs experimental liquid holdup preloading data

B.1.6. Newly Developed OkState Preload Model:

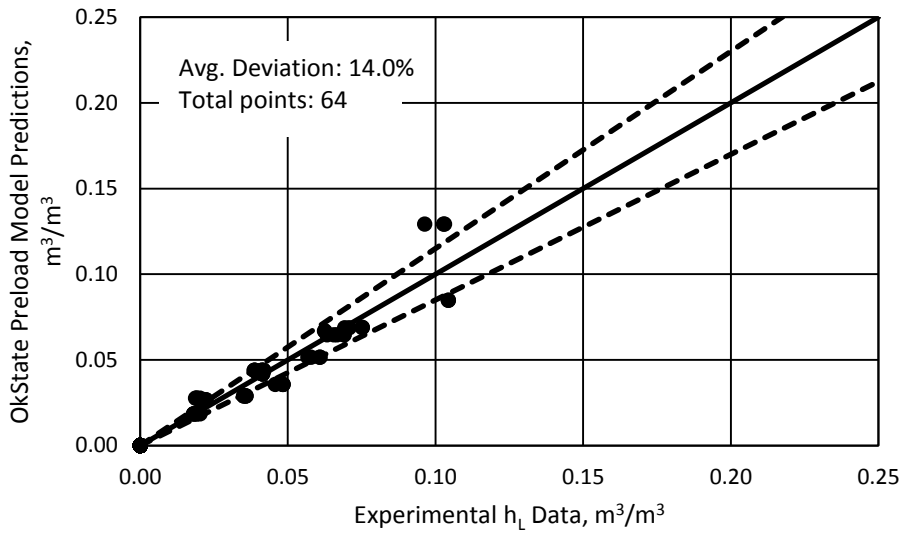

Fig. B.1.6. OkState preload model predictions vs experimental liquid holdup preloading data

B.1.7. Spiegel Model [31]:

$$h_L = \left(c\, a_d^{0.83}\, u_L^x \left(\frac{\mu_L}{\mu_{Water}}\right)^{0.25} \right)$$

$$c = 0.0169\ and\ x = 0.37\ if\ u_L < 40$$

$$c = 0.0075\ and\ x = 0.59\ if\ u_L > 40$$

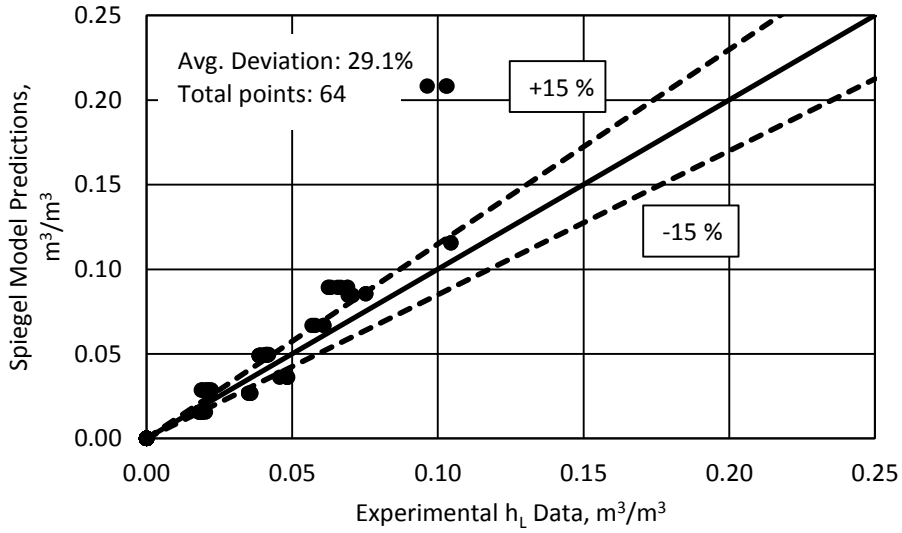

Fig. B.1.7. Spiegel preloading model predictions vs experimental liquid holdup preloading data

B.1.8. SRP Model [21]:

$$\left(\frac{\Delta P}{\Delta Z}\right)_{dry} = \left(\frac{\rho_G}{\rho_{(air,1\ bar)}}\right)^{0.4}\left(\frac{0.177\ \rho_G U_{GS}^2}{S\ \epsilon^2(\sin\theta)^2} + \frac{88.77\ u_G U_{GS}}{S^2\epsilon\sin\theta}\right)$$

$$F_t = \frac{a_e}{a_p} = \frac{(We_L Fr_L)^{0.15} 29.12\ S^{0.36}}{Re_L^{0.2}\ \epsilon^{0.6}(1-0.93\cos\gamma)(\sin\theta)^{0.3}}$$

Solve the below equations,

$$h_L = \left[\frac{4\ F_t}{S}\right]^{\frac{2}{3}}\left\{\frac{3\ \mu_L U_{Ls}}{\rho_L\epsilon\sin\theta\left[\left(\frac{\rho_L-\rho_G}{\rho_L}\right)\left(1-\frac{\left(\frac{\Delta P}{\Delta Z}\right)_{new}}{\left(\frac{\Delta P}{\Delta Z}\right)_{flood}}\right)\right]}\right\}^{\frac{1}{3}}$$

$$\frac{\Delta P}{\Delta Z} = \frac{\left(\frac{\Delta P}{\Delta Z}\right)_{dry}}{[1-(0.614+71.35\ S)h_L]^5}$$

$$\left(\frac{\Delta P}{\Delta Z}\right)_{flood} = 1025\ Pa/m$$

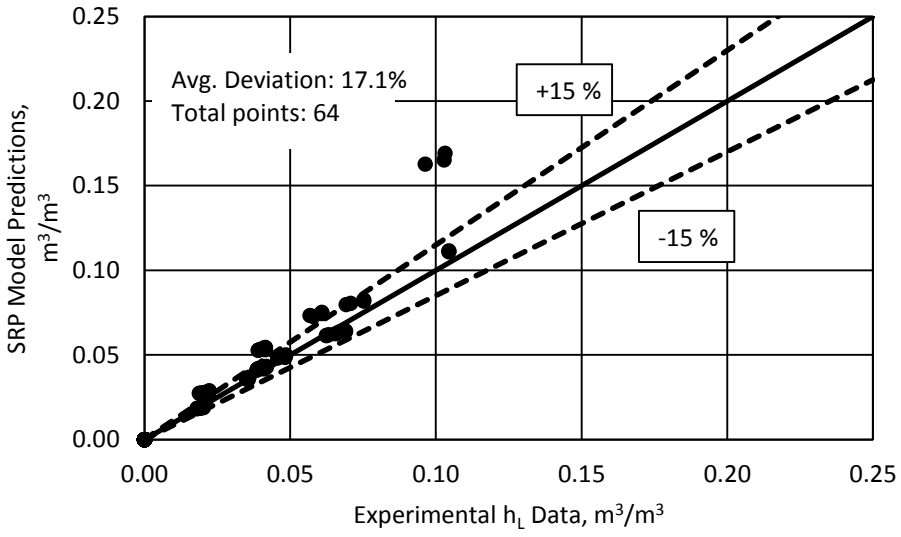

Fig. B.1.8. SRP preloading model predictions vs experimental liquid holdup preloading data

B.1.9. Stichlmair Model [43]:

$$h_L = 0.555 \left(U_L^2 \frac{a}{g\, \varepsilon^{4.65}} \right)^{\frac{1}{3}}$$

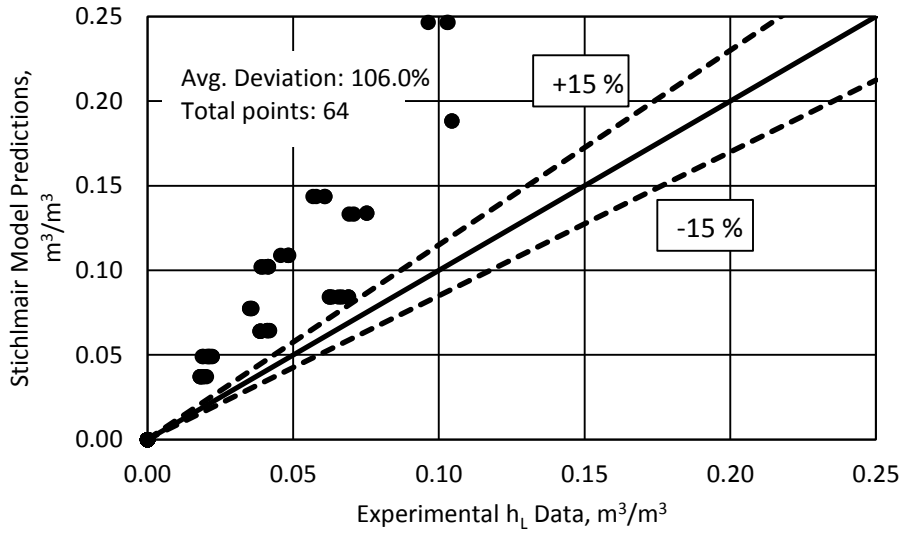

Fig. B.1.9. Stichlmair preloading model predictions vs experimental liquid holdup preloading data

C. Present model predictions for all the data

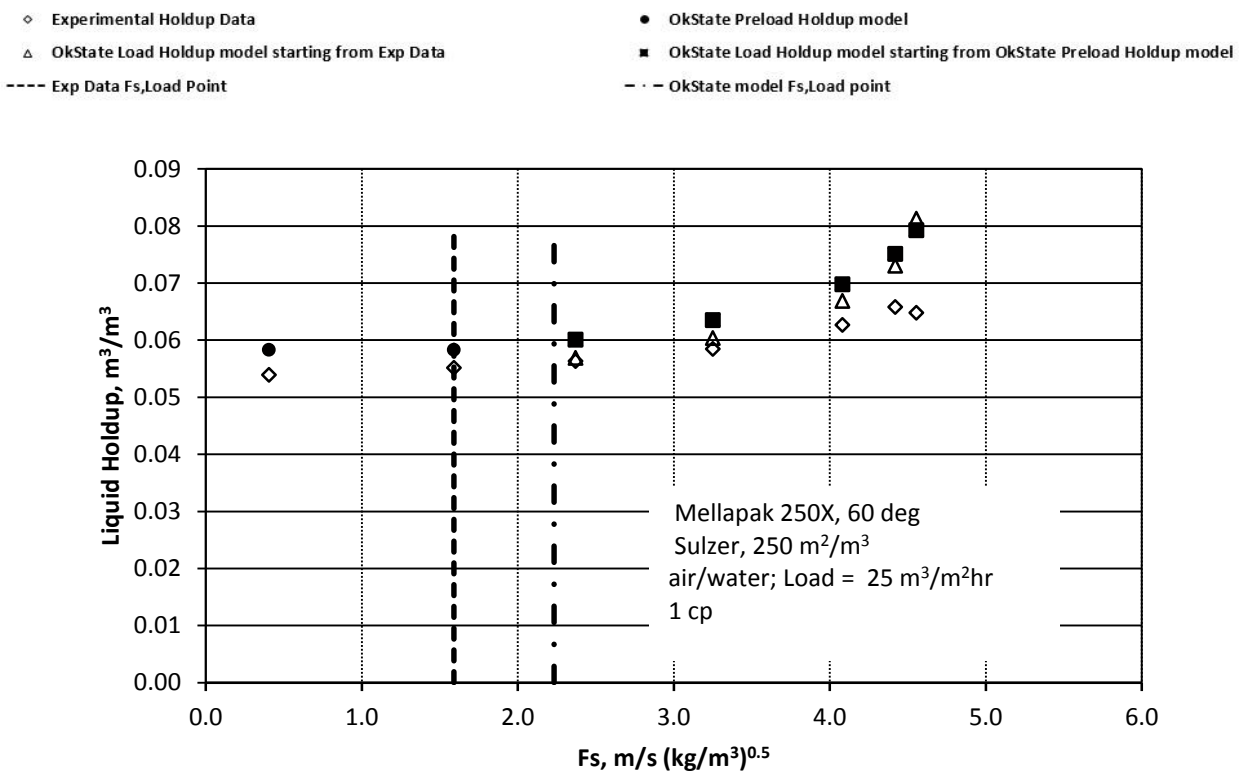

Fig. C.1. OkState liquid holdup model predictions vs. experimental liquid holdup data

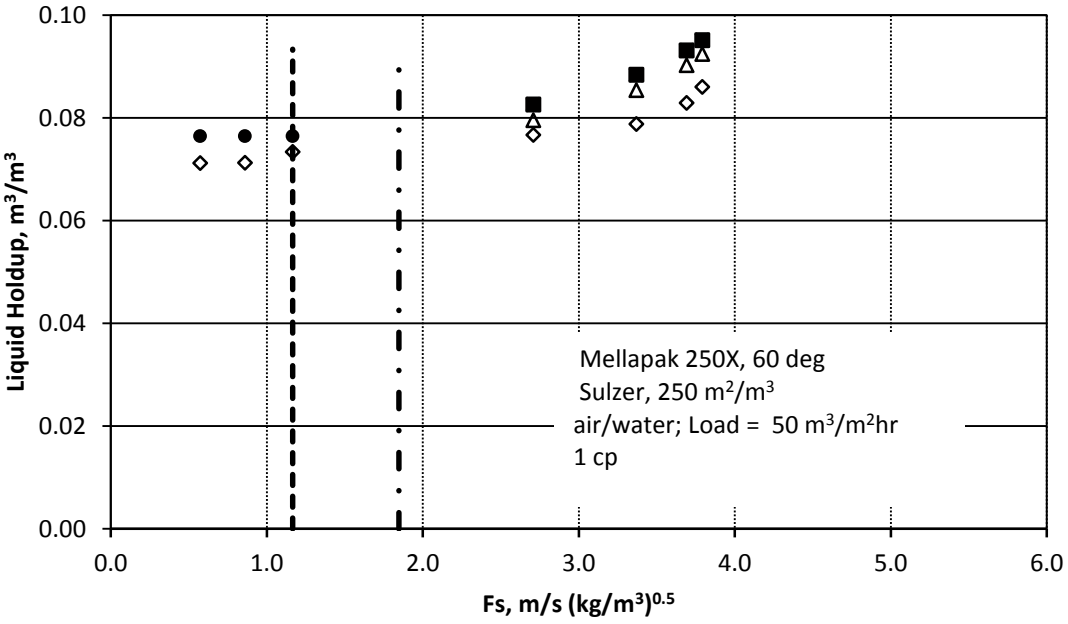

Fig. C.2. OkState liquid holdup model predictions vs. experimental liquid holdup data

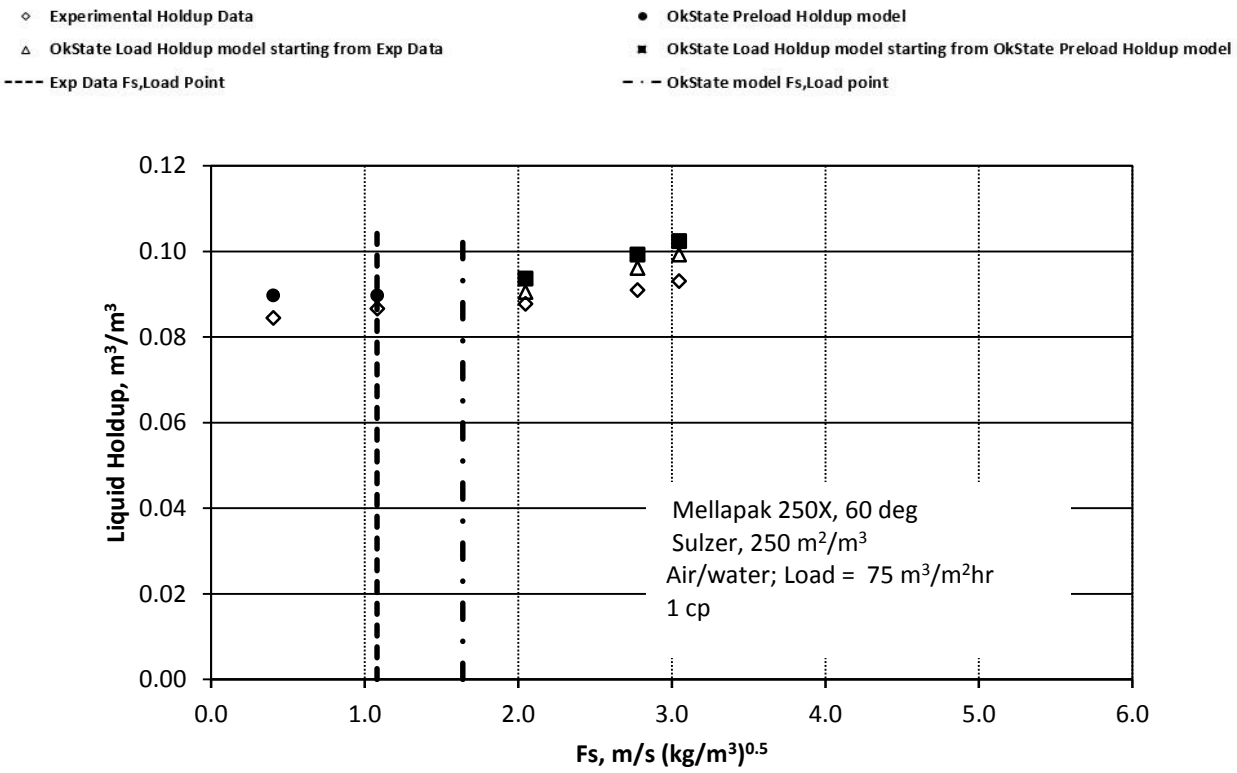

Fig. C.3. OkState liquid holdup model predictions vs. experimental liquid holdup data

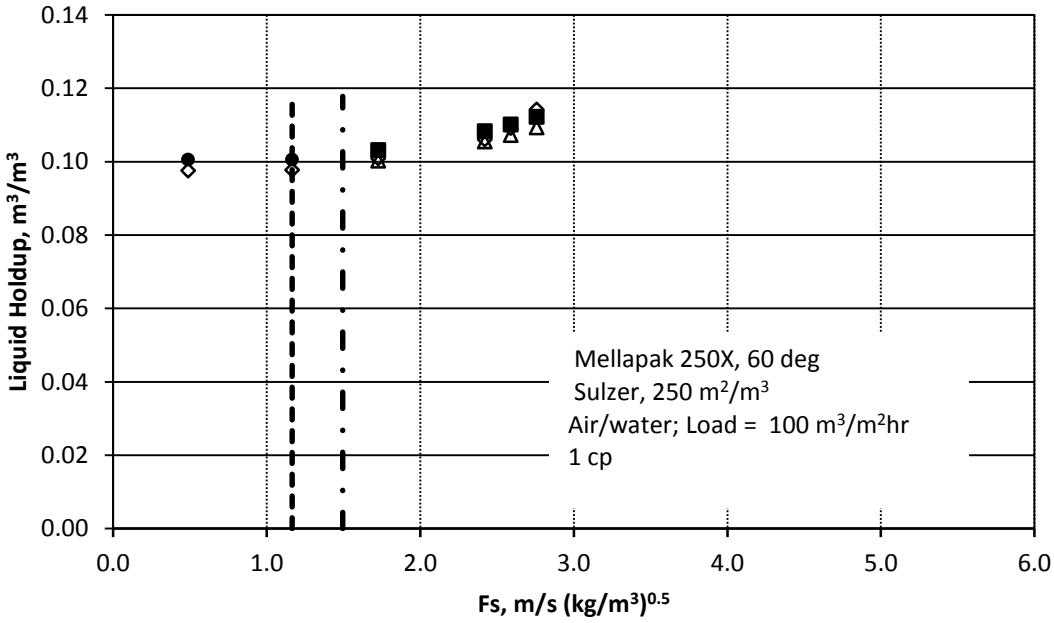

Fig. C.4. OkState liquid holdup model predictions vs. experimental liquid holdup data

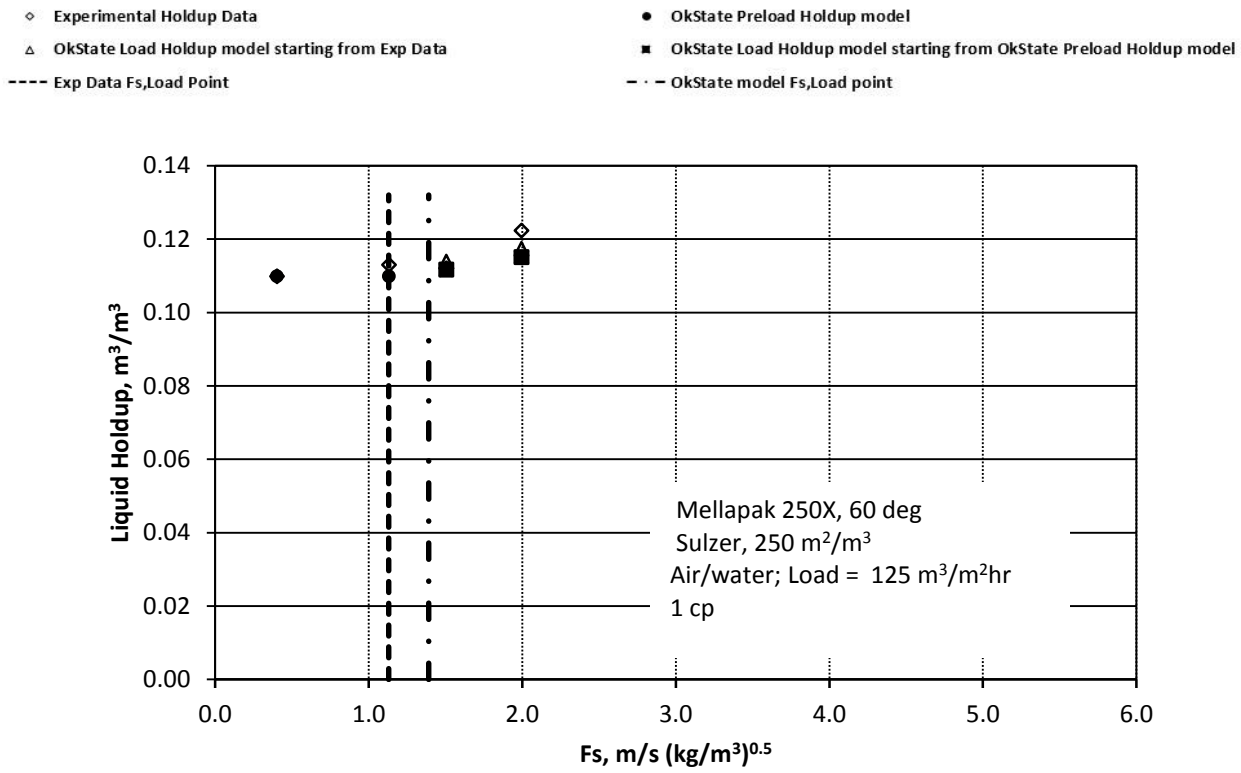

Fig. C.5. OkState liquid holdup model predictions vs. experimental liquid holdup data

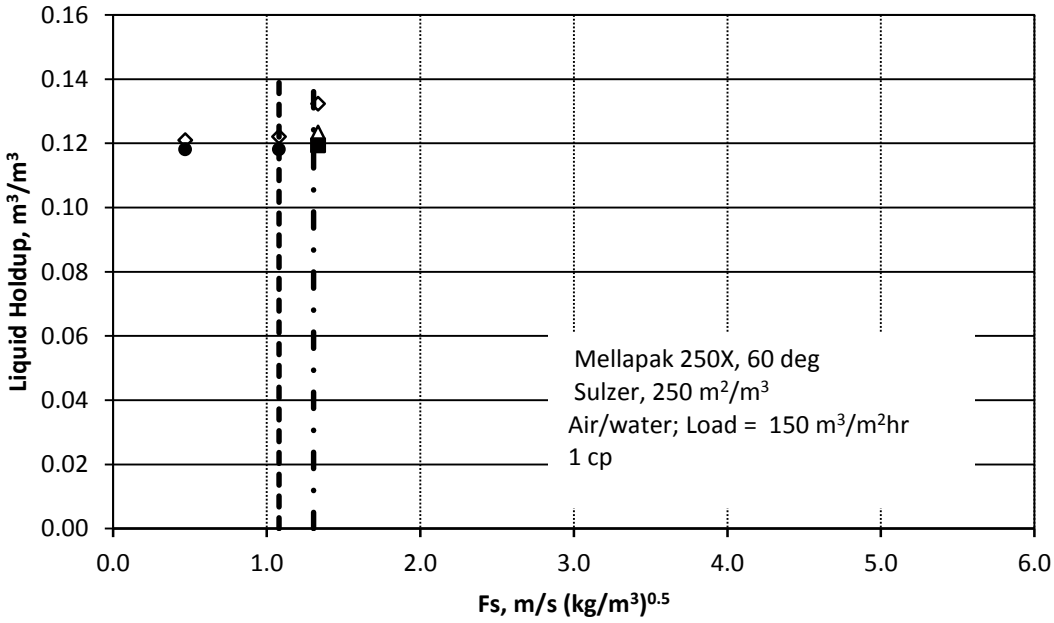

Fig. C.6. OkState liquid holdup model predictions vs. experimental liquid holdup data

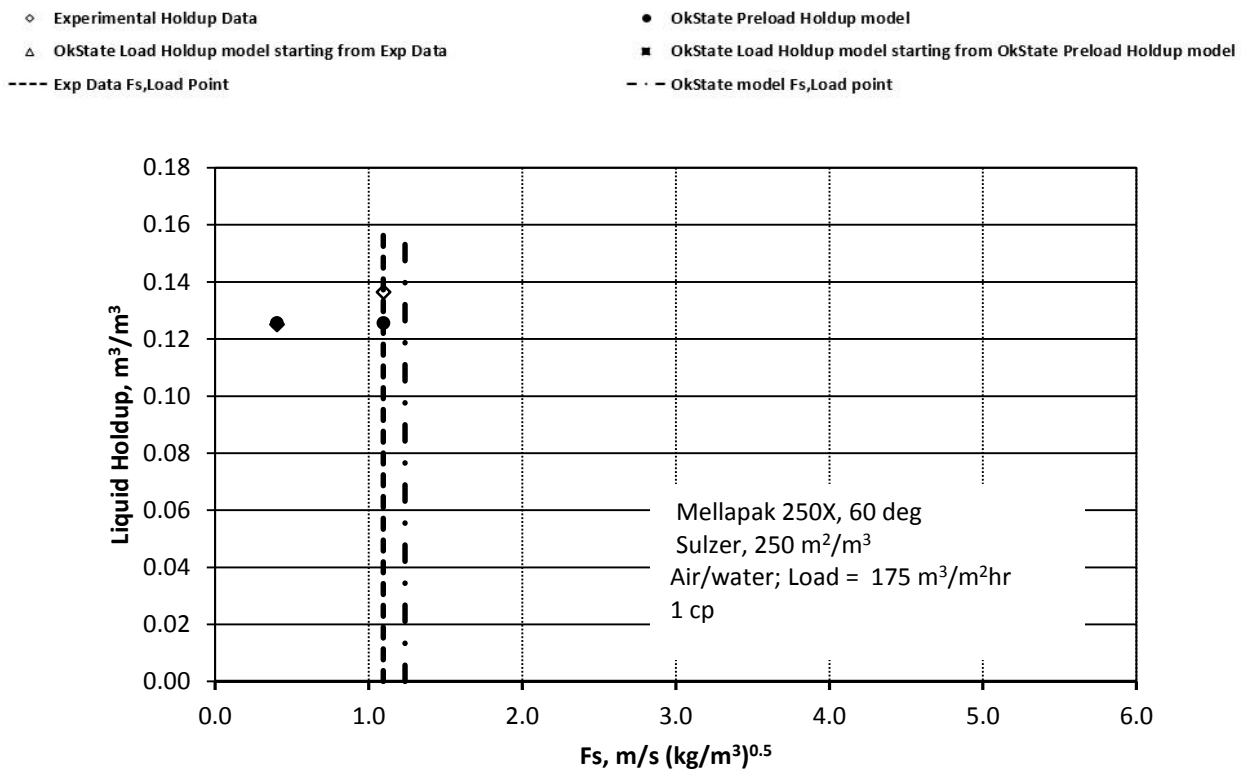

Fig. C.7. OkState liquid holdup model predictions vs. experimental liquid holdup data

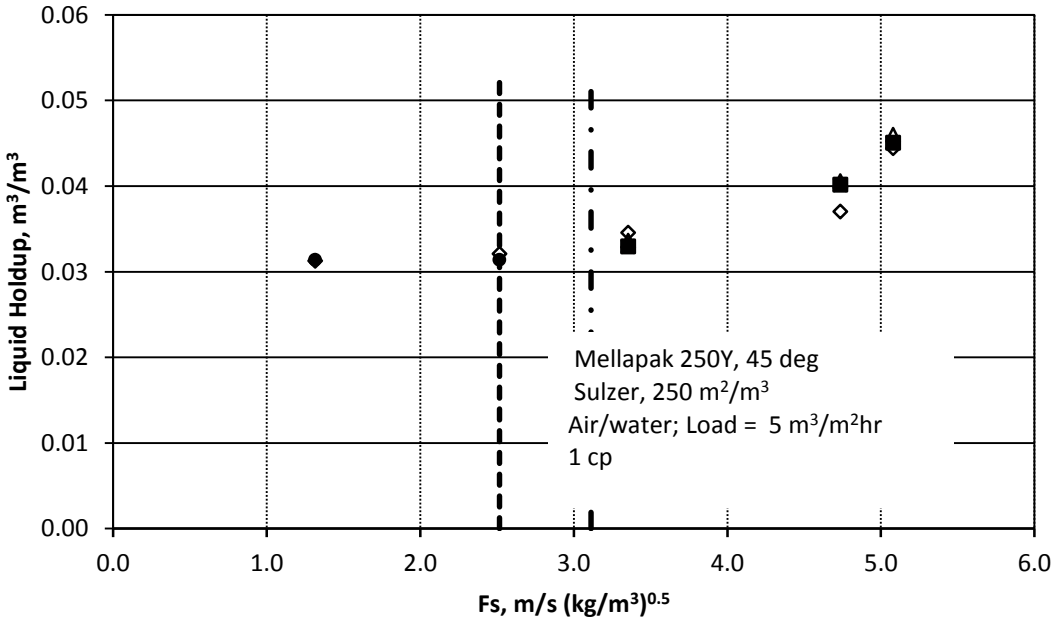

Fig. C.8. OkState liquid holdup model predictions vs. experimental liquid holdup data

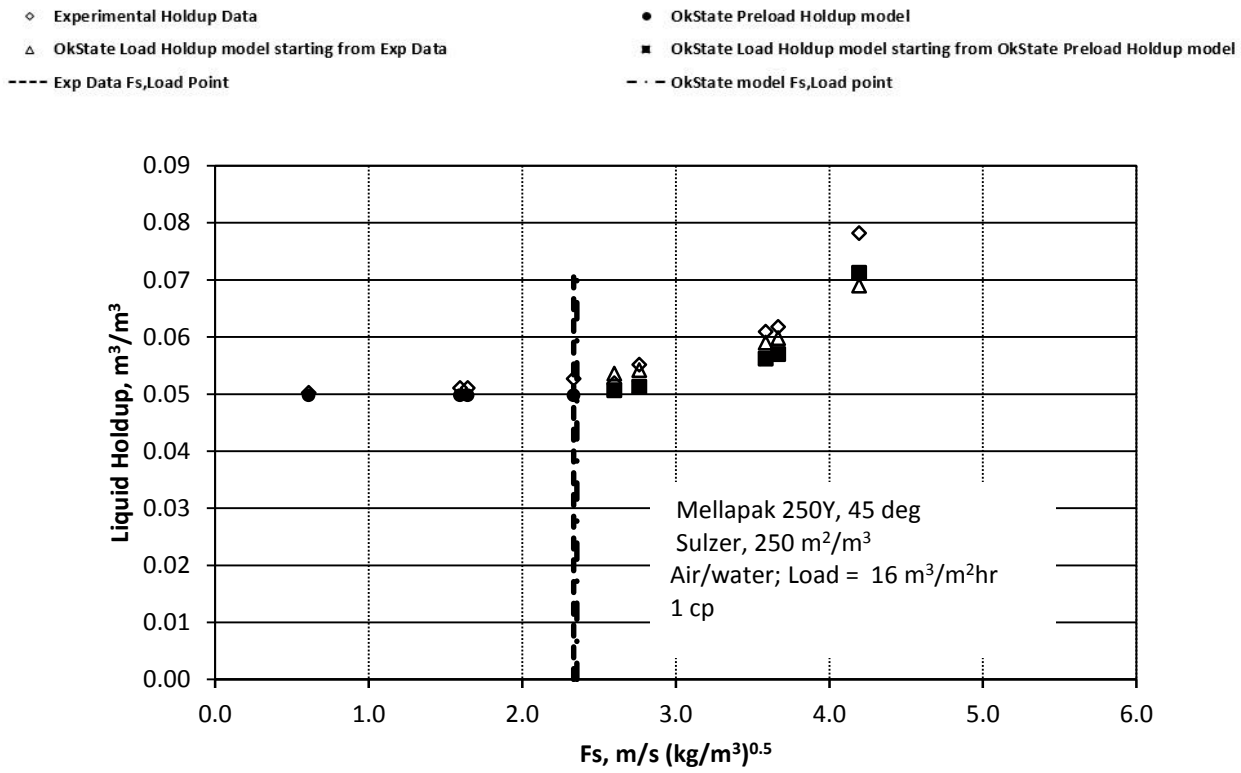

Fig. C.9. OkState liquid holdup model predictions vs. experimental liquid holdup data

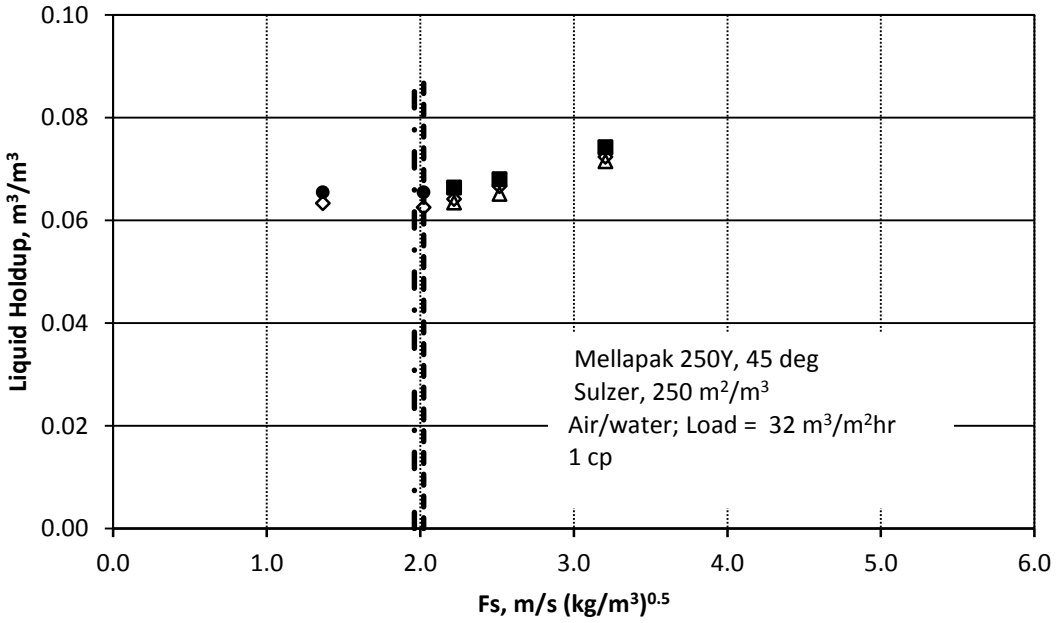

Fig. C.10. OkState liquid holdup model predictions vs. experimental liquid holdup data

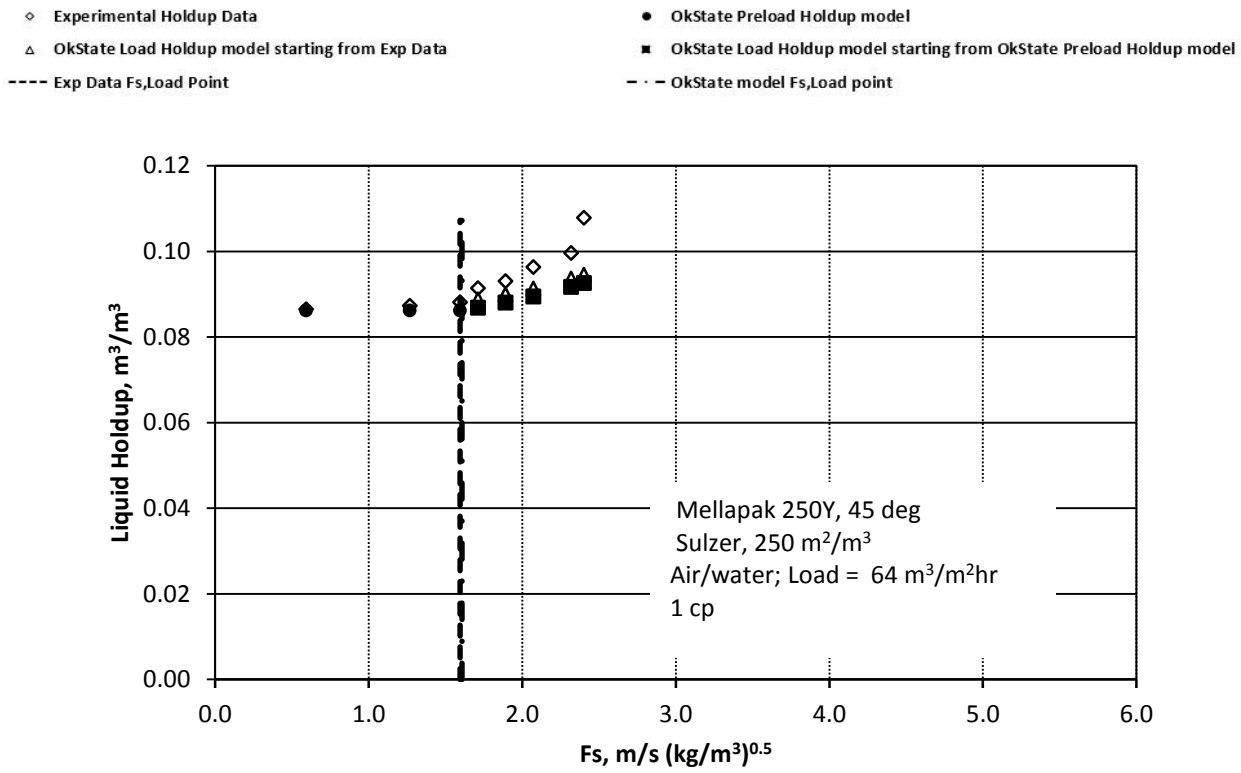

Fig. C.11. OkState liquid holdup model predictions vs. experimental liquid holdup data

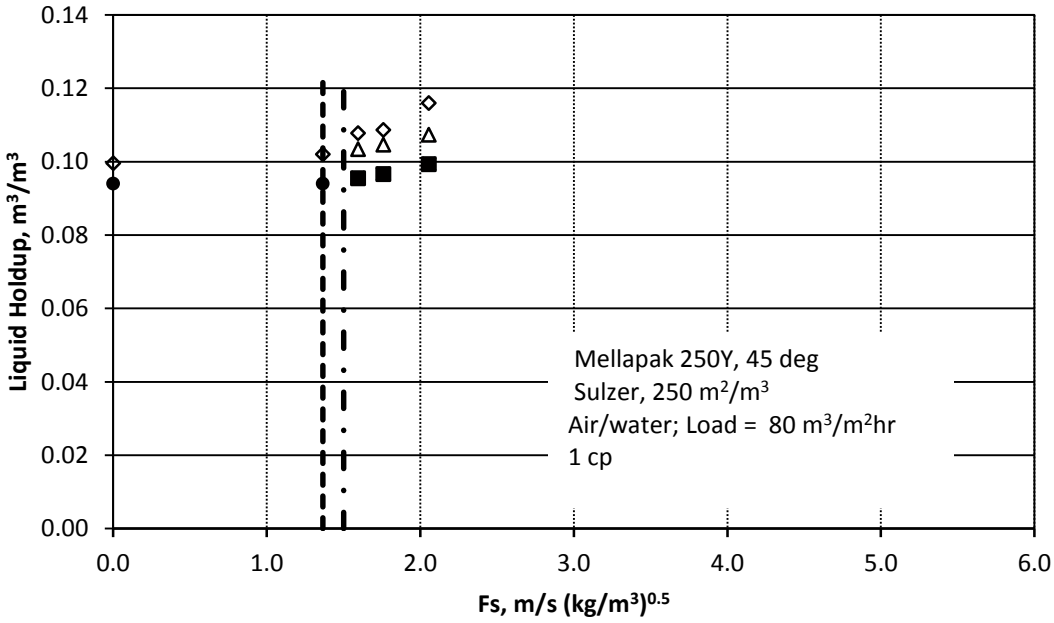

Fig. C.12. OkState liquid holdup model predictions vs. experimental liquid holdup data

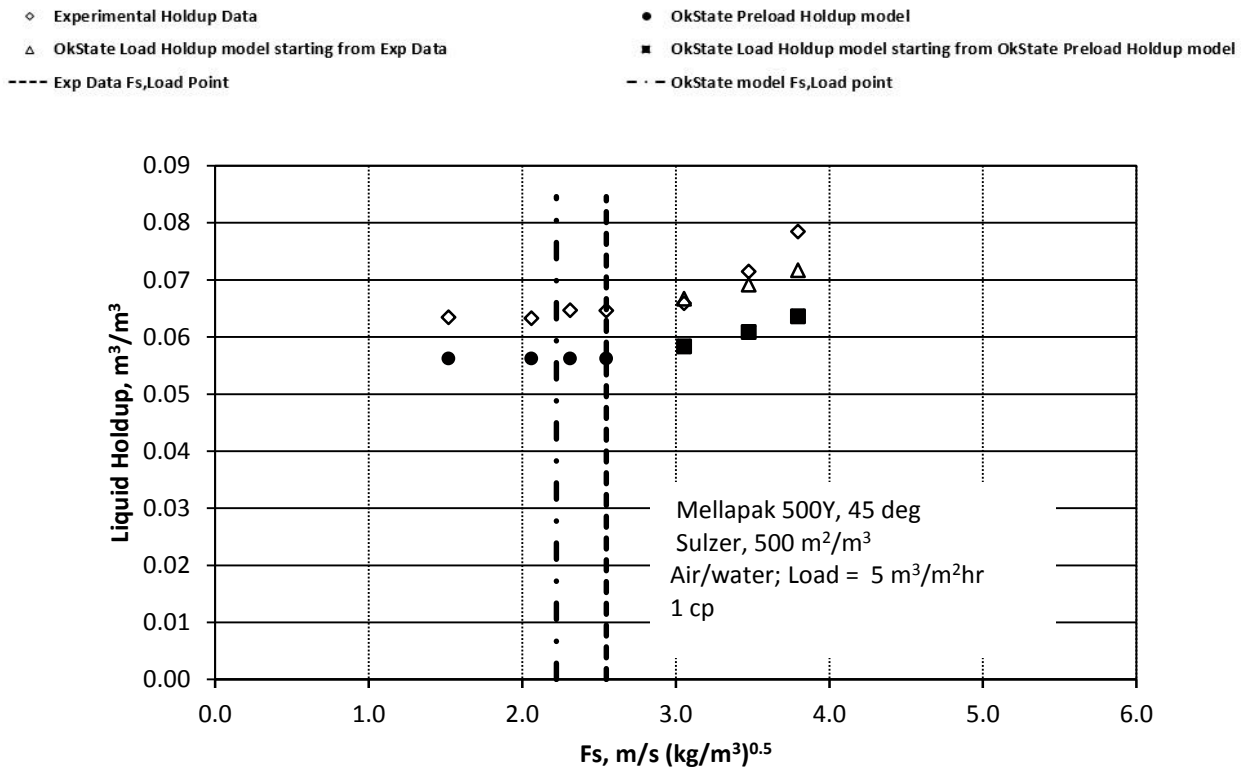

Fig. C.13. OkState liquid holdup model predictions vs. experimental liquid holdup data

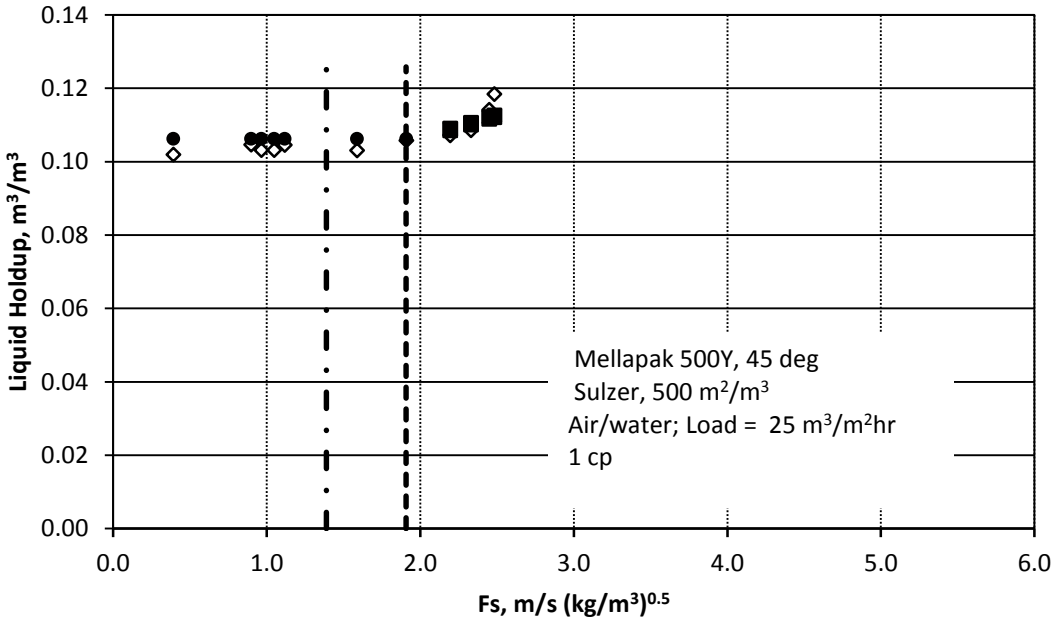

Fig. C.14. OkState liquid holdup model predictions vs. experimental liquid holdup data

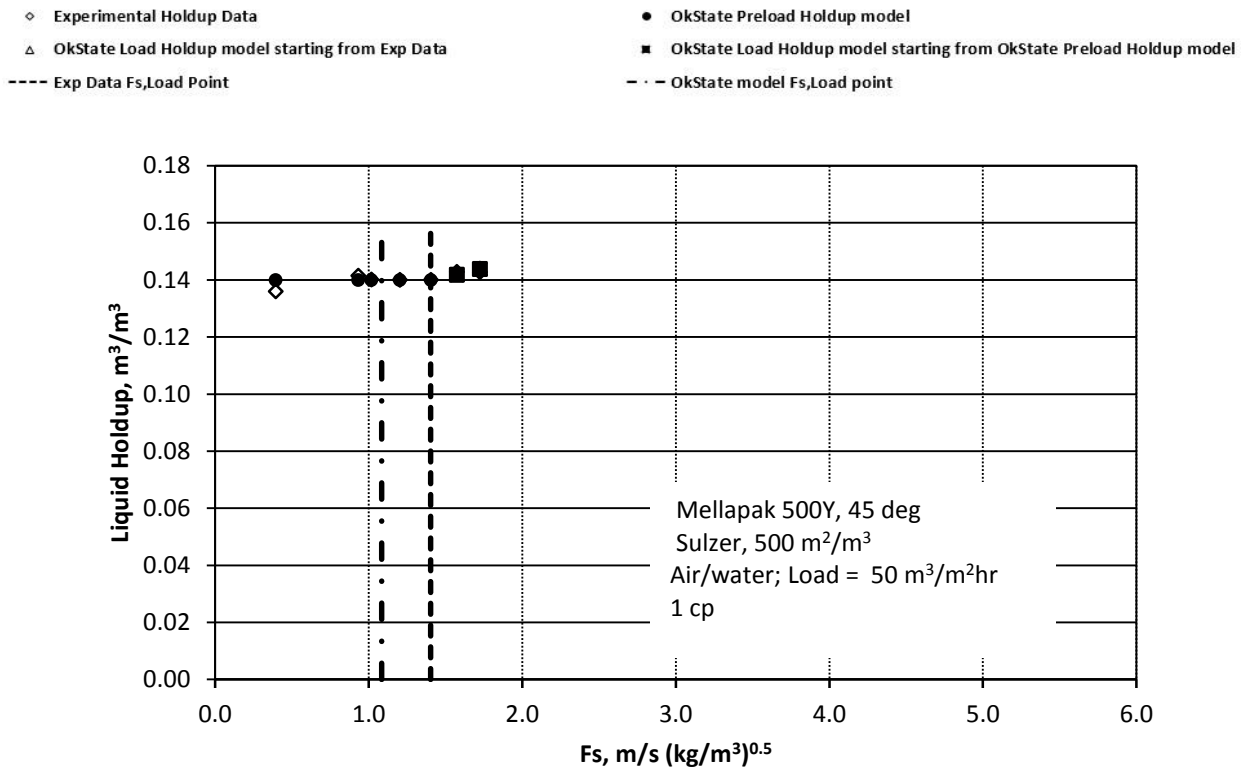

Fig. C.15. OkState liquid holdup model predictions vs. experimental liquid holdup data

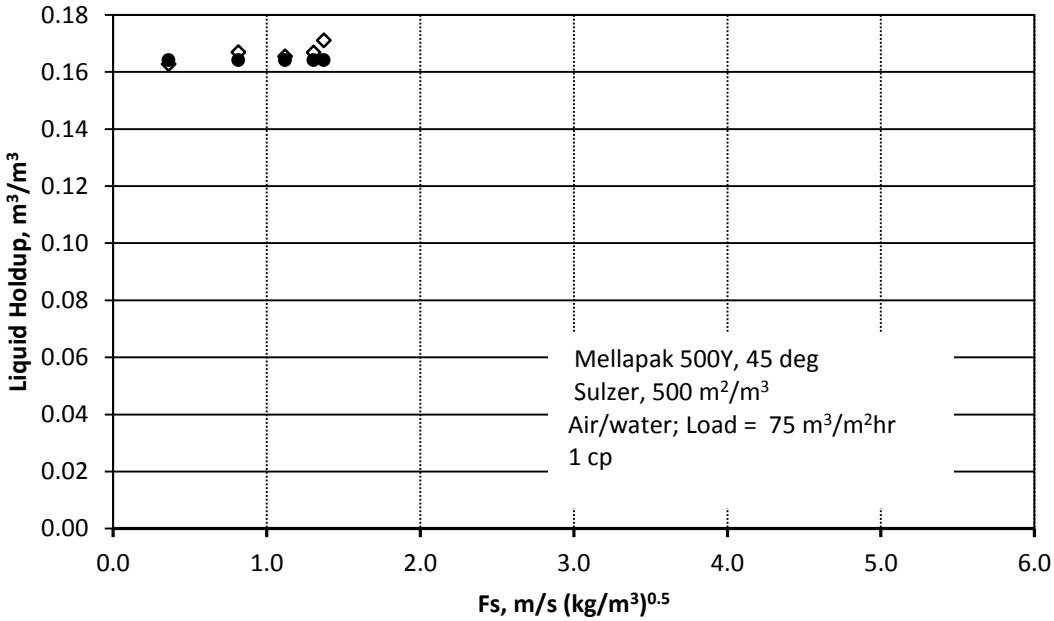

Fig. C.16. OkState liquid holdup model predictions vs. experimental liquid holdup data

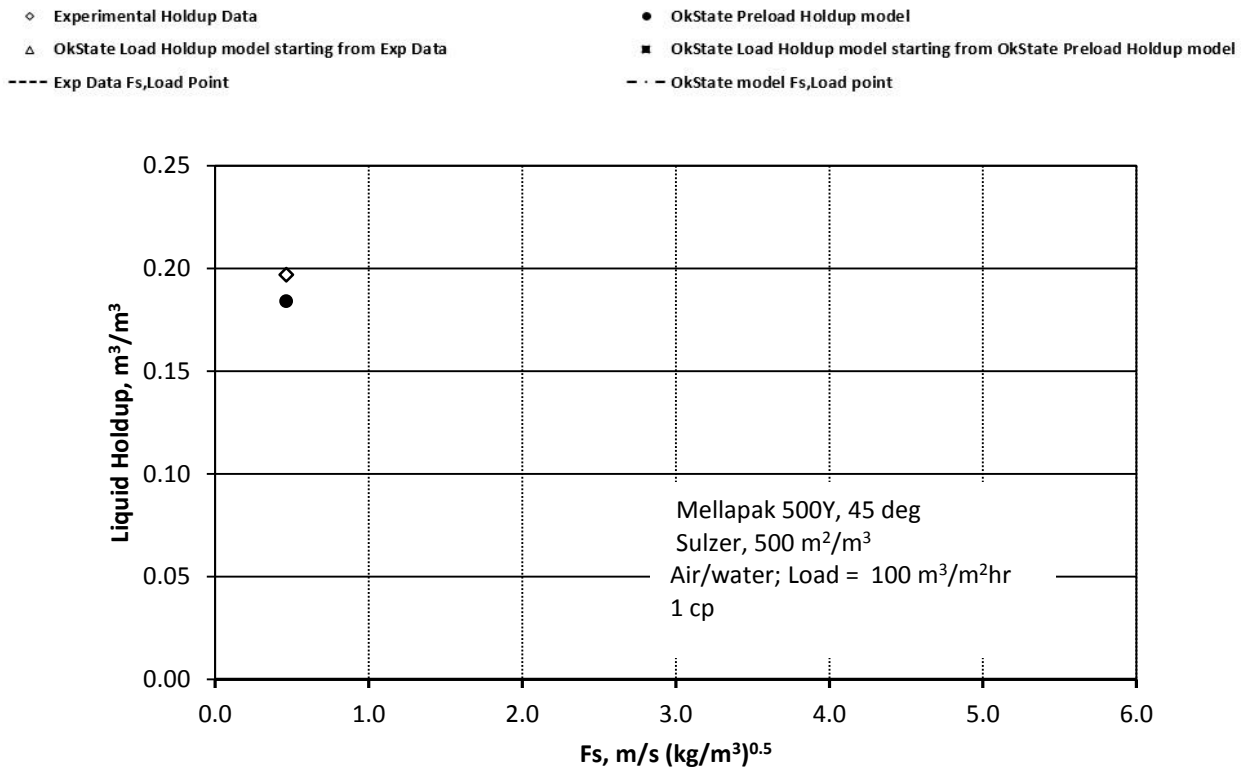

Fig. C.17. OkState liquid holdup model predictions vs. experimental liquid holdup data

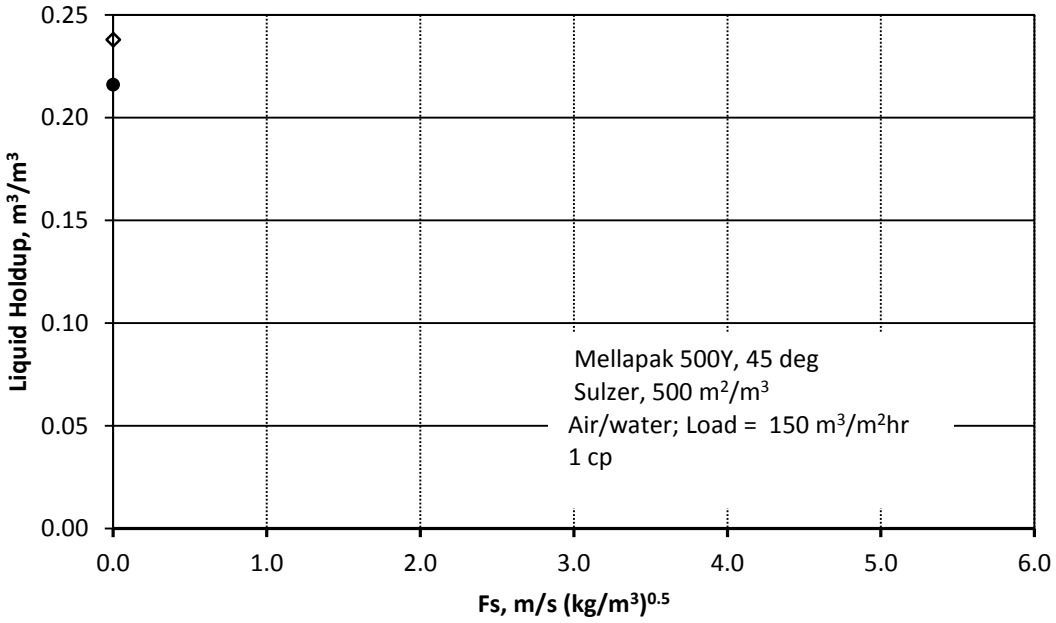

Fig. C.18. OkState liquid holdup model predictions vs. experimental liquid holdup data

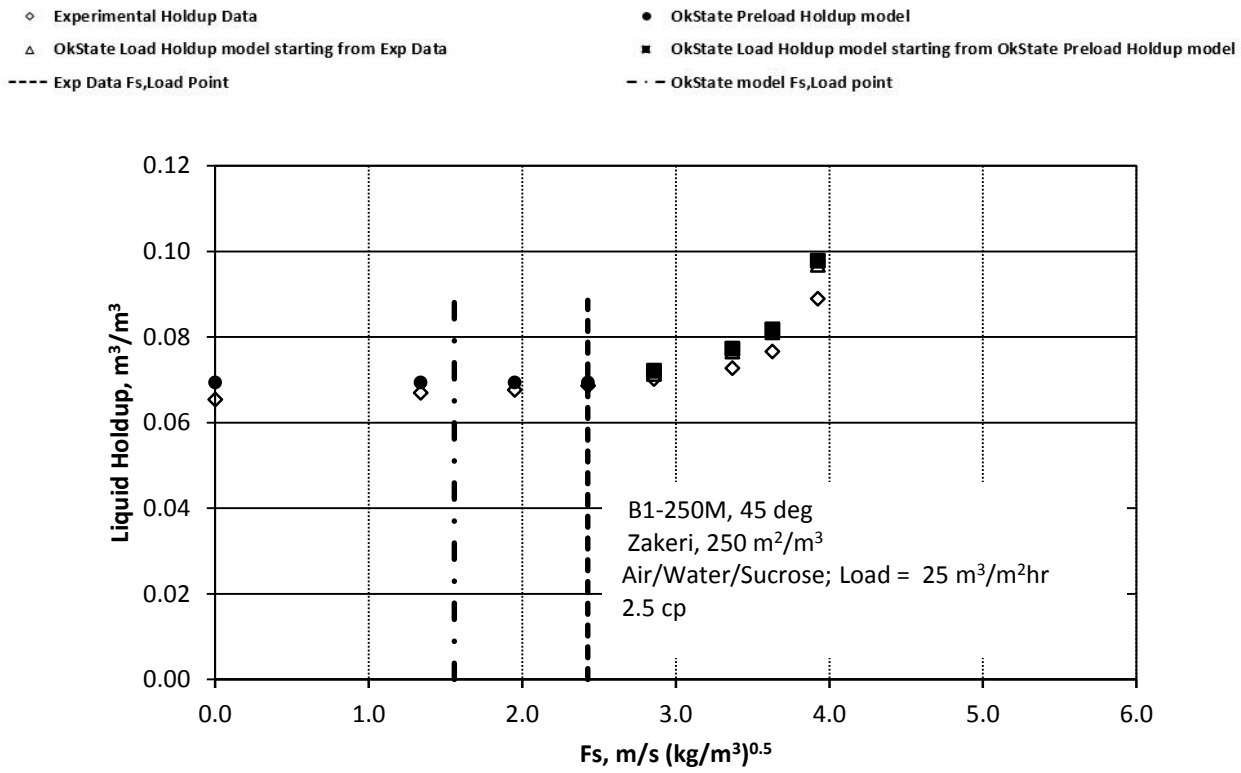

Fig. C.19. OkState liquid holdup model predictions vs. experimental liquid holdup data

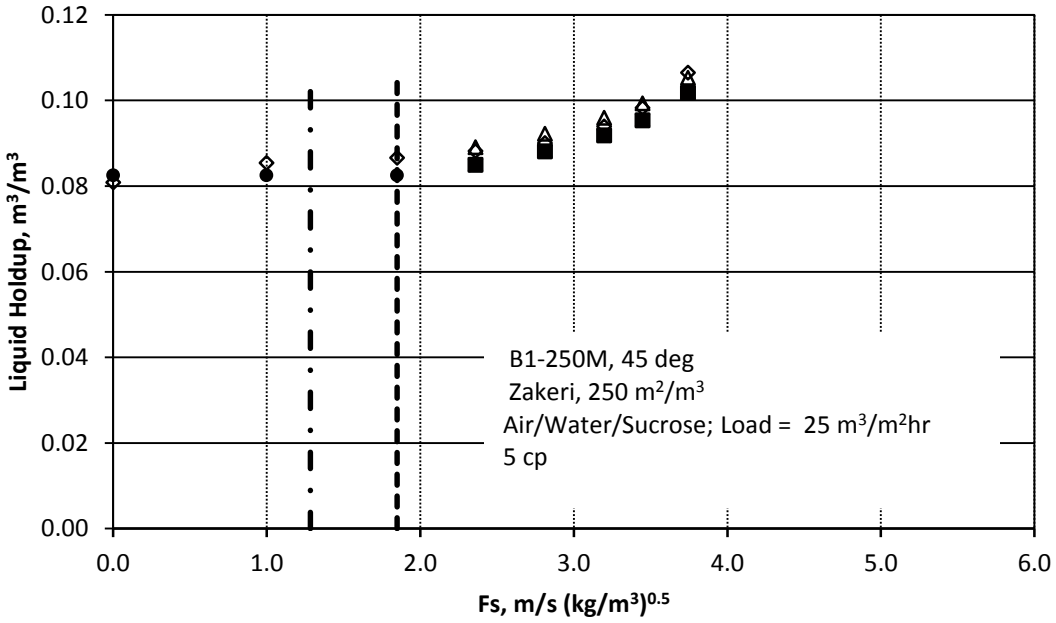

Fig. C.20. OkState liquid holdup model predictions vs. experimental liquid holdup data

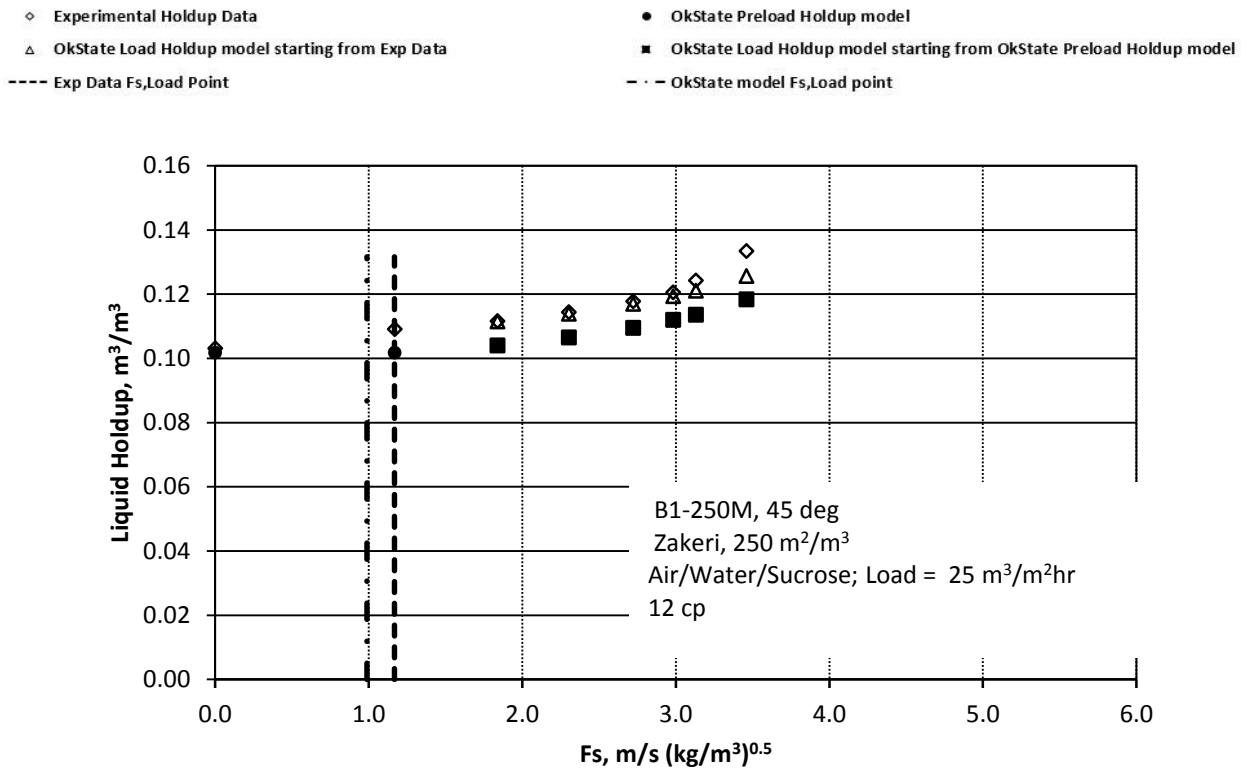

Fig. C.21. OkState liquid holdup model predictions vs. experimental liquid holdup data

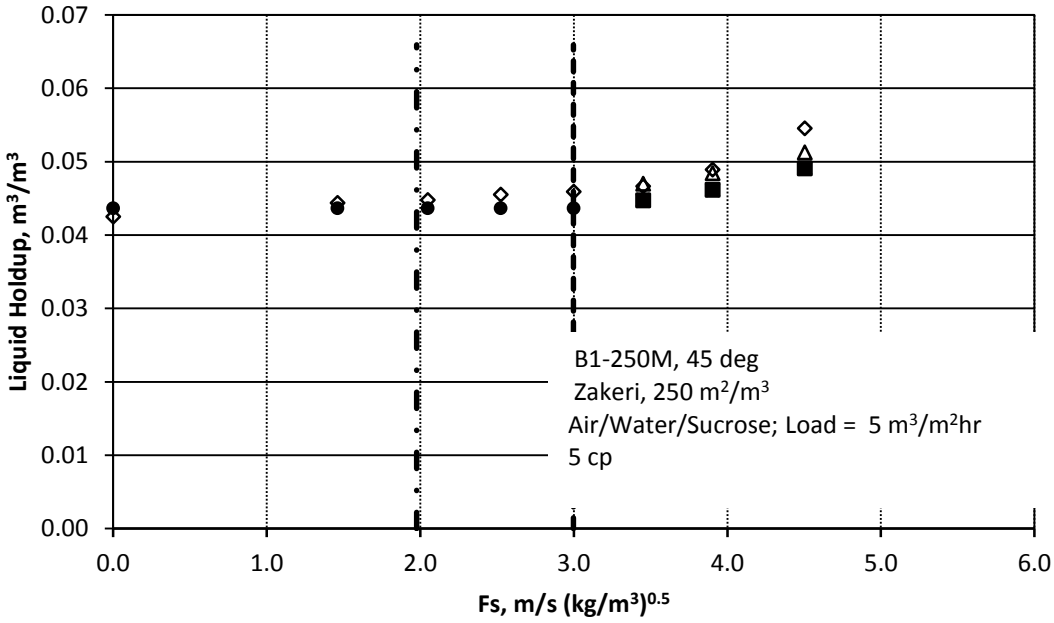

Fig. C.22. OkState liquid holdup model predictions vs. experimental liquid holdup data

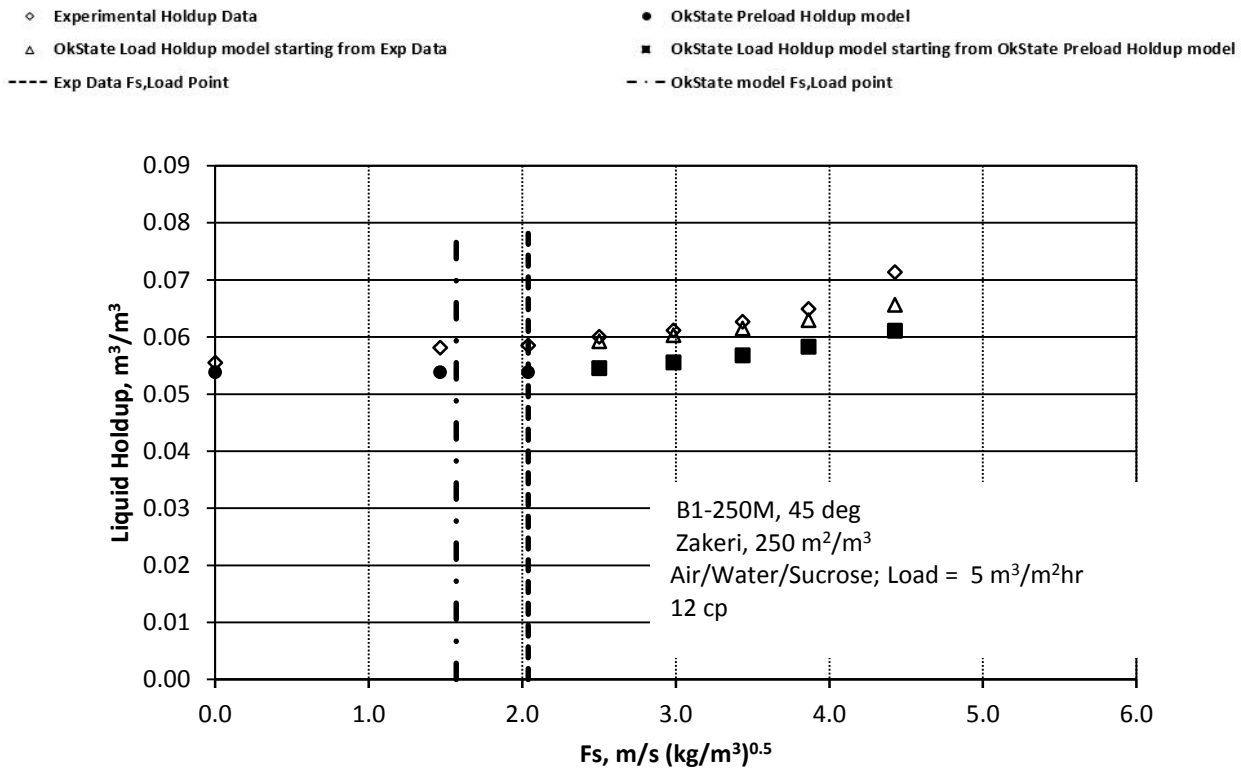

Fig. C.23. OkState liquid holdup model predictions vs. experimental liquid holdup data

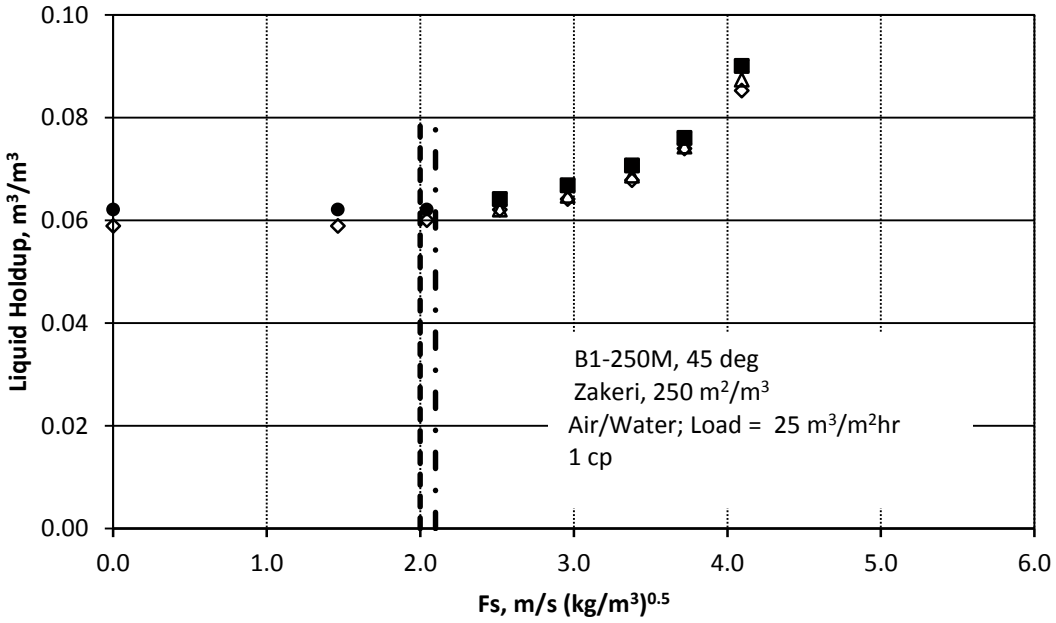

Fig. C.24. OkState liquid holdup model predictions vs. experimental liquid holdup data

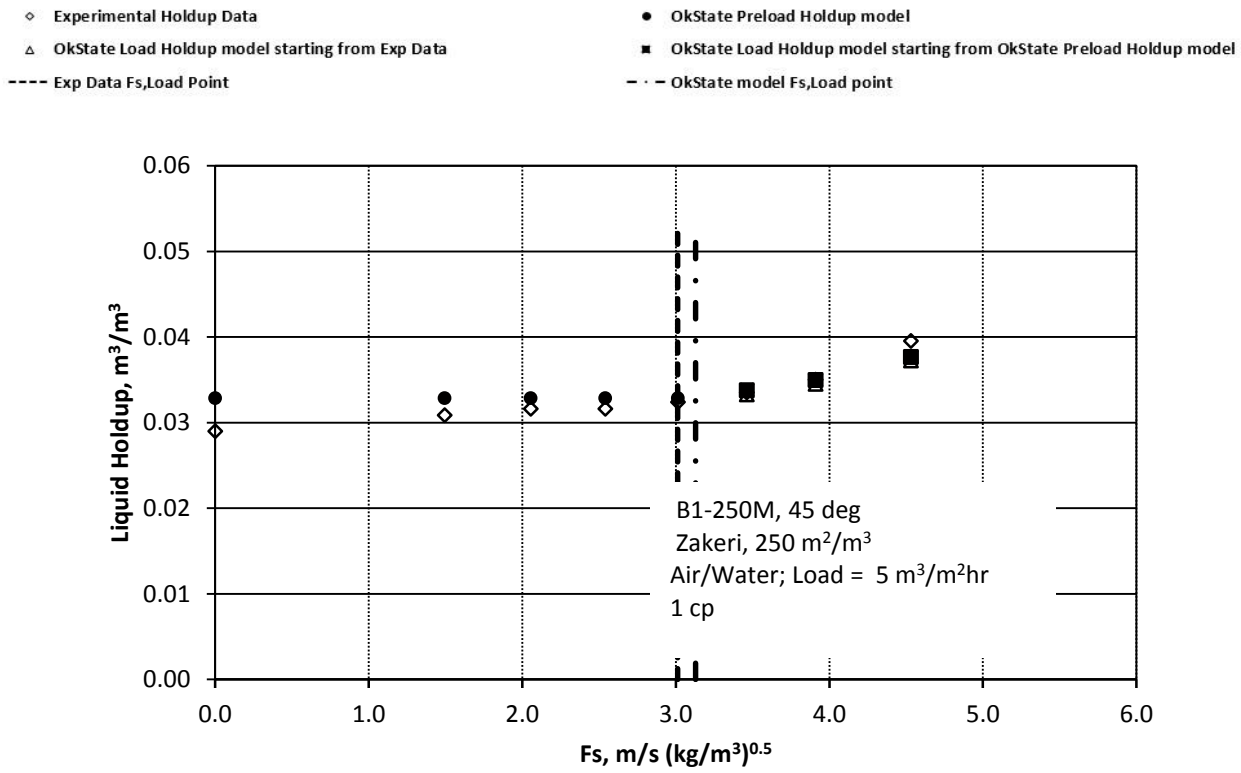

Fig. C.25. OkState liquid holdup model predictions vs. experimental liquid holdup data

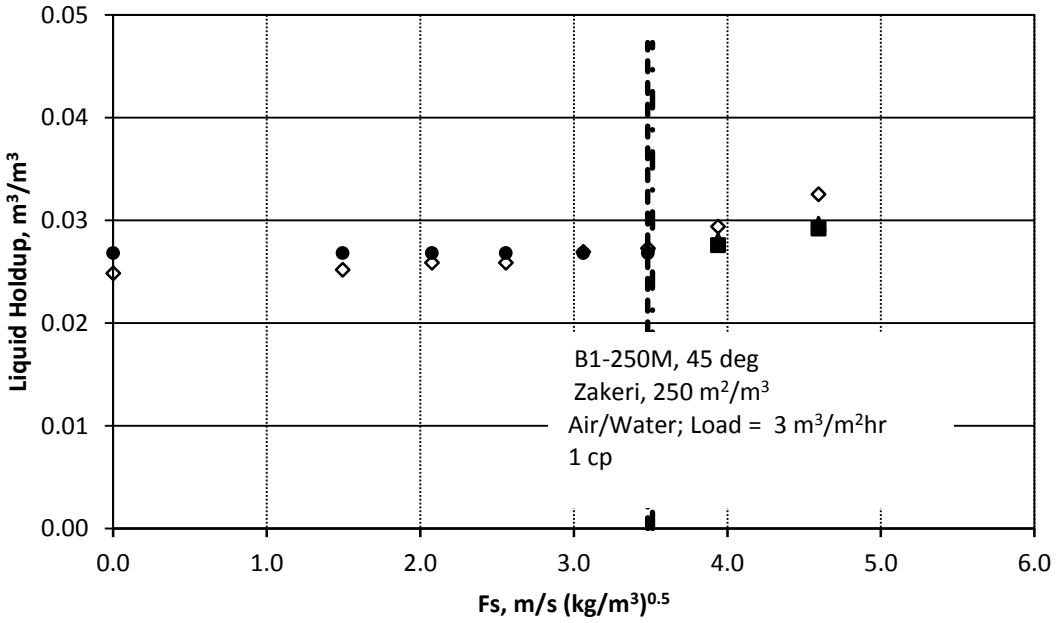

Fig. C.26. OkState liquid holdup model predictions vs. experimental liquid holdup data

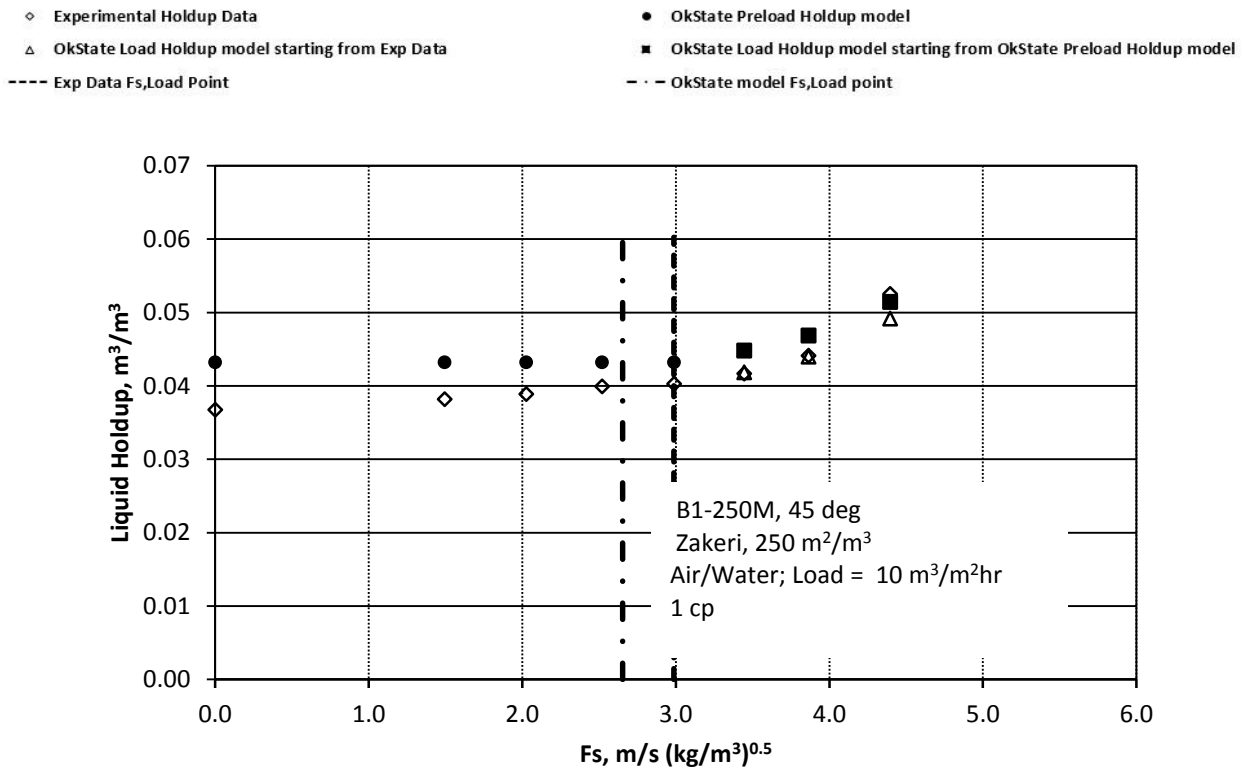

Fig. C.27. OkState liquid holdup model predictions vs. experimental liquid holdup data

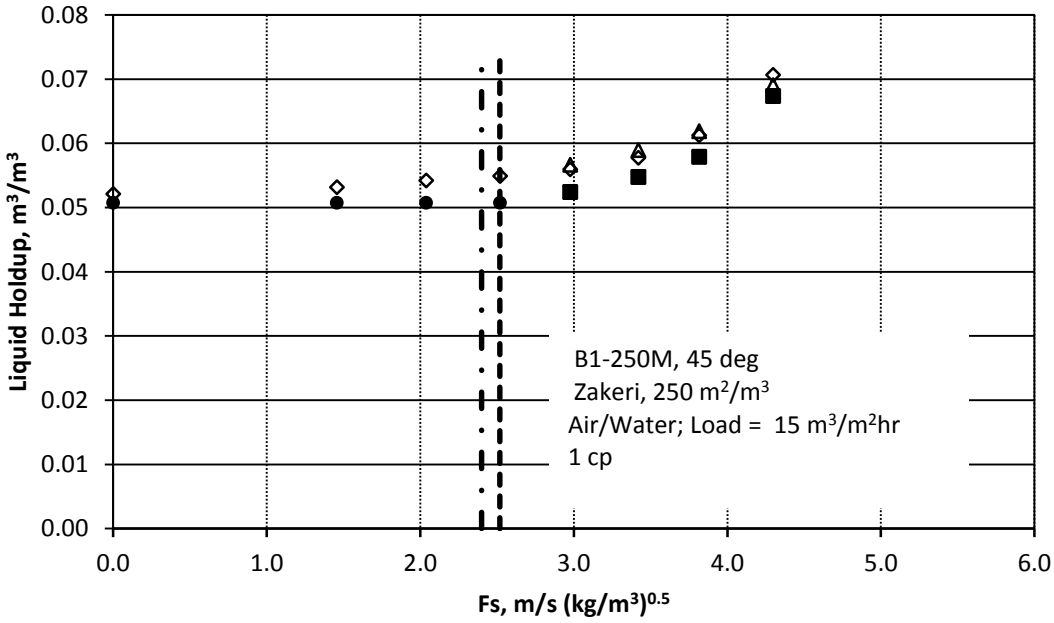

Fig. C.28. OkState liquid holdup model predictions vs. experimental liquid holdup data

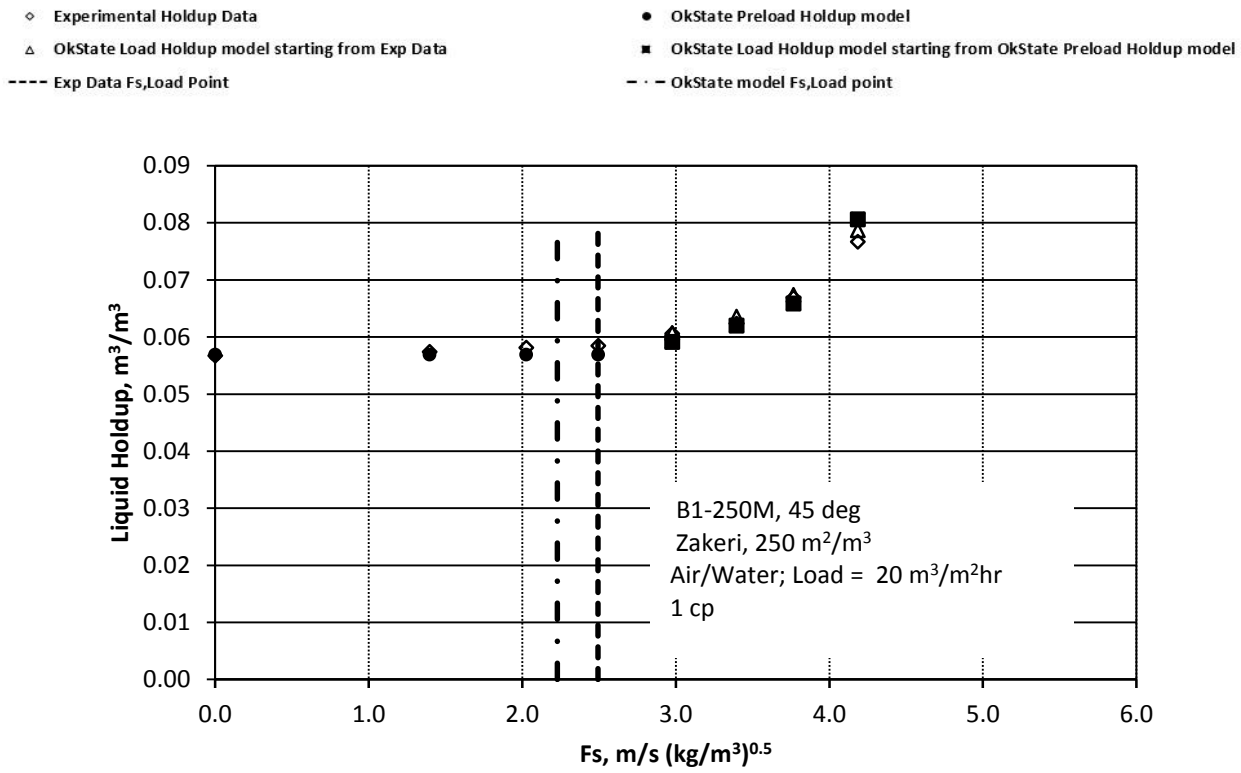

Fig. C.29. OkState liquid holdup model predictions vs. experimental liquid holdup data

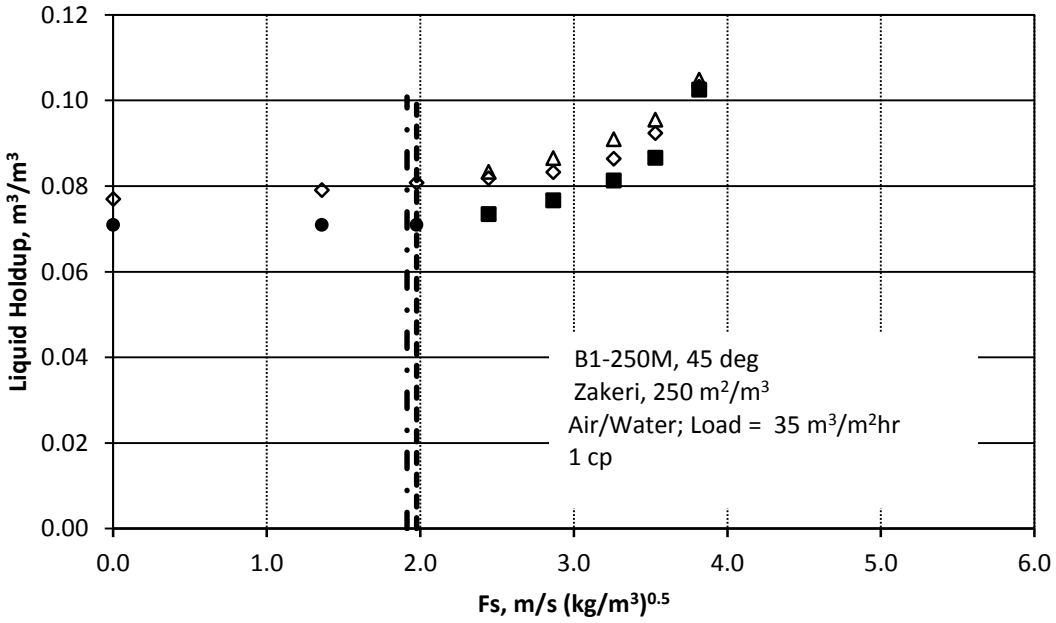

Fig. C.30. OkState liquid holdup model predictions vs. experimental liquid holdup data

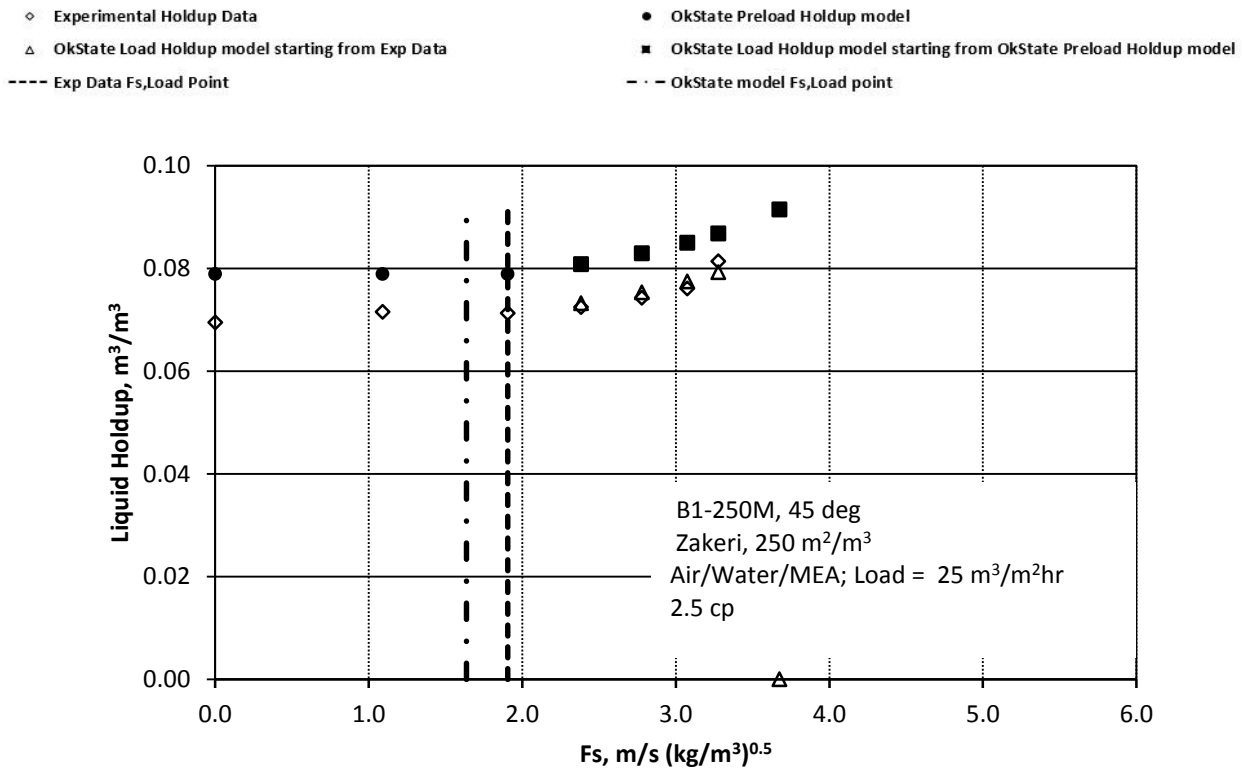

Fig. C.31. OkState liquid holdup model predictions vs. experimental liquid holdup data

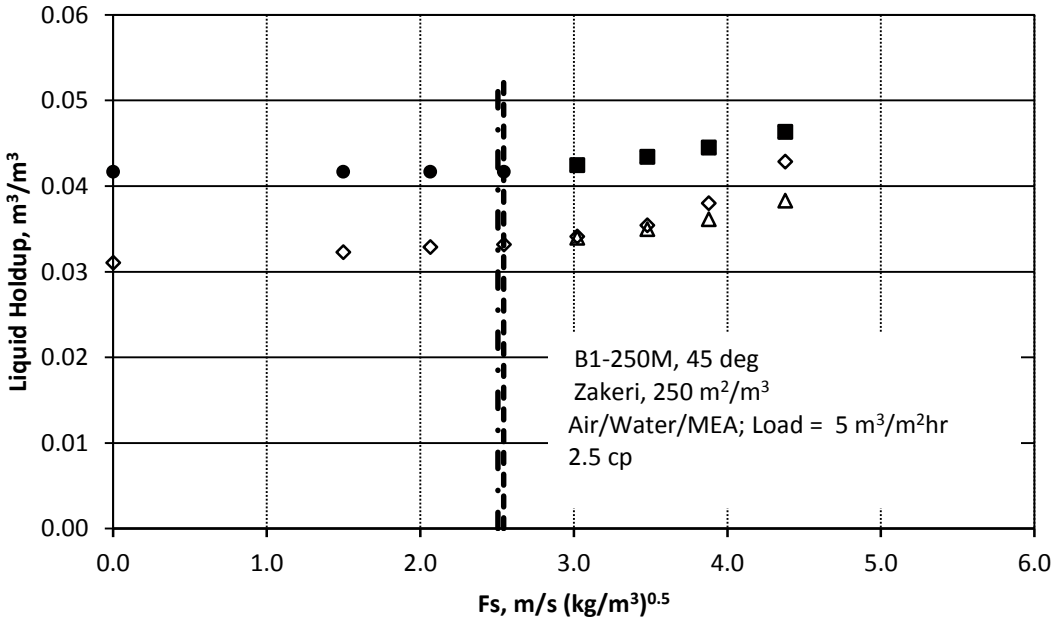

Fig. C.32. OkState liquid holdup model predictions vs. experimental liquid holdup data

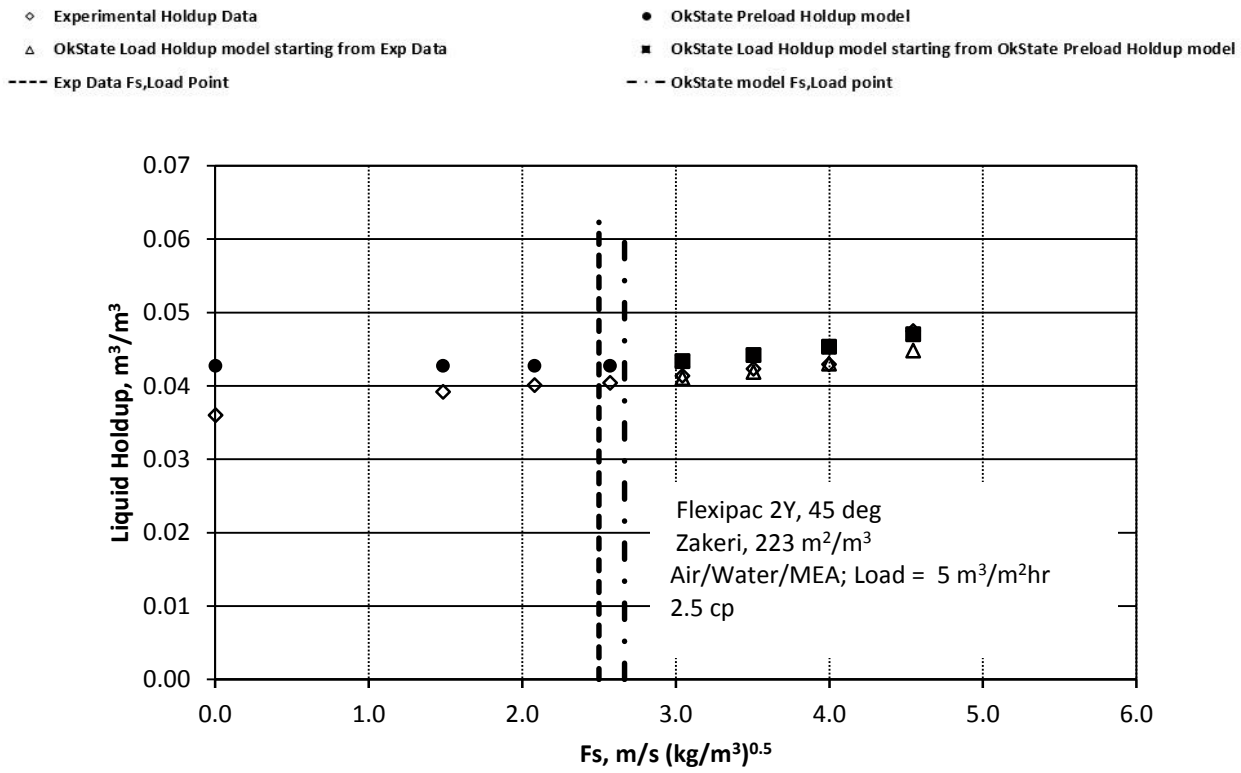

Fig. C.33. OkState liquid holdup model predictions vs. experimental liquid holdup data

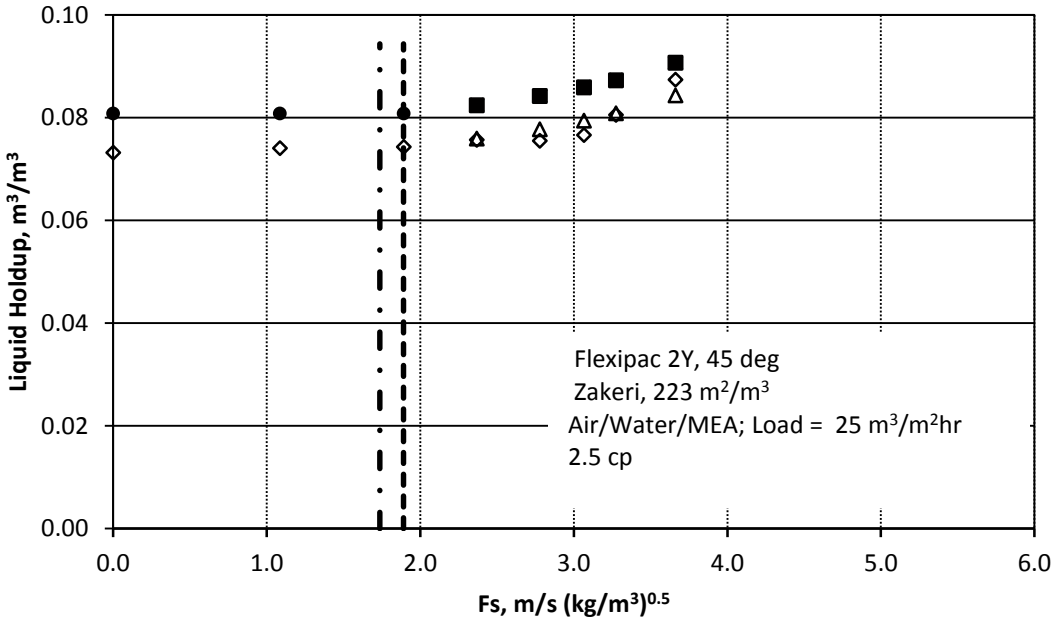

Fig. C.34. OkState liquid holdup model predictions vs. experimental liquid holdup data

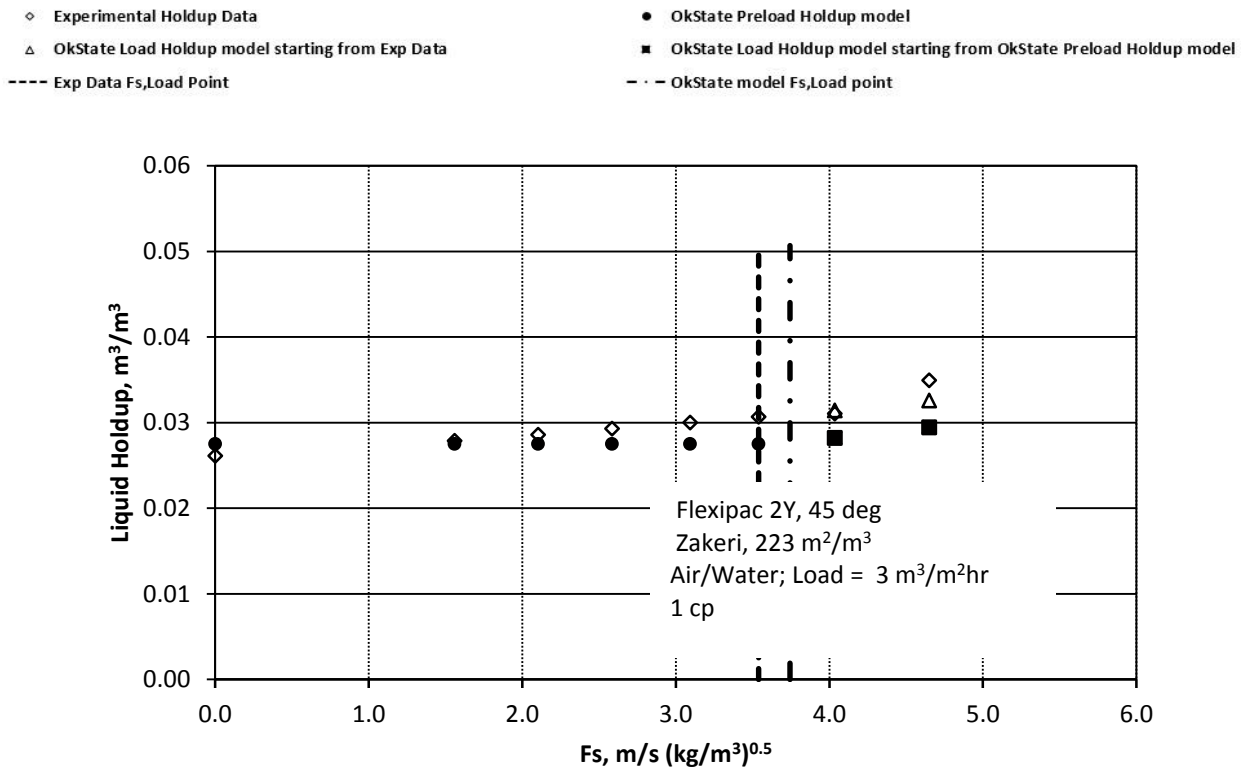

Fig. C.35. OkState liquid holdup model predictions vs. experimental liquid holdup data

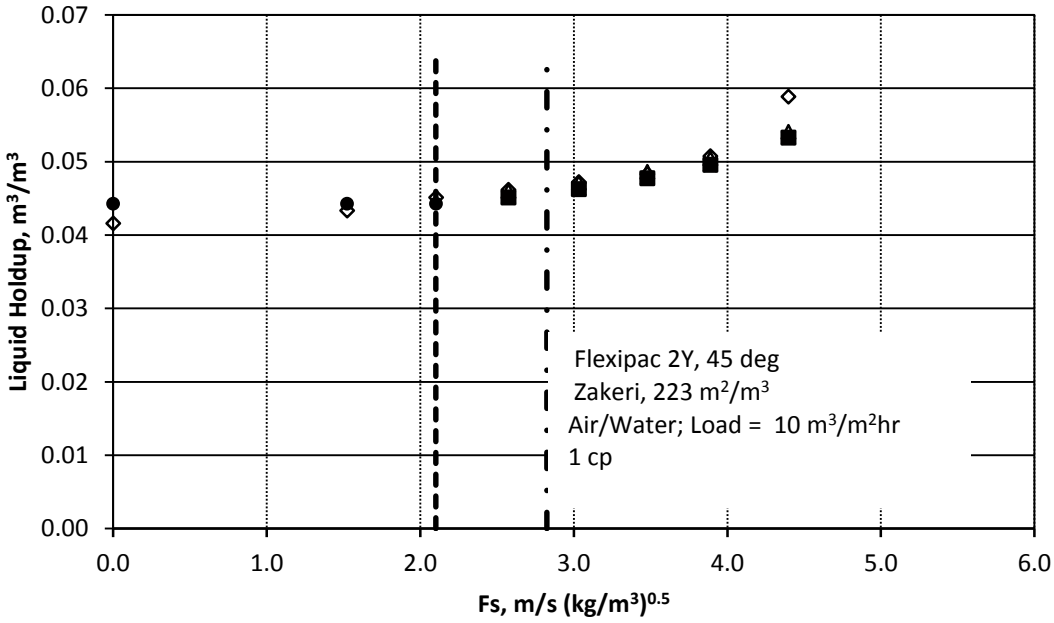

Fig. C.36. OkState liquid holdup model predictions vs. experimental liquid holdup data

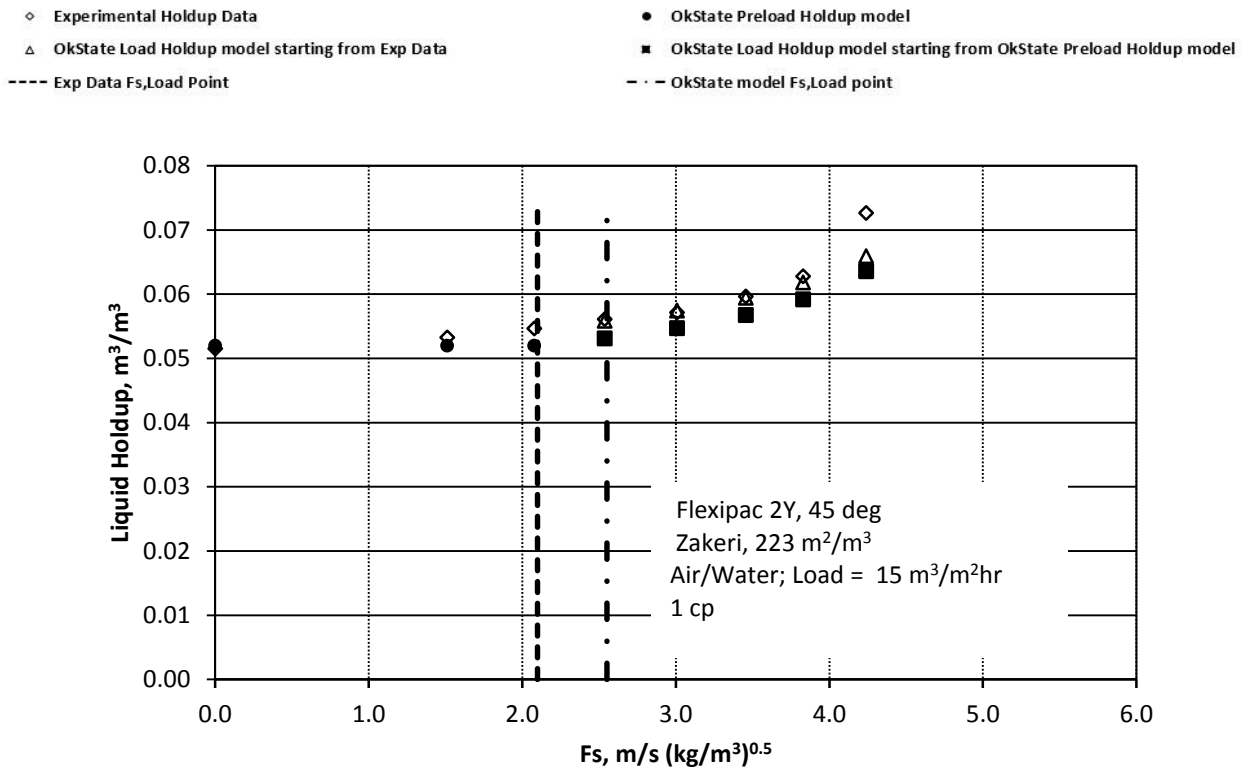

Fig. C.37. OkState liquid holdup model predictions vs. experimental liquid holdup data

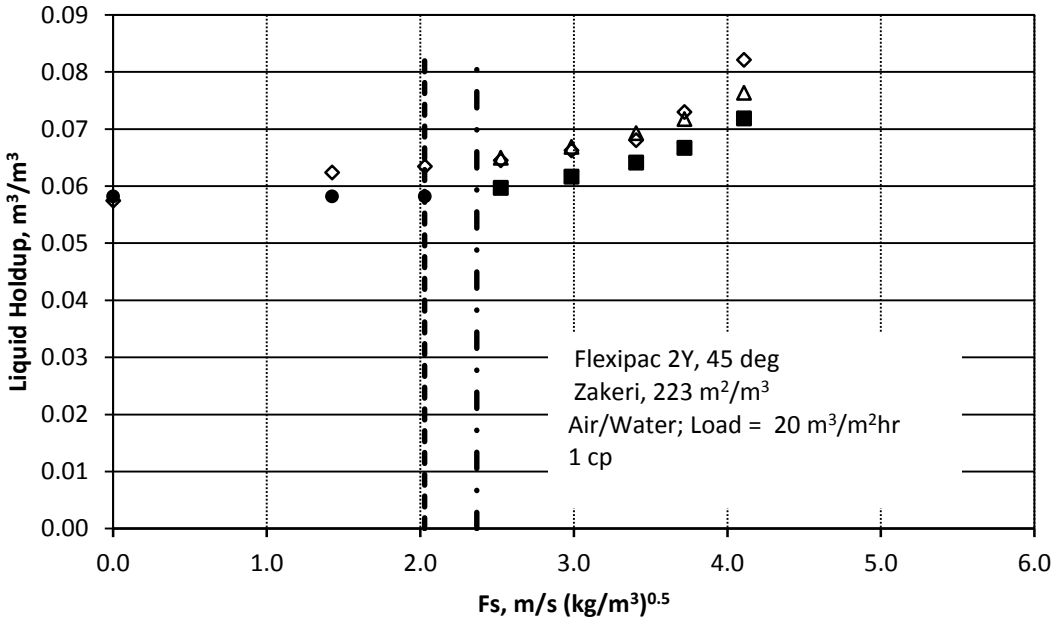

Fig. C.38. OkState liquid holdup model predictions vs. experimental liquid holdup data

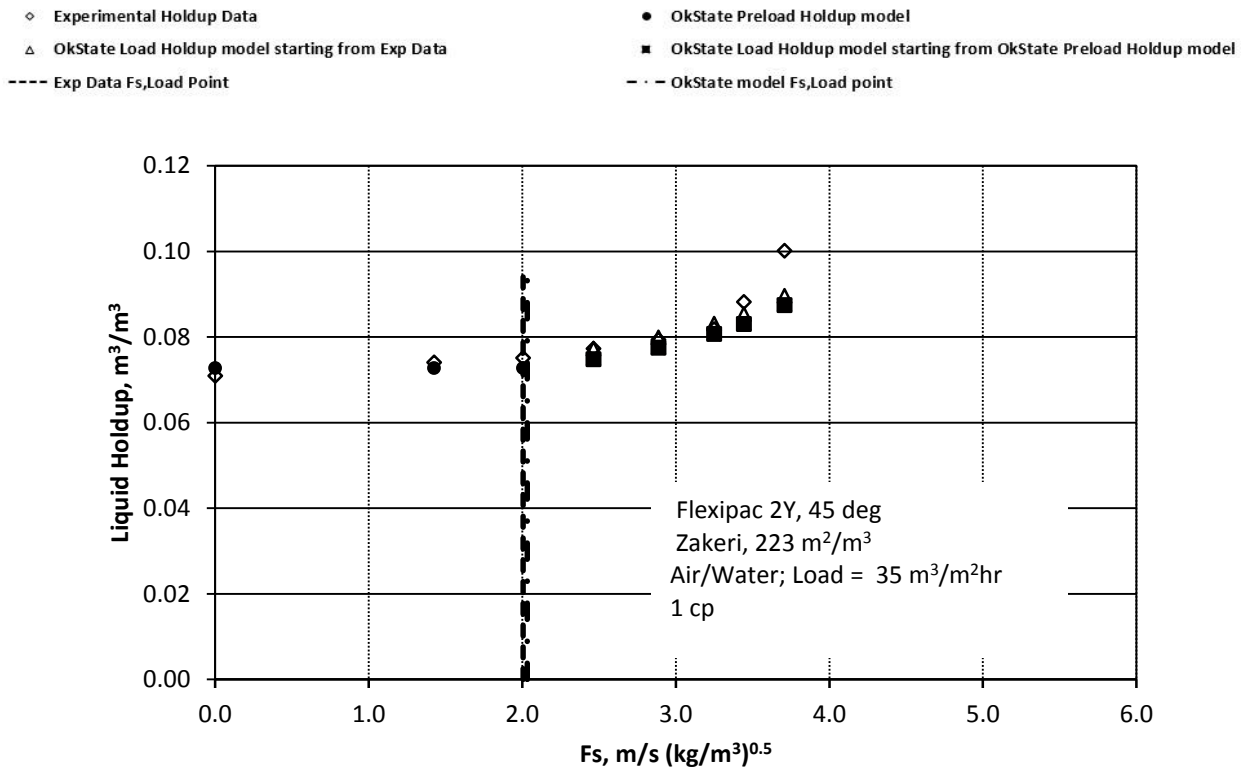

Fig. C.39. OkState liquid holdup model predictions vs. experimental liquid holdup data

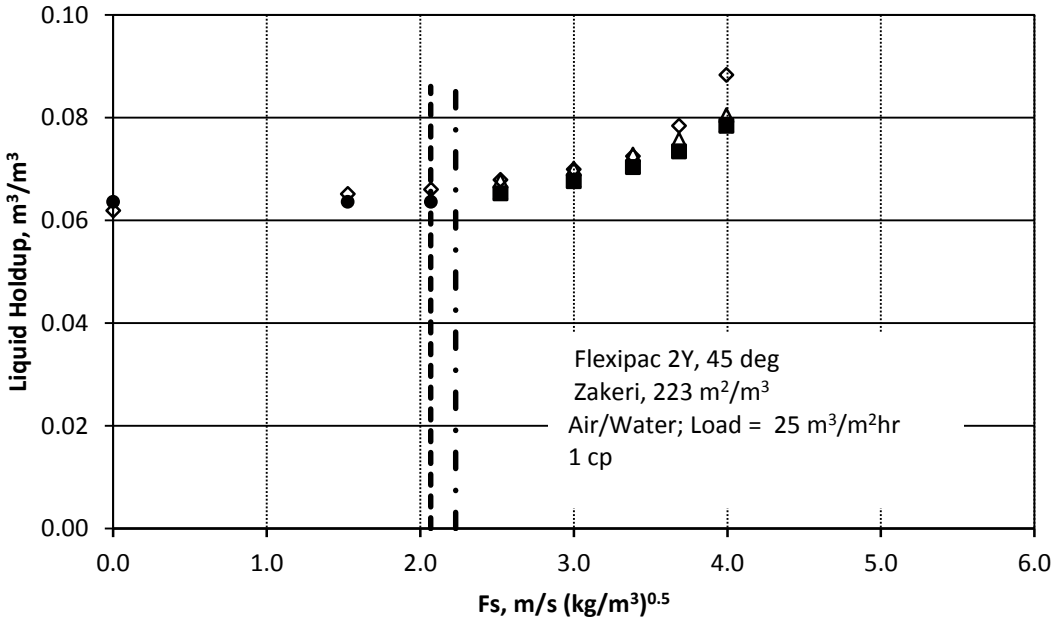

Fig. C.40. OkState liquid holdup model predictions vs. experimental liquid holdup data

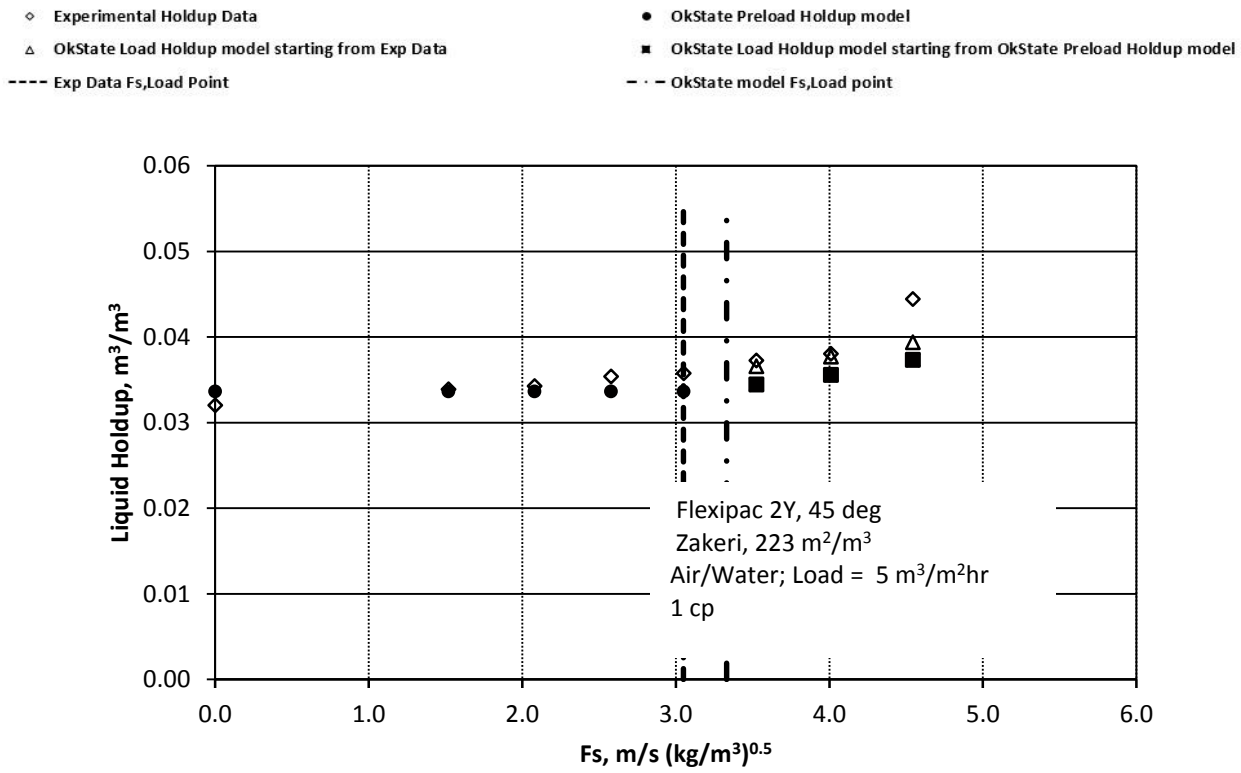

Fig. C.41. OkState liquid holdup model predictions vs. experimental liquid holdup data

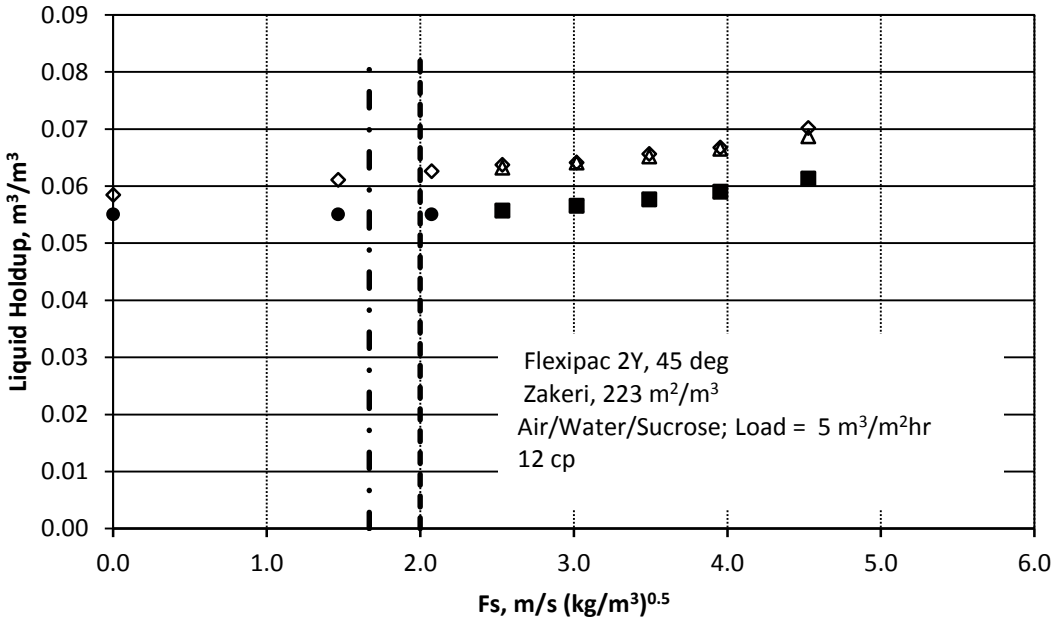

Fig. C.42. OkState liquid holdup model predictions vs. experimental liquid holdup data

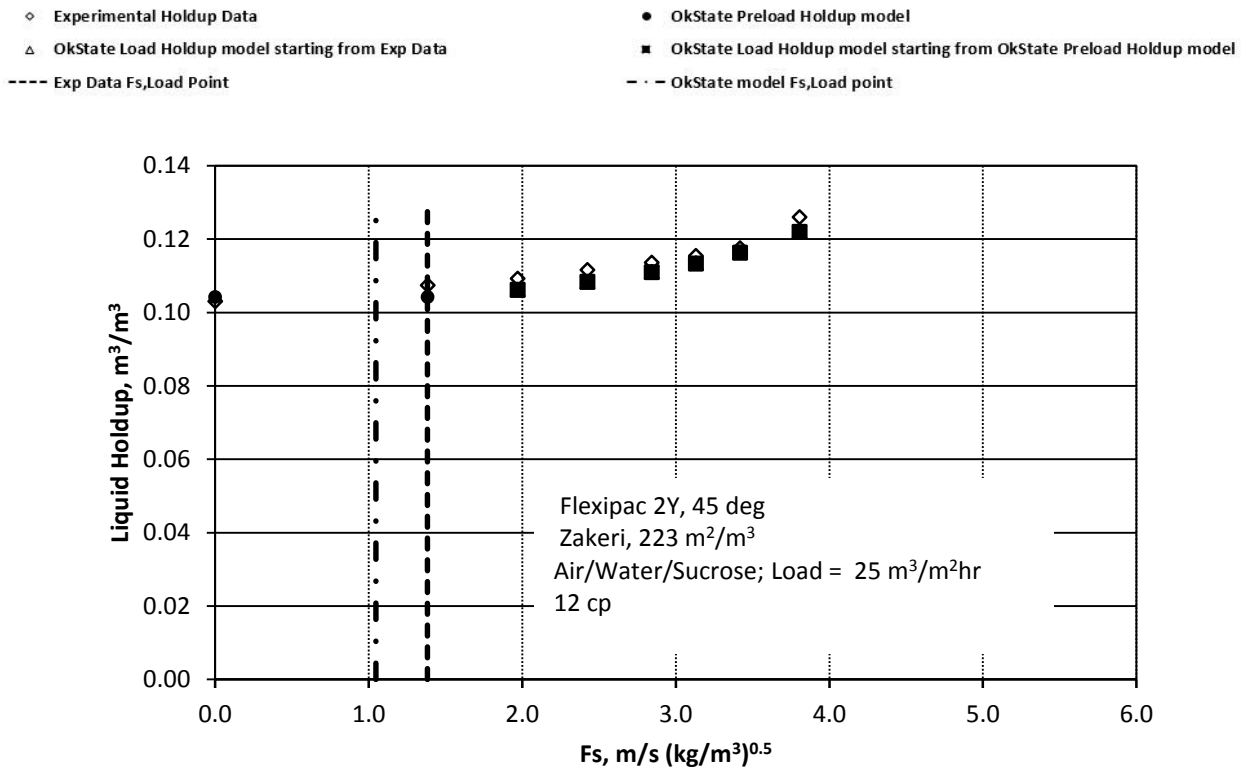

Fig. C.43. OkState liquid holdup model predictions vs. experimental liquid holdup data

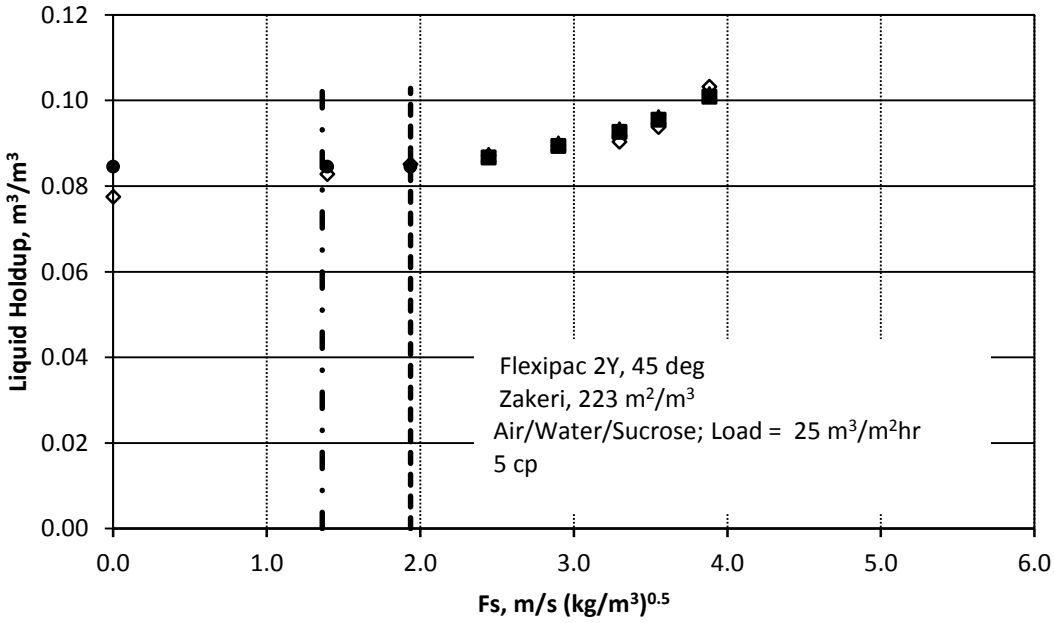

Fig. C.44. OkState liquid holdup model predictions vs. experimental liquid holdup data

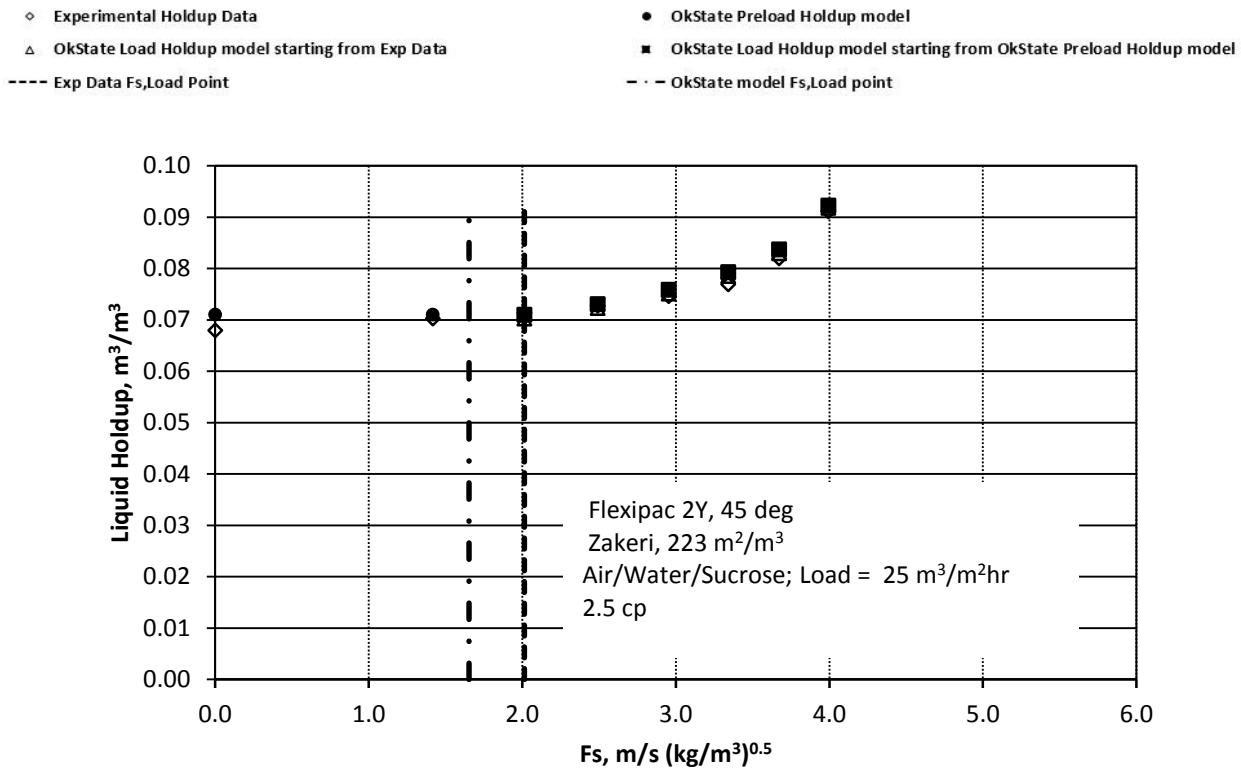

Fig. C.45. OkState liquid holdup model predictions vs. experimental liquid holdup data

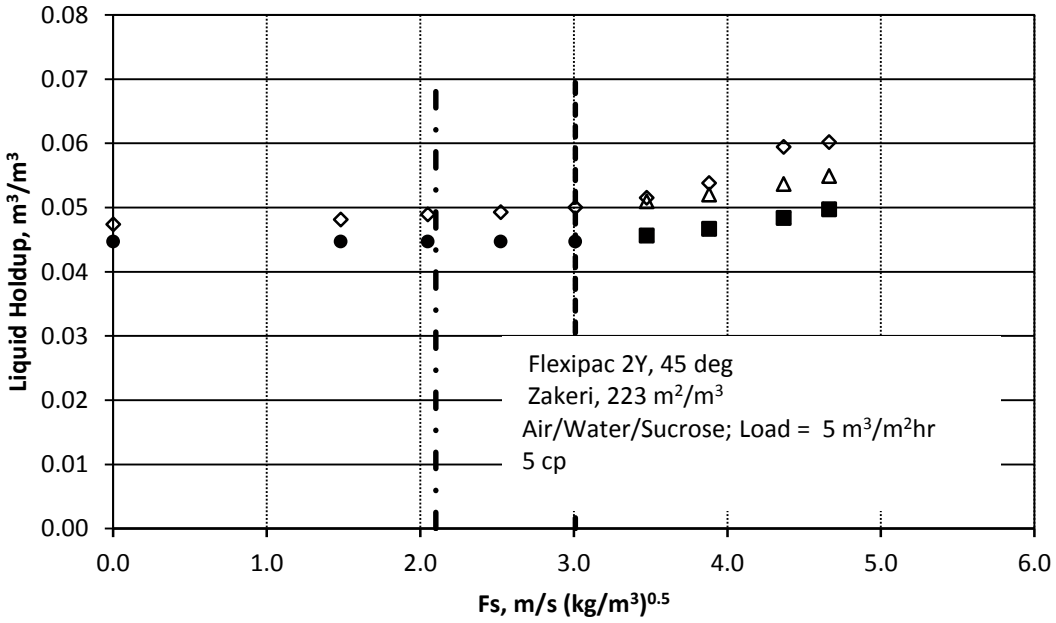

Fig. C.46. OkState liquid holdup model predictions vs. experimental liquid holdup data

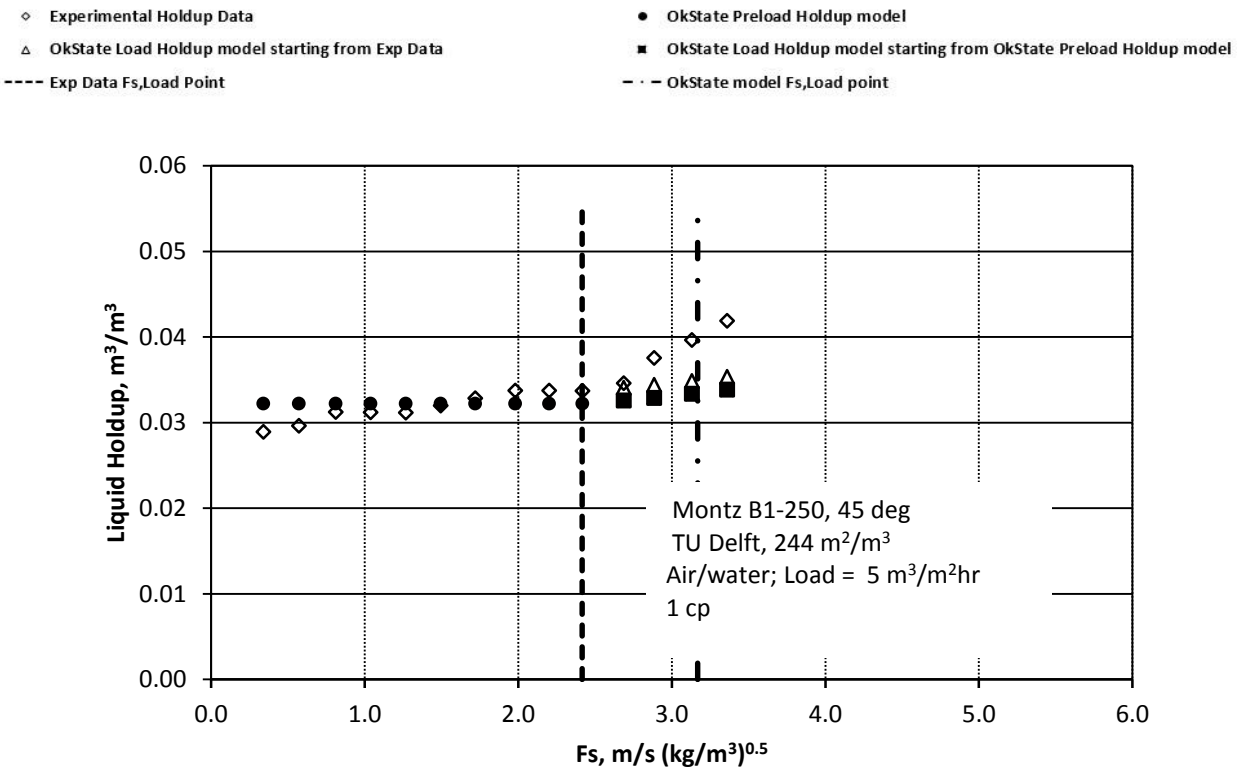

Fig. C.47. OkState liquid holdup model predictions vs. experimental liquid holdup data

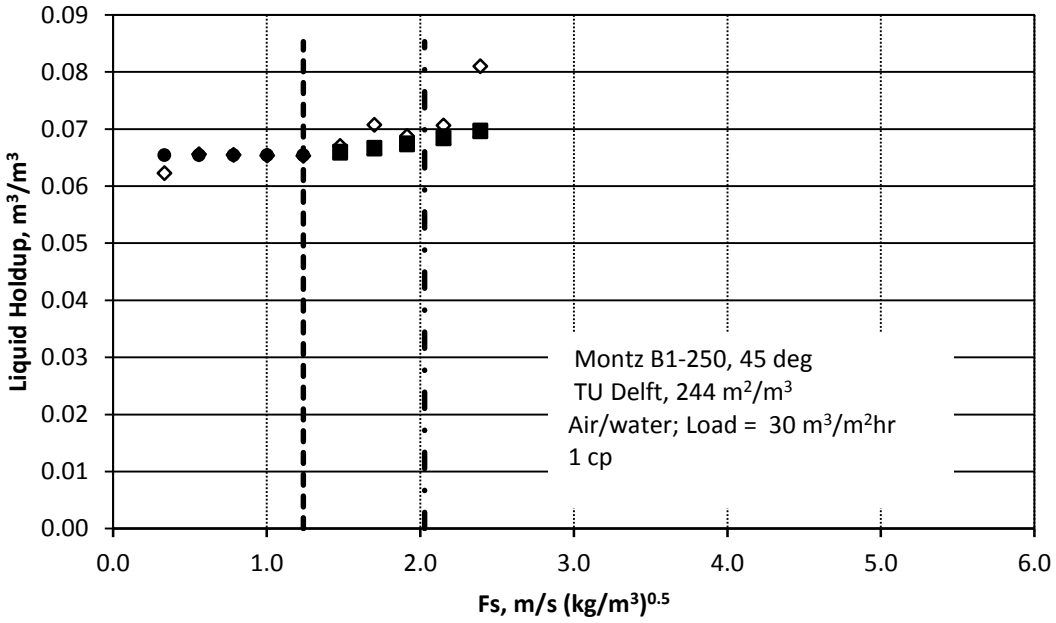

Fig. C.48. OkState liquid holdup model predictions vs. experimental liquid holdup data

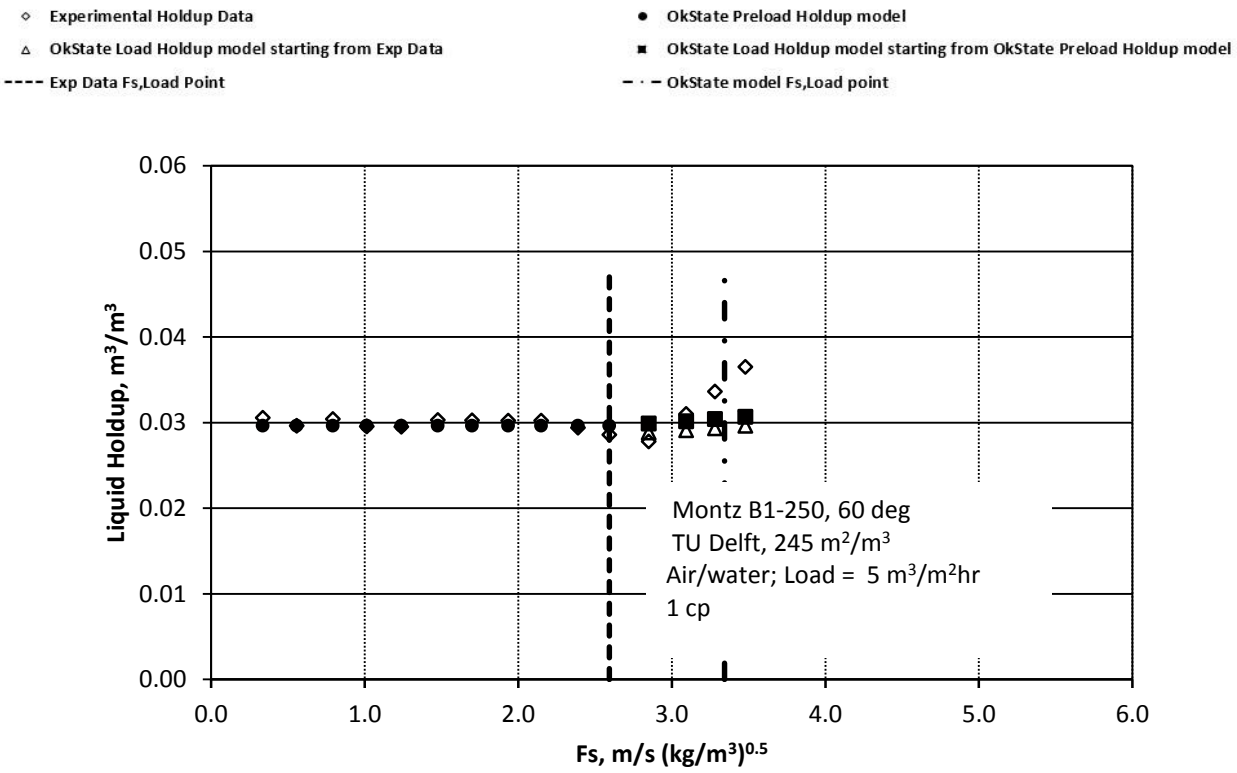

Fig. C.49. OkState liquid holdup model predictions vs. experimental liquid holdup data

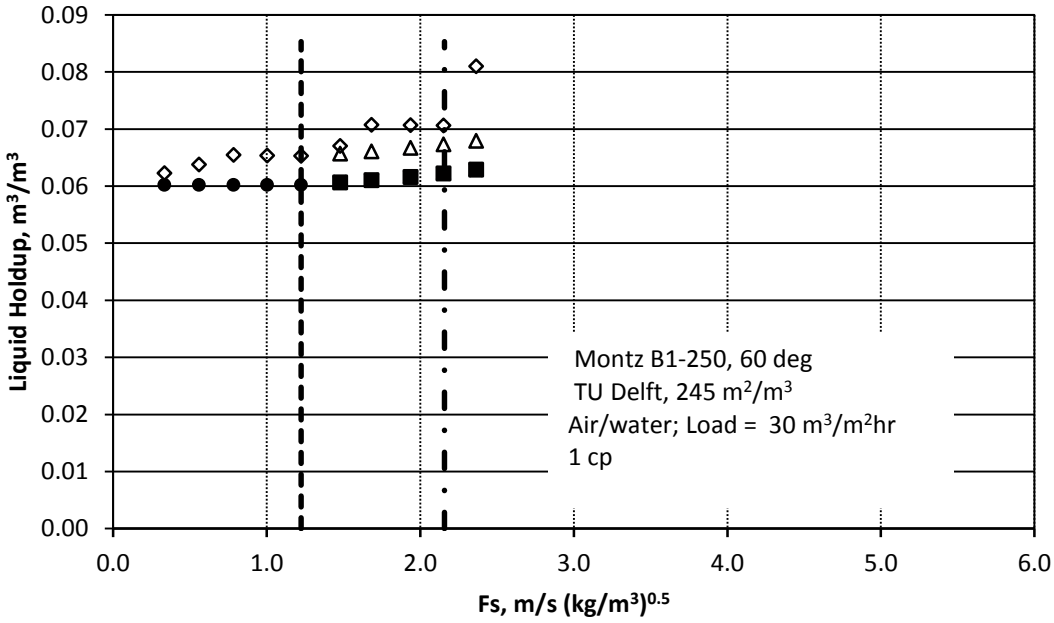

Fig. C.50. OkState liquid holdup model predictions vs. experimental liquid holdup data

D. Literature Loading Models performance using experimental liquid holdup loading data (Table 3.2)

D.1. SRP Model [21]:

$$\left(\frac{\Delta P}{\Delta Z}\right)_{dry} = \left(\frac{\rho_G}{\rho_{(air,1\ bar)}}\right)^{0.4}\left(\frac{0.177\ \rho_G U_{GS}^2}{S\ \epsilon^2(\sin\theta)^2} + \frac{88.77\ u_G U_{GS}}{S^2\epsilon\sin\theta}\right)$$

$$F_t = \frac{a_e}{a_p} = \frac{(We_L Fr_L)^{0.15} 29.12\ S^{0.36}}{Re_L^{0.2}\ \epsilon^{0.6}(1-0.93\cos\gamma)(\sin\theta)^{0.3}}$$

Solve the below equations,

$$h_L = \left[\frac{4\ F_t}{S}\right]^{\frac{2}{3}}\left\{\frac{3\ \mu_L U_{Ls}}{\rho_L\epsilon\sin\theta\left[\left(\frac{\rho_L-\rho_G}{\rho_L}\right)\left(1-\frac{\left(\frac{\Delta P}{\Delta Z}\right)_{new}}{\left(\frac{\Delta P}{\Delta Z}\right)_{flood}}\right)\right]}\right\}^{\frac{1}{3}}$$

$$\frac{\Delta P}{\Delta Z} = \frac{\left(\frac{\Delta P}{\Delta Z}\right)_{dry}}{[1-(0.614+71.35\ S)h_L]^5}$$

$$\left(\frac{\Delta P}{\Delta Z}\right)_{flood} = 1025\ Pa/m$$

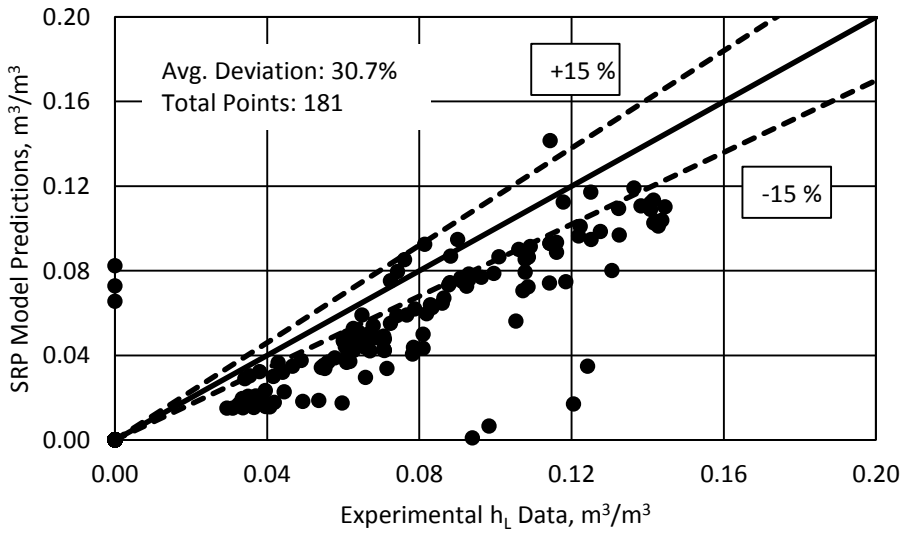

Fig. D.1. SRP loading model predictions vs experimental liquid holdup loading data

D.2. Gualito Model [52]:

$$\left(\frac{\Delta P}{\Delta Z}\right)_{dry} = \left(\frac{\rho_G}{\rho_{(air,1\ bar)}}\right)^{0.4}\left(\frac{0.177\ \rho_G U_{GS}^2}{S\ \epsilon^2(\sin\theta)^2} + \frac{88.77\ u_G U_{GS}}{S^2\epsilon\sin\theta}\right)$$

$$F_t = \frac{a_e}{a_p} = \frac{(We_L Fr_L)^{0.15} 29.12\ S^{0.36}}{Re_L^{0.2}\ \epsilon^{0.6}(1-0.93\cos\gamma)(\sin\theta)^{0.3}}$$

$$\left(\frac{\Delta P}{\Delta Z}\right)_{flood} = 1500 + 65000\ U_{LS}$$

Solve below equations,

$$h_L = \left[\frac{4\ F_t}{S}\right]^{\frac{2}{3}}\left\{\frac{3\ \mu_L U_{Ls}}{\rho_L \epsilon\sin\theta\left[\left(\frac{\rho_L-\rho_G}{\rho_L}\right)\left(1-\frac{\left(\frac{\Delta P}{\Delta Z}\right)_{new}}{\left(\frac{\Delta P}{\Delta Z}\right)_{flood}}\right)\right]}\right\}^{\frac{1}{3}}$$

$$\frac{\Delta P}{\Delta Z} = \frac{\left(\frac{\Delta P}{\Delta Z}\right)_{dry}}{[1-(0.614+71.35\ S)h_L]^5}$$

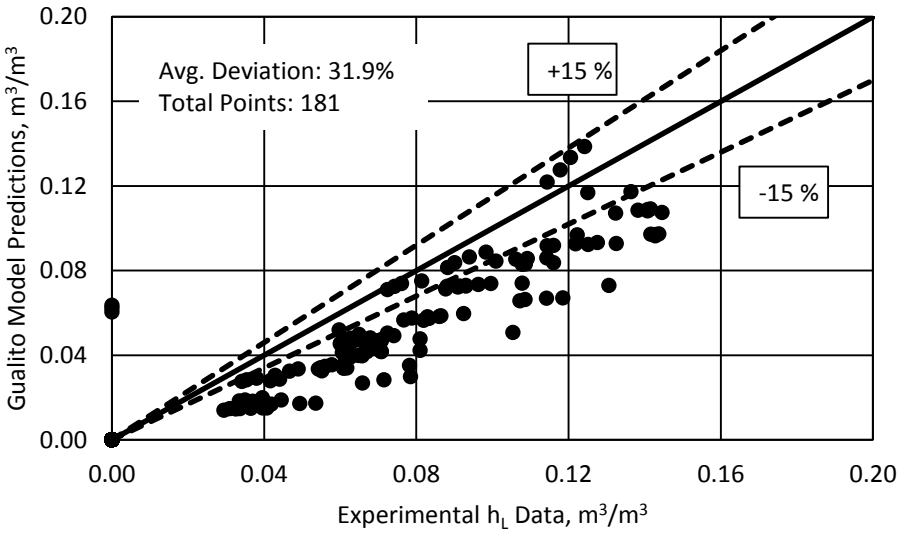

Fig. D.2. Gualito loading model predictions vs experimental liquid holdup loading data

D.3. Mackowiak Model [23]:

$$h_L = \left(\frac{3}{4}\right)\left(\frac{3}{g}\right)^{\frac{1}{3}} a^{\frac{2}{3}} \left(\frac{u_L \mu_L}{\rho_L}\right)^{\frac{1}{3}}$$

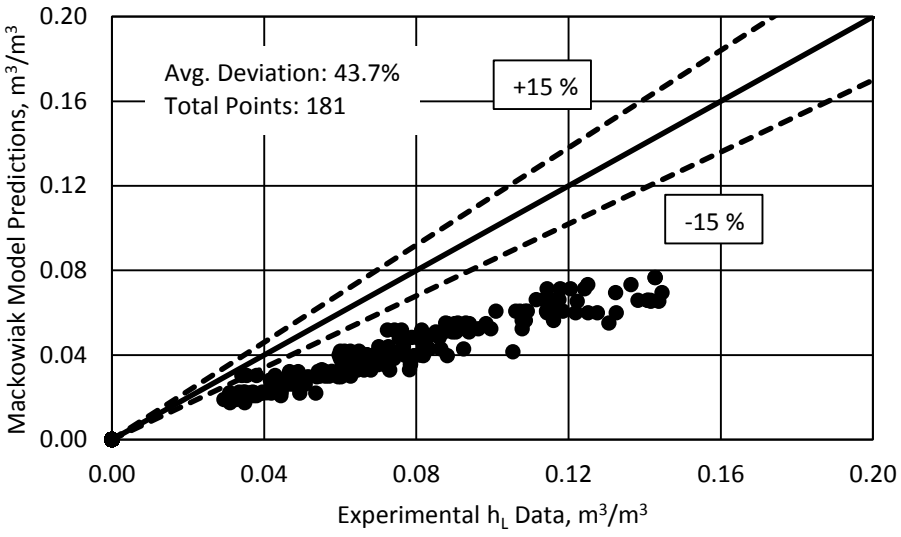

Fig. D.3. Mackowiak loading model predictions vs experimental liquid holdup loading data

E. Literature Load point Model performance using experimental load point data

E.1. Verschoof Model [40]:

Constant liquid load:

$$F_{G,lp} = \left[0.053\ \varepsilon^2\ g\ d_{hg} \frac{\rho_L - \rho_G}{\rho_G} \left(u_{Ls} \sqrt{\frac{\rho_L}{\rho_G}} \right)^{-0.25} (sin\ \alpha)^{1.24} \right]^{0.57} \sqrt{\rho_G}$$

Total reflux conditions (L/V = 1):

$$F_{G,lp} = \left[0.053\ \varepsilon^2\ g\ d_{hg}(\rho_L - \rho_G) \left(\frac{u_{Ls}}{u_{Gs}} \sqrt{\frac{\rho_L}{\rho_G}} \right)^{-0.25} (sin\ \alpha)^{1.15} \right]^{0.5} \sqrt{\rho_G}$$

$$d_{hG} = \frac{\frac{(bh - 2\delta s)^2}{bh}}{\left[\left(\frac{bh - 2\delta s}{2h} \right)^2 + \left(\frac{bh - 2\delta s}{b} \right)^2 \right]^{0.5} + \frac{bh - 2\delta s}{2h}}$$

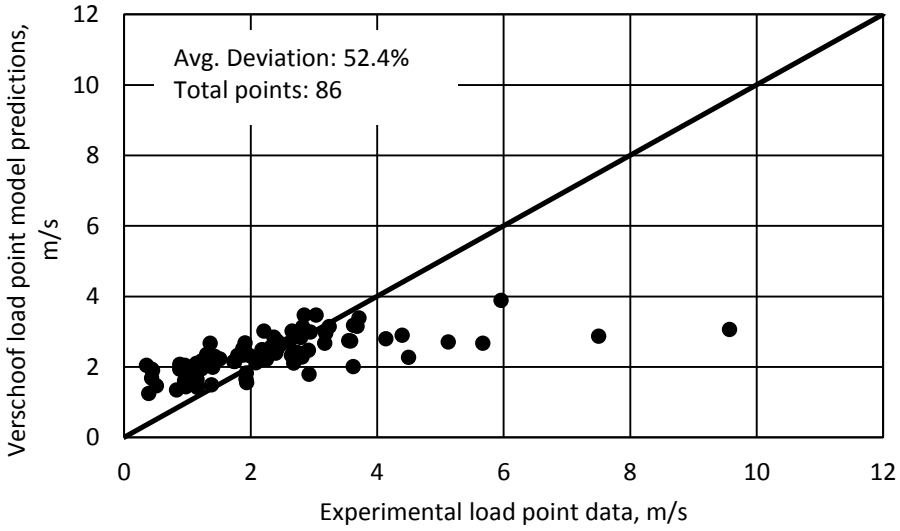

Fig. E.1. Verschoof load point model predictions vs experimental load point data

F. Data without packing surface area information

Table F.1. Summary of packing data without packing surface area information

Database	Packing	Effective area, (Approximated) m^2/m^3	Void fraction, ε	s, mm	Preloading	Loading	System
Koch [21]	Gempak 1A	115	96	36	8	7	Air/Water
	Gempak2A	220	95	18	6	7	
	Gempak 4A	453	91	9	5	11	
	Flexipac 1	453	91	9	5	10	
	Flexipac 2	220	95	18	9	15	
	Flexipac 3	115	96	36	15	13	
	Flexipac 4	55	98	72	16	12	
Total Points					64	75	

Table F.2. Summary of OkState liquid holdup load model and other literature liquid holdup model predictions using literature experimental liquid holdup data (with approximated packing surface area) in loading region

Database	Packing	Mean Absolute Relative Error, %				
		OkState liquid holdup load model (Eqn. 3.3)		SRP [21]	Mackowiak [23]	Gualito [52]
		Using Preloading Model Predictions	Using Experimental Preloading Data			
Koch [21]	Gempak 1A	26.0	**13.2**	29.4	28.3	19.8
	Gempak2A	9.1	**3.6**	7.6	28.1	7.8
	Gempak 4A	15.8	**4.6**	20.0	25.7	18.6
	Flexipac 1	10.2	**3.2**	9.3	31.6	13.3
	Flexipac 2	14.4	**4.4**	5.8	38.9	7.7
	Flexipac 3	17.0	**9.6**	20.2	31.8	16.0
	Flexipac 4	31.5	**12.7**	25.3	53.0	19.9
Average Deviation		17.8	**7.2**	16.3	35.0	14.6

- Lowest error for each packing were bolded
- For models requiring packing dimension information, error was displayed as NA where the packing dimension information is not available

$$MARE,\ \% = \frac{(Measured\ Holdup\ -Predicted\ Holdup)}{(Measured\ Holdup)}\ X\ 100$$

F.1. Literature Loading Models performance using experimental liquid holdup loading data (Table F.2)

F.1.1. Newly Developed OkState liquid holdup load model using Experimental liquid holdup preloading data:

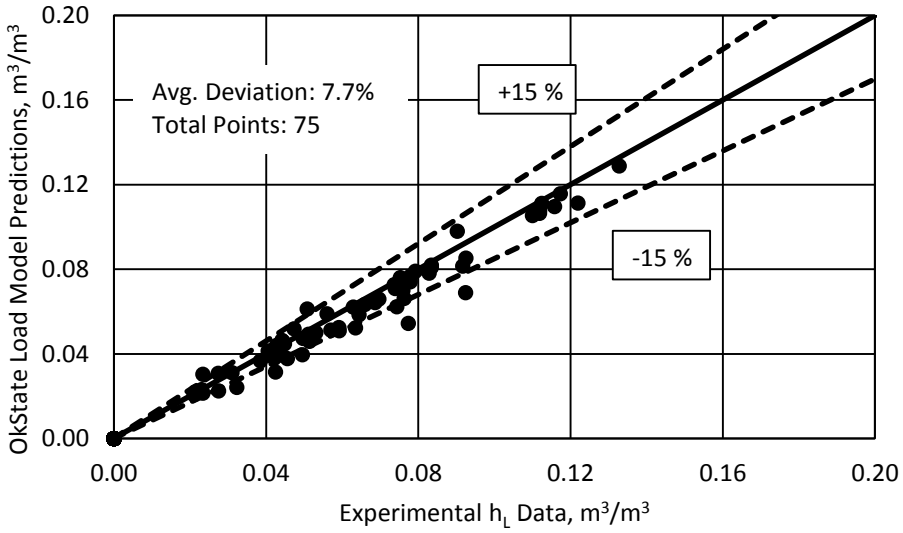

Fig. F.1.1. OkState liquid holdup load model predictions using Experimental liquid holdup preloading data vs experimental liquid holdup loading data

F.1.2. Newly Developed OkState liquid holdup load model using OkState liquid holdup preload model:

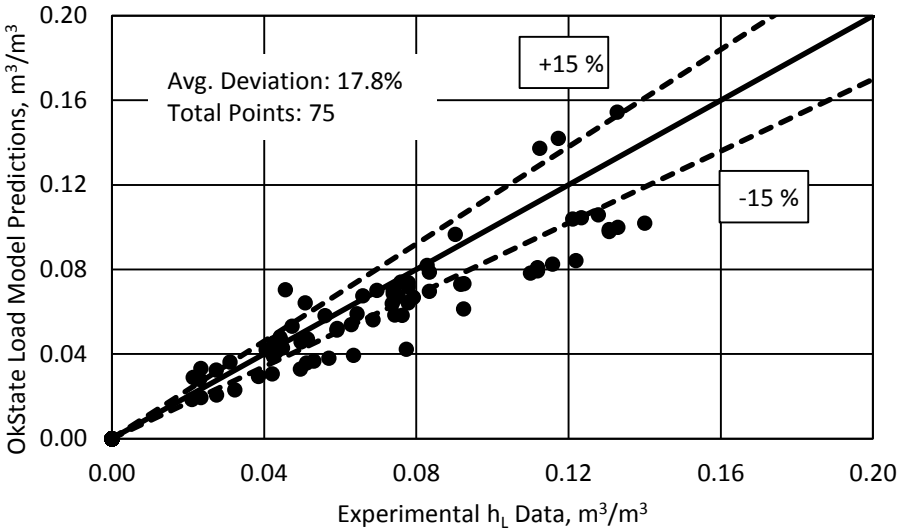

Fig. F.1.2. OkState liquid holdup load model predictions using Experimental liquid holdup preloading data vs experimental liquid holdup loading data

F.1.3. SRP Model [21]:

$$\left(\frac{\Delta P}{\Delta Z}\right)_{dry} = \left(\frac{\rho_G}{\rho_{(air,1\ bar)}}\right)^{0.4}\left(\frac{0.177\ \rho_G U_{GS}^2}{S\ \epsilon^2(\sin\theta)^2} + \frac{88.77\ u_G U_{GS}}{S^2\epsilon\sin\theta}\right)$$

$$F_t = \frac{a_e}{a_p} = \frac{(We_L Fr_L)^{0.15} 29.12\ S^{0.36}}{Re_L^{0.2}\ \epsilon^{0.6}(1-0.93\cos\gamma)(\sin\theta)^{0.3}}$$

Solve the below equations,

$$h_L = \left[\frac{4\ F_t}{S}\right]^{\frac{2}{3}}\left\{\frac{3\ \mu_L U_{Ls}}{\rho_L\epsilon\sin\theta\left[\left(\frac{\rho_L-\rho_G}{\rho_L}\right)\left(1-\frac{\left(\frac{\Delta P}{\Delta Z}\right)_{new}}{\left(\frac{\Delta P}{\Delta Z}\right)_{flood}}\right)\right]}\right\}^{\frac{1}{3}}$$

$$\frac{\Delta P}{\Delta Z} = \frac{\left(\frac{\Delta P}{\Delta Z}\right)_{dry}}{[1-(0.614+71.35\ S)h_L]^5}$$

$$\left(\frac{\Delta P}{\Delta Z}\right)_{flood} = 1025\ Pa/m$$

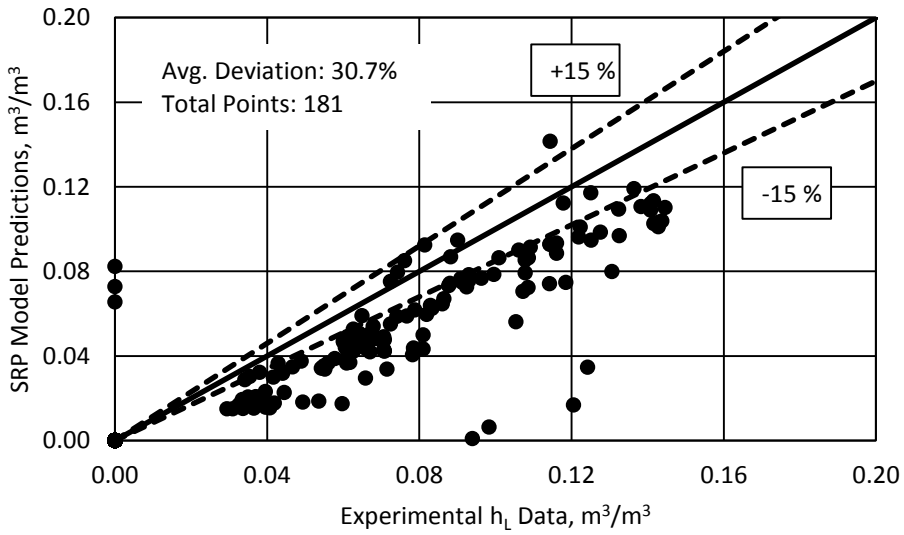

Fig. F.1.3. SRP loading model predictions vs experimental liquid holdup loading data

F.1.4. Gualito Model [52]:

$$\left(\frac{\Delta P}{\Delta Z}\right)_{dry} = \left(\frac{\rho_G}{\rho_{(air,1\ bar)}}\right)^{0.4}\left(\frac{0.177\ \rho_G U_{GS}^2}{S\ \epsilon^2(\sin\theta)^2} + \frac{88.77\ u_G U_{GS}}{S^2\epsilon\sin\theta}\right)$$

$$F_t = \frac{a_e}{a_p} = \frac{(We_L Fr_L)^{0.15} 29.12\ S^{0.36}}{Re_L^{0.2}\ \epsilon^{0.6}(1-0.93\cos\gamma)(\sin\theta)^{0.3}}$$

$$\left(\frac{\Delta P}{\Delta Z}\right)_{flood} = 1500 + 65000\ U_{LS}$$

Solve below equations,

$$h_L = \left[\frac{4\ F_t}{S}\right]^{\frac{2}{3}}\left\{\frac{3\ \mu_L U_{Ls}}{\rho_L\epsilon\sin\theta\left[\left(\frac{\rho_L-\rho_G}{\rho_L}\right)\left(1-\frac{\left(\frac{\Delta P}{\Delta Z}\right)_{new}}{\left(\frac{\Delta P}{\Delta Z}\right)_{flood}}\right)\right]}\right\}^{\frac{1}{3}}$$

$$\frac{\Delta P}{\Delta Z} = \frac{\left(\frac{\Delta P}{\Delta Z}\right)_{dry}}{[1-(0.614+71.35\ S)h_L]^5}$$

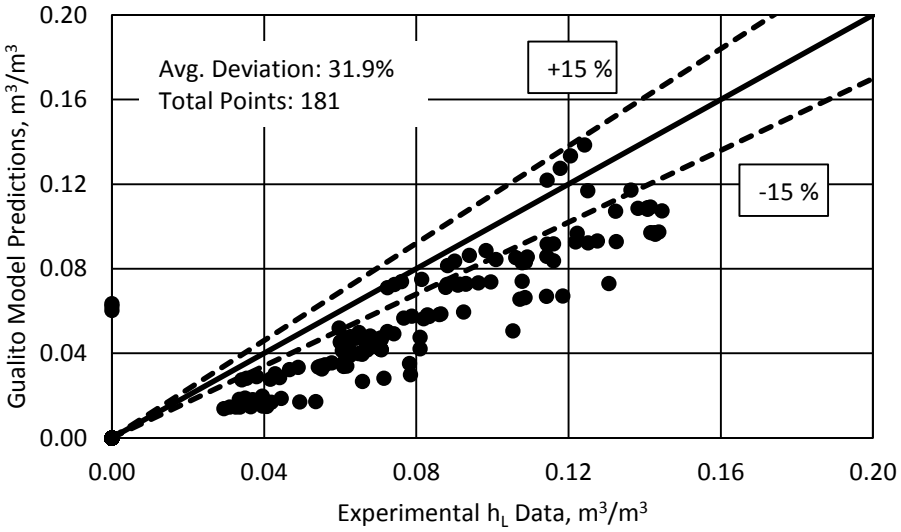

Fig. F.1.4. Gualito loading model predictions vs experimental liquid holdup loading data

F.1.5. Mackowiak Model [23]:

$$h_L = \left(\frac{3}{4}\right)\left(\frac{3}{g}\right)^{\frac{1}{3}} a^{\frac{2}{3}} \left(\frac{u_L \mu_L}{\rho_L}\right)^{\frac{1}{3}}$$

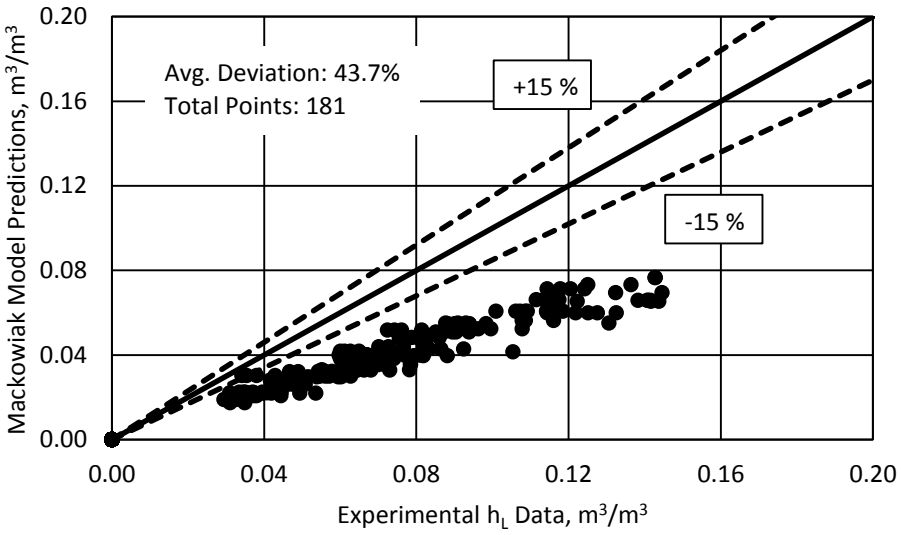

Fig. F.1.5. Mackowiak loading model predictions vs experimental liquid holdup loading data

F.2. Literature Load point Model performance using experimental load point data

F.2.1. Newly Developed OkState load point model using Experimental load point data:

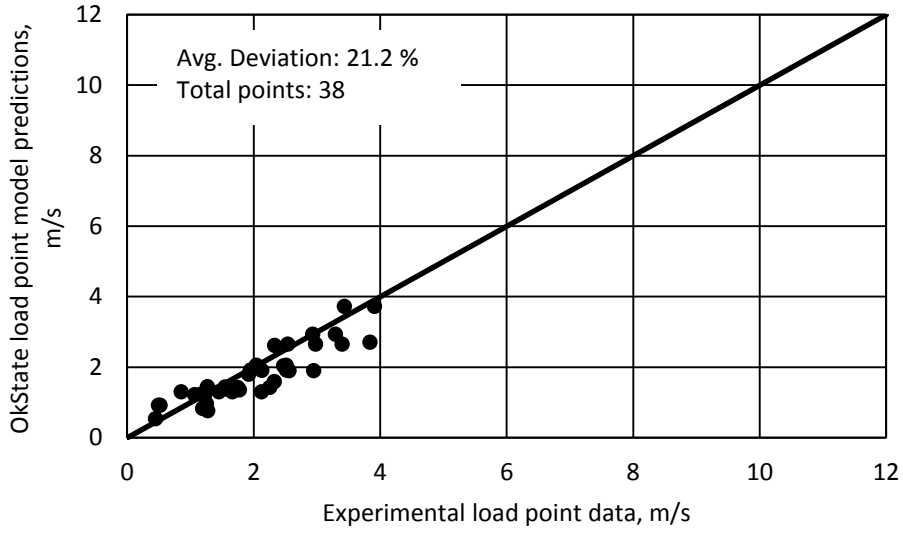

Fig. F.2.1. OkState load point model predictions vs experimental load point data

F.2.2. Verschoof Model [40]:

Constant liquid load:

$$F_{G,lp} = \left[0.053\ \varepsilon^2\ g\ d_{hg} \frac{\rho_L - \rho_G}{\rho_G} \left(u_{Ls} \sqrt{\frac{\rho_L}{\rho_G}} \right)^{-0.25} (sin\ \alpha)^{1.24} \right]^{0.57} \sqrt{\rho_G}$$

Total reflux conditions (L/V = 1):

$$F_{G,lp} = \left[0.053\ \varepsilon^2\ g\ d_{hg}(\rho_L - \rho_G) \left(\frac{u_{Ls}}{u_{Gs}} \sqrt{\frac{\rho_L}{\rho_G}} \right)^{-0.25} (sin\ \alpha)^{1.15} \right]^{0.5} \sqrt{\rho_G}$$

$$d_{hG} = \frac{\frac{(bh - 2\delta s)^2}{bh}}{\left[\left(\frac{bh - 2\delta s}{2h} \right)^2 + \left(\frac{bh - 2\delta s}{b} \right)^2 \right]^{0.5} + \frac{bh - 2\delta s}{2h}}$$

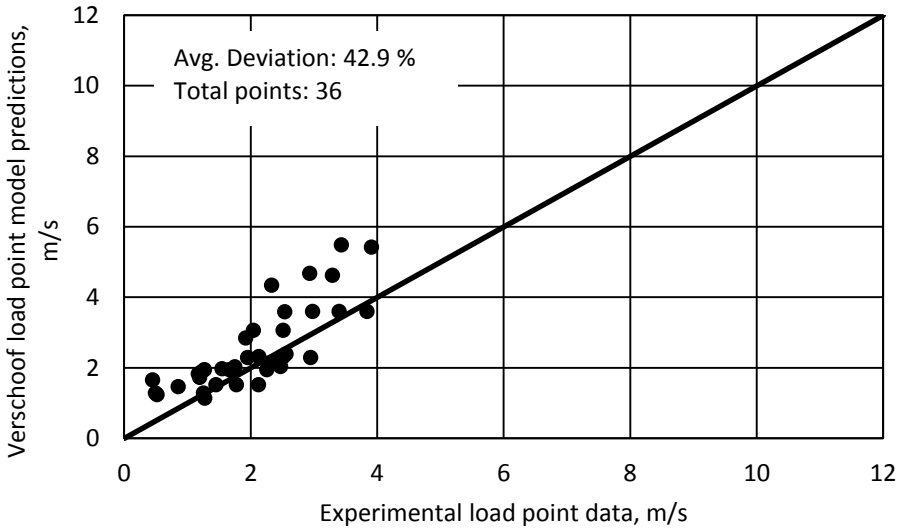

Fig. F.2.2. Verschoof load point model predictions vs experimental load point data

G. Summary of Literature Load point Data and OkState Load point Model predictions

Table G.1. Summary of Literature Load point Data and OkState Load point Model predictions

Pressure bar	System	Packing	Beta	Load m^3/m^2h	Exp Load Point m/s $(kg/m^3)^{0.5}$	OkState Load Point m/s $(kg/m^3)^{0.5}$
1.018	air/water	Montz B1-250	45	5	2.42	3.17
1.018	air/water	Montz B1-250	45	30	1.24	2.03
1.018	air/water	Montz B1-250	60	5	2.59	3.34
1.018	air/water	Montz B1-250	60	30	1.22	2.16
1	air/water	Mellapak 250X	60	25	1.59	2.23
1	air/water	Mellapak 250X	60	50	1.17	1.85
1	air/water	Mellapak 250X	60	75	1.08	1.64
1	air/water	Mellapak 250X	60	100	1.16	1.49
1	air/water	Mellapak 250X	60	125	1.13	1.39
1	air/water	Mellapak 250X	60	150	1.08	1.30
1	air/water	Mellapak 250X	60	175	1.10	1.24
1	air/water	Mellapak 250Y	45	5	2.52	3.11
1	air/water	Mellapak 250Y	45	16	2.33	2.36
1	air/water	Mellapak 250Y	45	32	2.02	1.96
1	air/water	Mellapak 250Y	45	64	1.59	1.61
1	air/water	Mellapak 250Y	45	80	1.36	1.50
1	air/water	Mellapak 500Y	45	5	2.55	2.22
1	air/water	Mellapak 500Y	45	25	1.91	1.39
1	air/water	Mellapak 500Y	45	50	1.40	1.08
1	Air/Water/Sucrose	B1-250M	45	25	2.43	1.56
1	Air/Water/Sucrose	B1-250M	45	25	1.85	1.28
1	Air/Water/Sucrose	B1-250M	45	25	1.17	0.99
1	Air/Water/Sucrose	B1-250M	45	5	3.00	1.98
1	Air/Water/Sucrose	B1-250M	45	5	2.04	1.57
1	Air/Water	B1-250M	45	25	2.00	2.10
1	Air/Water	B1-250M	45	5	3.01	3.13
1	Air/Water	B1-250M	45	3	3.48	3.51
1	Air/Water	B1-250M	45	10	2.99	2.65
1	Air/Water	B1-250M	45	15	2.52	2.40
1	Air/Water	B1-250M	45	20	2.49	2.23
1	Air/Water	B1-250M	45	35	1.98	1.91
1	MEA	B1-250M	45	25	1.90	1.64
1	MEA	B1-250M	45	5	2.54	2.50

Pressure bar	System	Packing	Beta	Load m3/m2h	Exp Load Point m/s (kg/m3)0.5	OkState Load Point m/s (kg/m3)0.5
1	MEA	Flexipac 2Y	45	5	2.50	2.67
1	MEA	Flexipac 2Y	45	25	1.89	1.74
1	Air/Water	Flexipac 2Y	45	3	3.54	3.74
1	Air/Water	Flexipac 2Y	45	10	2.10	2.82
1	Air/Water	Flexipac 2Y	45	15	2.10	2.55
1	Air/Water	Flexipac 2Y	45	20	2.03	2.37
1	Air/Water	Flexipac 2Y	45	35	2.00	2.03
1	Air/Water	Flexipac 2Y	45	25	2.07	2.23
1	Air/Water	Flexipac 2Y	45	5	3.05	3.33
1	Air/Water/Sucrose	Flexipac 2Y	45	5	2.00	1.67
1	Air/Water/Sucrose	Flexipac 2Y	45	25	1.38	1.05
1	Air/Water/Sucrose	Flexipac 2Y	45	25	1.94	1.36
1	Air/Water/Sucrose	Flexipac 2Y	45	25	2.01	1.65
1	Air/Water/Sucrose	Flexipac 2Y	45	5	3.01	2.10

H. Literature Liquid Holdup Flooding Model performance using Experimental Liquid Holdup Flooding Data

H.1. Mackowiak Model [59]:

$$\lambda_0 = \left(\frac{u_L}{u_V}\right)_{FL}$$

When $Re_L \geq 2$:

$$h_{L,Fl}^{O} = \frac{\left(\sqrt{1.44\,\lambda_0^2 + 0.8\,\lambda_0\,(1-\lambda_0)} - 1.2\,\lambda_0\right)}{0.4\,(1-\lambda_0)}\left[\frac{m^3}{m^3}\right]$$

When $e_L < 2$:

$$h_{L,Fl}^{O} = \frac{\left(\sqrt{1.254\,\lambda_0^2 + 0.48\,\lambda_0\,(1-\lambda_0)} - 1.12\,\lambda_0\right)}{0.24\,(1-\lambda_0)}\left[\frac{m^3}{m^3}\right]$$

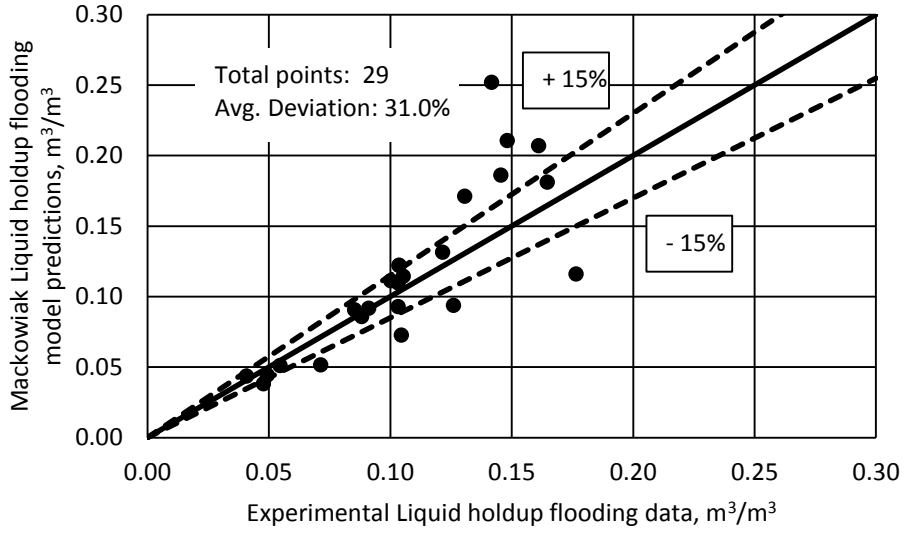

Fig. H.1. Mackowiak liquid holdup flooding model predictions vs experimental liquid holdup flooding data

I. Literature Flooding Velocity Models Performance using Experimental Flooding Velocity Data

I.1. Lockett Model [61]:

$$u_{v,fl} = c_g \left(\frac{\rho_l - \rho_g}{\rho_g}\right)^{0.5}$$

$$c_g = \left(\frac{Nu}{d_e}\right)^2$$

$$d_e = (1 + m \left(\frac{\rho_G}{\rho_l}\right)^{0.5} \left(\frac{\rho_l - \rho_G}{\rho_G}\right)^{0.25} \left(\frac{L}{V}\right)^{0.5}$$

$$Nu = \left(1.57\, a^{-0.25} \left(\frac{\mu_l}{\mu_w}\right)^{-0.03}\right)$$

$$m = 0.78 \exp(0.00058\ \mathrm{a})$$

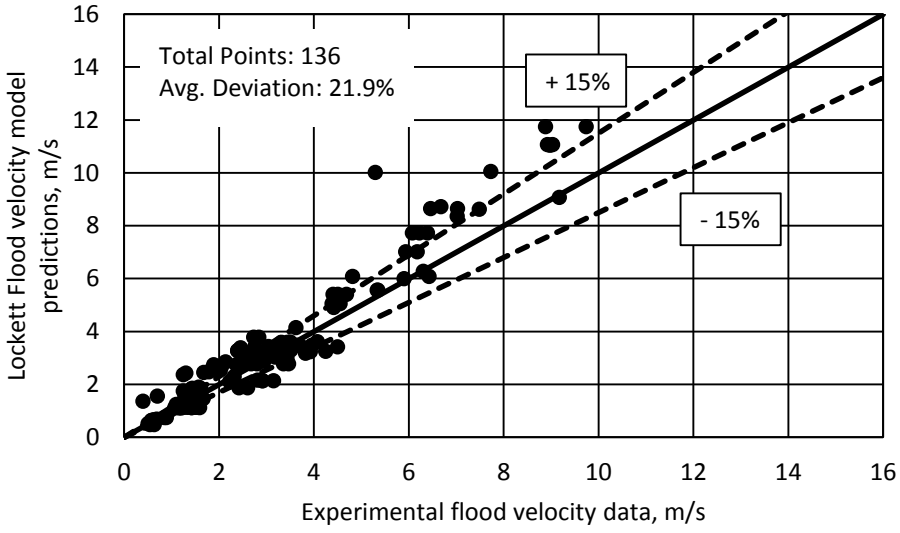

Fig. I.1. Lockett flooding velocity model predictions vs experimental flooding velocity data

I.2. Kuzniewska Model [63]:

$$u_{g,fl} = A_1 \epsilon \left(\frac{a}{\epsilon^3}\right)^{B_1}$$

$$A_1 = A \frac{\left(\frac{\rho_a \rho_l}{\rho_g \rho_w}\right)^{0.5}}{\left(\frac{\sigma_L}{\sigma_w}\right)^{0.25} \left(\frac{\eta_l}{\eta_w}\right)^{0.02}}$$

$$B_1 = B \frac{\left(\frac{v_l}{v_w}\right)^{0.02}}{\left(\frac{\eta_g}{\eta_a}\right)^{0.1} \left(\frac{\sigma_l}{\sigma_w}\right)^{0.15}}$$

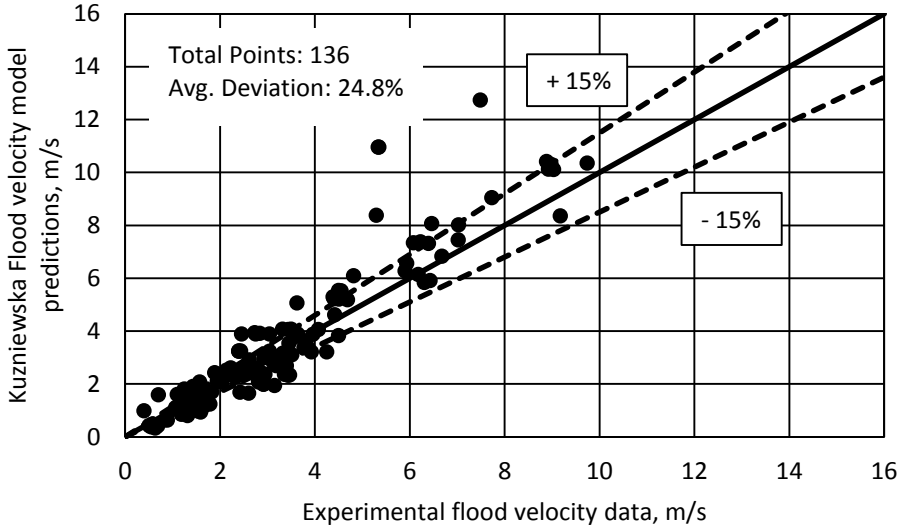

Fig. I.2. Kuzniewska flooding velocity model predictions vs experimental flooding velocity data

J. Literature Flooding Data summary without packing surface area information

Table J.1. Summary of packing data without packing surface area information

Database	Packing	Effective area, (Approximated) m2/m3	Void fraction, ε	s, mm	System
Koch [21]	Gempak 1A	115	96	36	Air/Water
	Gempak2A	220	95	18	
	Gempak 4A	453	91	9	
	Flexipac 1	453	91	9	
	Flexipac 2	220	95	18	
	Flexipac 3	115	96	36	
	Flexipac 4	55	98	72	

J.1. Literature Liquid Holdup Flooding Model performance using Experimental Liquid Holdup Flooding Data

J.1.1. OkState Liquid holdup flooding model:

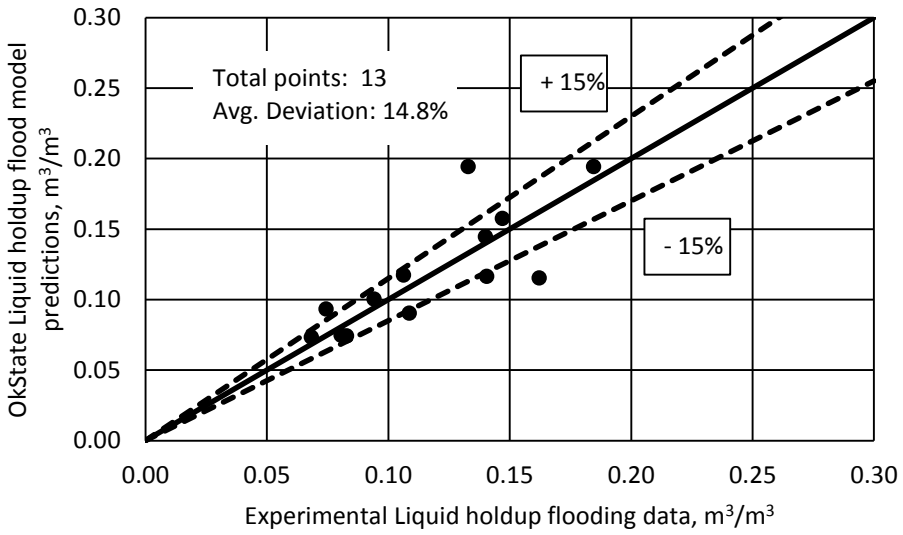

Fig. J.1.1. OkState liquid holdup flooding model predictions vs experimental liquid holdup flooding data

J.1.2. Mackowiak Model [59]:

$$\lambda_0 = \left(\frac{u_L}{u_V}\right)_{FL}$$

When $Re_L \geq 2$:

$$h^O_{L,Fl} = \frac{\left(\sqrt{1.44\,\lambda_0^2 + 0.8\,\lambda_0\,(1-\lambda_0)} - 1.2\,\lambda_0\right)}{0.4\,(1-\lambda_0)}\left[\frac{m^3}{m^3}\right]$$

When $e_L < 2$:

$$h^O_{L,Fl} = \frac{\left(\sqrt{1.254\,\lambda_0^2 + 0.48\,\lambda_0\,(1-\lambda_0)} - 1.12\,\lambda_0\right)}{0.24\,(1-\lambda_0)}\left[\frac{m^3}{m^3}\right]$$

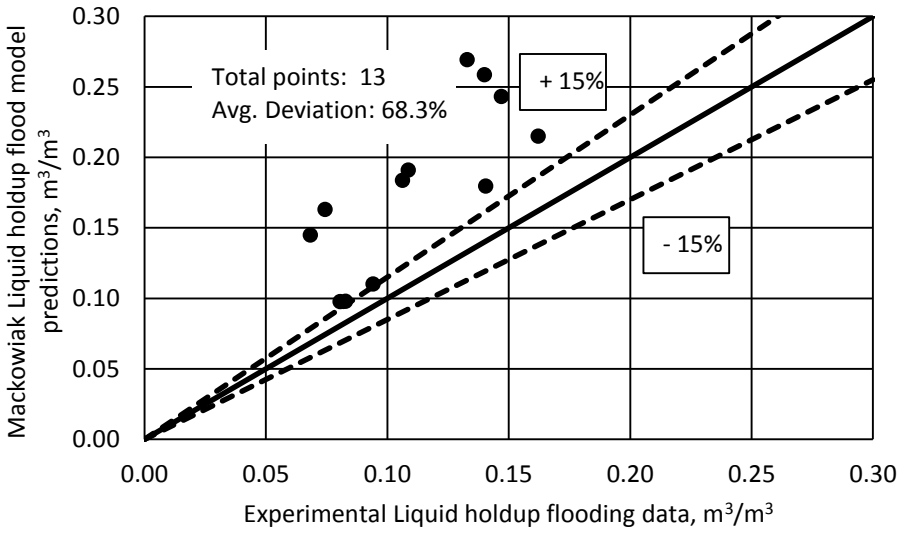

Fig. J.1.2. Mackowiak liquid holdup flooding model predictions vs experimental liquid holdup flooding data

J.2. Literature Flooding Velocity Models performance using Experimental Flooding Velocity Data

Table J.2.1. Summary of literature flood velocity model performance using experimental flood velocity data (Table J.1)

Model	Average Mean Absolute Relative Error, %
OkState	17.4
Lockett	32.6
Kuzniewska	17.4

$$MARE,\ \% = \frac{(Measured\ Flooding\ velocity\ - Predicted\ looding\ velocity)}{(Measured\ looding\ velocity)}\ X\ 100$$

J.2.1. Lockett Model [61]:

$$u_{v,fl} = c_g \left(\frac{\rho_l - \rho_g}{\rho_g}\right)^{0.5}$$

$$c_g = \left(\frac{Nu}{d_e}\right)^2$$

$$d_e = (1 + m \left(\frac{\rho_G}{\rho_l}\right)^{0.5} \left(\frac{\rho_l - \rho_G}{\rho_G}\right)^{0.25} \left(\frac{L}{V}\right)^{0.5}$$

$$Nu = \left(1.57\, a^{-0.25} \left(\frac{\mu_l}{\mu_w}\right)^{-0.03}\right)$$

$$m = 0.78 \exp(0.00058\, a)$$

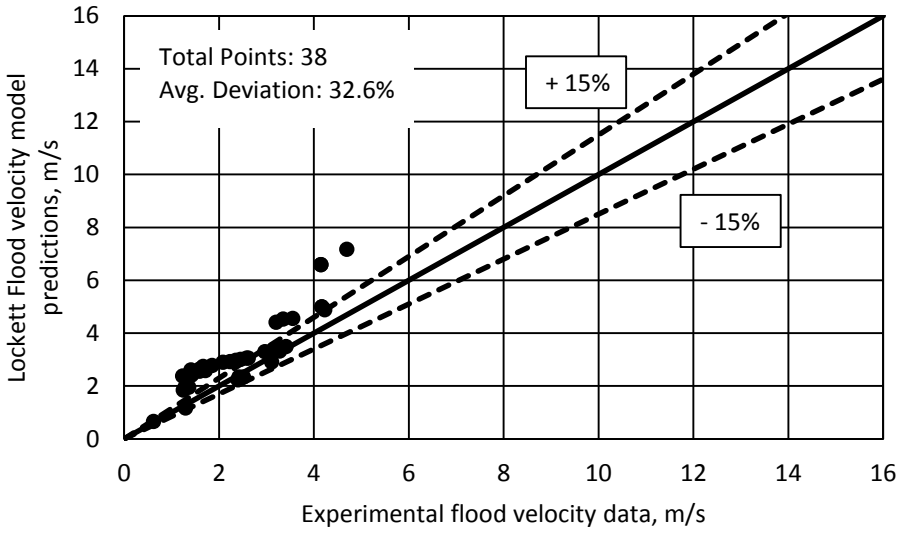

Fig. J.2.1. Lockett flooding velocity model predictions vs experimental flooding velocity data

J.2.2. Kuzniewska Model [63]:

$$u_{g,fl} = A_1 \epsilon \left(\frac{a}{\epsilon^3}\right)^{B_1}$$

$$A_1 = A \frac{\left(\frac{\rho_a \rho_l}{\rho_g \rho_w}\right)^{0.5}}{\left(\frac{\sigma_L}{\sigma_w}\right)^{0.25} \left(\frac{\eta_l}{\eta_w}\right)^{0.02}}$$

$$B_1 = B \frac{\left(\frac{v_l}{v_w}\right)^{0.02}}{\left(\frac{\eta_g}{\eta_a}\right)^{0.1} \left(\frac{\sigma_l}{\sigma_w}\right)^{0.15}}$$

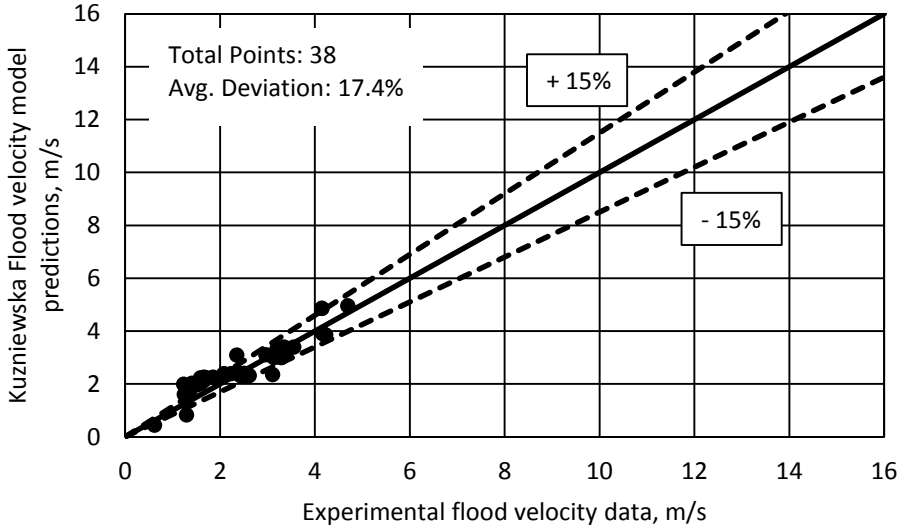

Fig. J.2.2. Kuzniewska flooding velocity model predictions vs experimental flooding velocity data

J.2.3. OkState Flood velocity model:

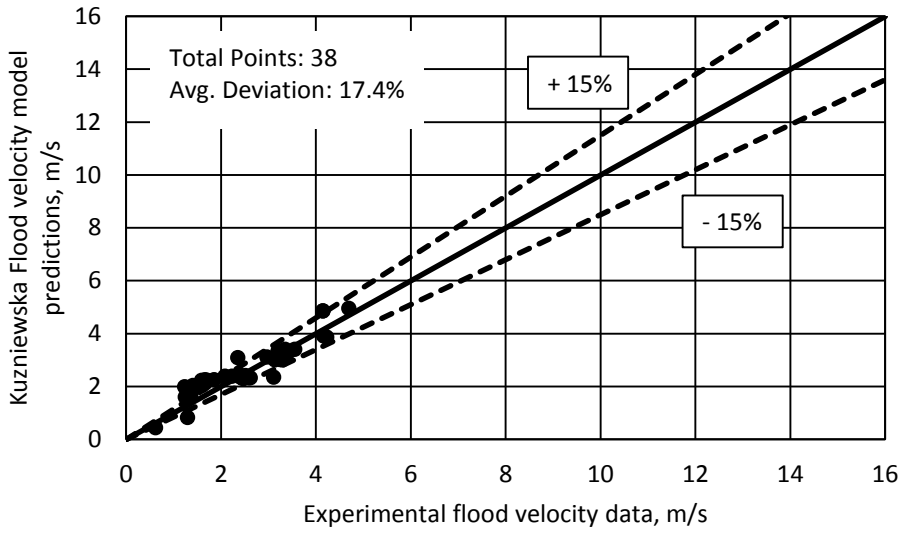

Fig. J.2.3. OkState flooding velocity model predictions vs experimental flooding velocity data

VITA

Anil Krishna Jammula

Candidate for the Degree of

Doctor of Philosophy

Thesis: NEW LIQUID HOLDUP, LOAD POINT AND FLOODING VELOCITY MODELS IN DIFFERENT REGIONS OF OPERATIONS FOR A STRUCTURED PACKED COLUMN

Major Field: Chemical Engineering

Biographical:

Personal Data: Born in Vijayawada, AP, India on March 4, 1986.

Education:

Completed the requirements for the Doctor of Philosophy in Chemical Engineering at Oklahoma State University, Stillwater, Oklahoma in December, 2014.
Completed the requirements for the Master of Engineering in Chemical Engineering at Lamar University, Beaumont, Texas, USA in 2008.
Completed the requirements for the Bachelor of Technology in Chemical Engineering at Acharya Nagarjuna University, Guntur, Andhra Pradesh, India in 2007.

Experience:

Worked as Development Engineer-Intern at Optimized Gas Treating Inc., between May and December of 2013
Worked as Chemical Engineer-Intern at Flowserve between May and August of 2012

Professional Memberships:

Member - International Society of Automation, American Institute of Chemical Engineers, and Omega Chi Epsilon

Name: Anil Krishna Jammula Date of Degree: DECEMBER, 2014

Institution: Oklahoma State University Location: Stillwater, Oklahoma

Title of Study: NEW LIQUID HOLDUP, LOAD POINT AND FLOODING VELOCITY MODELS IN DIFFERENT REGIONS OF OPERATIONS FOR A STRUCTURED PACKED COLUMN

Pages in Study: 164 Candidate for the Degree of Doctor of Philosophy

Major Field: Chemical Engineering

Scope and Method of Study: Liquid holdup of structured packed column affects the pressure drop, flooding velocity, and HETP. For this reason, liquid holdup was used as an important model parameter by different researchers such as Billet (1999) and SRP (1995). However, despite its importance, the amount of work available on liquid holdup is much less in the open literature. When the performance of available literature models were evaluated using the experimental data from the open literature, the literature models were not properly capturing the effect of packing geometry and operating conditions. The main reason for the lack of performance is because a majority of these liquid holdup models were adopted from the random packing. So there is a clear need for liquid holdup models to be developed for a structured packed column using an experimental structured packed column. In the present work, new liquid holdup models were developed in different regions of operation using experimental data of a structured packed column. Furthermore, these new liquid holdup models were used in developing new load point and flood point models.

Findings and Conclusions: A brief summary of the new models is presented below:

- Both OkState preloading and flooding liquid holdup models were developed using a film thickness model.
- An OkState loading liquid holdup model was developed using vapor kinetic energy term.
- An OkState load point model was developed using dimensional analysis.
- An OkState flooding velocity model was developed using the Wallis equation and also liquid holdup flooding term as the main model parameter

Overall multiple models were developed using packing geometrical area and packing void fraction as the main model parameters. These new models were properly capturing the effect of operating conditions and packing geometry on the experimental conditions than any of the literature models. The current models will be useful in improving the pressure drop and HETP models of a structured packed column.